Energy efficiency of fog computing in access networks

Abdullah AL Qahtani

Submitted in accordance with the requirements for the degree of Doctor of Philosophy

The University of Leeds

School of Electronic and Electrical Engineering

November 2022

The candidate confirms that the work submitted is his own, except where work which has formed part of jointly authored publications has been included. The contribution of the candidate and the other authors to this work has been explicitly indicated below. The candidate confirms that appropriate credit has been given within the thesis where reference has been made to the work of others.

Chapter 3 is based partly on the work from:

A.M. Alqahtani, S. H. Mohamed, T. E. H. El-Gorashi, and J. M. H. Elmirghani, 'PON-Based Connectivity for Fog Computing', in 2020 22nd International Conference on Transparent Optical Networks (ICTON), 2020, pp. 1–6, doi: 10.1109/ICTON51198.2020.9203425

Prof. Elmirghani, the supervisor, suggested the study of 'PON-Based Connectivity for Fog Computing' and MILP optimisation. The co-supervisor Dr El-Gorashi, worked with the student on the MILP model development and revised the paper. The co-author Dr. S.H. Mohamed, helped in the initial model preparation and revised the work. The PhD student developed the model analysed the results and wrote paper.

Chapter 4 is based partly on the work from:

A. M. Alqahtani, B. Yosuf, S. H. Mohamed, T. E. H. El-Gorashi, and J. M. H. Elmirghani, 'Energy Efficient Resource Allocation in Federated Fog Computing Networks', in 2021 IEEE Conference on Standards for Communications and Networking (CSCN), 2021, pp. 199–204, doi: 10.1109/CSCN53733.2021.9686117

Prof. Elmirghani suggested the study of 'Energy Efficient Resource Allocation in Federated Fog Computing Networks' and MILP optimisation. Dr El-Gorashi, worked with the student on the MILP model development and revised the paper. The co-authors Dr B. Yosuf and Dr S.H. Mohamed , helped in the initial model preparation and revised the work. The PhD student developed the model analysed the results and wrote paper.

Chapter 5 is based partly on the work from:

A.M. Alqahtani, B. Yosuf, S. H. Mohamed, T. E. H. El-Gorashi, and J. M. H. Elmirghani, 'Energy Minimized Federated Fog Computing over Passive Optical Networks', 2021 Int. Symp. Networks, Comput. Commun., pp. 1–6, Oct. 2021, doi: 10.1109/ISNCC52172.2021.9615749.

Prof Elmirghani suggested the study of 'Energy Minimized Federated Fog Computing over Passive Optical Networks' and MILP optimisation. Dr El-Gorashi worked with the student on the MILP model development and revised the paper. The co-authors Dr B. Yosuf and Dr S.H. Mohamed helped in the initial model preparation and revised the models and the work. The PhD student developed the model analysed the results and wrote paper.

Acknowledgements

I would like to express my great gratitude to my PhD supervisor Prof. Jaafar Elmirghani for the support during my PhD, for his constant support, patience, comments and for sharing of his immense knowledge. Working with my PhD supervisor has been an invaluable experience that shaped my research career.

I would also like to sincerely acknowledge Dr Taisir El-Gorashi, my second supervisor for the support, encouragement, comments, and the great feedback and discussions of my research. I would also like to acknowledge Dr Sanaa H. Mohamed and Dr Barzan Yosuf for the help and support during my PhD. I would also like to acknowledge all research group members for their academic and personal support throughout this journey.

I would like to acknowledge the Government of Saudi Arabia for funding my PhD study and for their support.

I would like to express my love and gratitude to my beloved wife Seham who has been a constant source of support, patient, and encouragement during the challenges of my PhD and life. I am truly thankful for having you in my life.

I would like to express my love to my daughter Jwana and my son Bassel who fill me with pleasure and joy.

Finally, I would like to dedicate this thesis to my parents; to my father Mohammed, and my mother Hadbaa. I have been extremely fortunate in my life to have parents who have shown me unconditional love and support. Also, many thanks to my beloved brothers and sisters; Saad, Maha, Manal, Noha, Rahaf and Roaa for their support and for making my life enjoyable and full of fun.

Abstract

Today's and future delay-sensitive applications, such as connected vehicles, smart grids, smart cities, and Internet of things (IoT) applications generate tremendous amount of data that can overwhelm data centres in cloud computing infrastructures. Using these cloud data centres can cause a remarkable increase in the applications response time and in the power consumption. Thus, the efficiency of cloud computing is marred by such delay-sensitive applications due to the distance between the end-users and the cloud servers. To address these issues, fog computing units are placed in the access network to be close to the end-users and to offer processing and storage, resources. Passive Optical Network (PON) architectures are efficient technology choices in the access networks and data centres as their capacity provides high-bandwidth and their passive components offer reduction in the power consumption compared to electronic switching.

In this thesis, we propose an energy efficient distributed fog computing architecture containing multiple fog nodes connected by a Wavelength Division Multiplexing (WDM) PON based on Arrayed Waveguide Grating Routers (AWGRs). The fog nodes can collaborate with each other through PON connectivity, and hence can meet the delay sensitive application requirements in access networks. Firstly, we develop a Mixed Integer Linear Programming (MILP) model to optimise the AWGRs connectivity between the distributed fog computing units to facilitate fog nodes collaboration through inter-fog communications. In addition to optimising the connectivity in the proposed collaborative architecture, we developed an energy-efficient resource allocation MILP model along with a heuristic model to optimise the placement of virtual

machines (VMs) while considering the inter-VMs traffic for fog units' collaboration. The results show that optimising the placement of VMs in the distributed fog computing units saves up to 44% of the total power consumption compared to placing VMs while neglecting the power consumption and inter-VMs traffic. The impact of the volume of the inter-VMs traffic on the total power consumption is also investigated.

In addition, we evaluate the collaborative proposed architecture capacity using a MILP model that optimises the placement of end-users' demands while aiming to reduce the total networking and processing power consumption. The results show an increase in processing capacity utilisation and a reduction in the power consumption compared to a non-collaborative architecture.

Finally, we study optimising processing user demands considering user-mobility which necessitate VMs migration between collaborative fog computing units over the WDM PON architecture. A MILP model is developed to minimise the total power consumption and propagation delay in case of conducting VMs migrations due to user mobility for delay-sensitive application. The optimal allocation results show that migrating the VMs over the AWGR-based PON achieves a significant decrease in networking power consumption and in propagation delay by 55% and 92%, respectively compared to using other routes with active components via the access network for the VMs migrations.

Table of Contents

Acknowledgements .... **III**
Abstract .... **IV**
Table of Contents .... **VI**
List of Figures .... **IX**
List of Tables .... **XII**
Abbreviations .... **XIII**
Chapter 1 Introduction **1**
1.1 Motivation 1
1.2 Objectives 5
1.3 Thesis contributions 6
1.4 Publications 7
1.5 Thesis structure 8
Chapter 2 : Literature Review **10**
2.1 Telecommunication Networks 10
2.1.1 Access network 12
2.1.2 Metro Network 13
2.1.3 Core Network 14
2.2 Passive Optical Networks (PON) 15
2.2.1 Passive Optical Network (PON) Devices 17
2.2.2 PONs Multiplexing Techniques 19
2.2.3 Software-Defined Networking (SDN) for PON Networks 20
2.2.4 Energy-Efficient Networking using PONs 20
2.3 Cloud computing 23
2.4 Data Centres 24
2.4.1 Electronic Data centre 25
2.4.2 Hybrid Data Centre Architectures 26
2.4.3 Optical Data Centre Architecture 27
2.4.4 Traffic Patterns in Data centre 27
2.5 Fog Computing 29
2.5.1 Fog Computing Architectures 31
2.5.2 Characteristic and Challenges of Fog Computing 31
2.5.3 Energy-efficiency in Fog Computing 32
2.6 Virtualisation in cloud and fog Computing. 33
2.7 User Mobility 36

2.7.1 Individual-Mobility Model 37
2.8 Summary 40
Chapter 3 PON-Based Connectivity for Collaborative Fog Computing units 41
3.1 PON-Based Collaborative Fog Computing units 41
3.2 Collaborative Fog Computing units based on the SDN-PON Architecture 45
3.3 The MILP Model for the Connectivity 49
3.4 Results and discussion..54
3.5 Benchmarking the Power Consumption 57
3.6 Summary. 61
Chapter 4 Energy Efficient VM Placement in the Collaborative Fog Computing Architecture 62
4.1 Introduction 62
4.2 MILP Optimisation Model 64
4.3 Results and Discussion...71
4.4 Impact of Inter-VM Traffic on The Power Consumption. 75
4.5 Heuristic Approach to Energy Efficient Virtual Machines (VM) Placement in PON-based Fog Computing.....................................79
Summary 84
Chapter 5 Energy Efficient Placement for End Users' demands in a Collaborative Fog Computing Architecture 85
5.1 Introduction 85
5.1 Related Work 86
5.2 The Proposed PON-based collaborative FOG architecture 87
5.2.1 The Networking Layer 88
5.2.2 The Processing Layer 88
5.3 MILP Optimisation Model for Energy Efficient Placement of End Users' demands 89
5.4 MILP MODEL RESULT...100
5.5 Energy Efficient VM Placement in a Heterogeneous Collaborative-Fog Computing Architecture..105
5.5.1 The Proposed Architecture 106
5.5.2 Results...107
5.6 Summary 112
Chapter 6 User Mobility-Aware Collaborative Fog computing Units Architecture 113
6.1 Introduction 113

6.2 Related Work 114
6.3 User-Mobility scenarios..116
6.4 MILP Model..117
6.5 MILP MODEL RESULT..132
6.5.1 Scenario 1: Joint minimisation model of Total Power Consumption and Propagation Delay (Ô) 135
6.5.2 Scenario 2: Variation of the objectives....................................140
6.6 Summary 146
Chapter 7 Conclusions and Future Work 147
7.1 Conclusions..147
7.2 Future Work..149
7.2.1 Architecture and Model Optimisation 149
7.2.2 Resilience in the Proposed Architecture 150
7.2.3 Experimental demonstration 150
7.2.4 Extending the model’s objective 150

List of Figures

FIGURE 2.1 TELECOMMUNICATION NETWORKS. 11
FIGURE 2.2 PON ARCHITECTURE. 17
FIGURE 2.3 (A) AWGR ($\boldsymbol{n}$X$\boldsymbol{n}$),(B) AWG (1X$\boldsymbol{n}$), AND (C) AWG ($\boldsymbol{n}$X1). 18
FIGURE 2.4 THE TRADITIONAL DATA CENTRE. 25
FIGURE 2.5 EDGE COMPUTING ARCHITECTURE. 30
FIGURE 2.6 CLASSIFICATION OF USER-MOBILITY MODELS. 37
FIGURE 3.1 PON-BASED COLLABORATIVE FOG COMPUTING. 43
FIGURE 3.2 SPINE AND LEAF-BASED COLLABORATIVE FOG COMPUTING. 44
FIGURE 3.3 COLLABORATIVE FOG COMPUTING CELLS BASED ON PON CONNECTIVITY. 47
FIGURE 3.5 WAVELENGTH ASSIGNMENTS AND ROUTING. 55
FIGURE 3.6 THE POWER CONSUMPTION OF THE PROPOSED ARCHITECTURE VS SPINE AND LEAF ARCHITECTURE. 60
FIGURE 3.7 POWER SAVING BY THE PROPOSED ARCHITECTURE COMPARED TO SPINE AND LEAF. 61
FIGURE 4.1 THE POWER CONSUMPTION OF SYSTEM OF THE PROPOSED MODEL AND THE BASELINE MODEL. 74
FIGURE 4.2 NUMBERS OF ACTIVATED SERVERS OF THE PROPOSED MODEL AND THE BASELINE MODEL. 75
FIGURE 4.3 THE POWER CONSUMPTION OF PROPOSED MODEL WITH INTER-VM TRAFFIC DEMAND VERSUS NO-INTER-VM TRAFFIC DEMAND. 76
FIGURE 4.4 NUMBERS OF ACTIVATED SERVERS OF NO INTER-VMS TRAFFIC DEMAND VERSUS VARIED INTER-VMS TRAFFIC DEMAND. 76
FIGURE 4.5 THE POWER CONSUMPTION OF DIFFERENT SETS OF INTER-VM TRAFFIC DEMAND. 77
FIGURE 4.6 THE NUMBER OF ACTIVATED SERVERS OF DIFFERENT SETS OF INTER-VM TRAFFIC DEMAND. 78
FIGURE 4.7 TOTAL TRAFFIC BETWEEN THE SERVERS. 78
FIGURE 4.8 FLOWCHART OF THE HEURISTIC MODEL. 81
FIGURE 4.9 THE POWER CONSUMPTION RESULTS OF THE MILP OPTIMISATION MODEL VERSUS THE HEURISTIC MODEL. 82
FIGURE 4.10 THE NUMBER OF ACTIVATED SERVERS TO PLACE THE VMS IN THE MILP OPTIMISATION MODEL AND THE HEURISTIC MODEL. 83

FIGURE 5.1 THE COLLABORATIVE FOG ARCHITECTURE OVER PON… 87
FIGURE 5.2 NUMBER OF PROCESSED VERSUS BLOCKED VMS IN THE NON-COLLABORATIVE FOG……………………………………………103
FIGURE 5.3 NUMBER OF PROCESSED VERSUS BLOCKED VMS IN THE COLLABORATIVE FOG……………………………………..…………103
FIGURE 5.4 TOTAL POWER CONSUMPTION (i.e., networking and processing) OF BOTH FOG ARCHITECTURES…………………………...104
FIGURE 5.5 PROCESSING POWER CONSUMPTION IN BOTH FOG ARCHITECTURES……………………………………………………..…104
FIGURE 5.6 NETWORKING POWER CONSUMPTION IN BOTH FOG ARCHITECTURES……………………………………………………..…105
FIGURE 5.7 NUMBER OF USED SERVERS IN BOTH FOG ARCHITECTURES. 105
FIGURE 5.8 THE EVALUATED HETEROGENEOUS COLLABORATIVE-FOG COMPUTING ARCHITECTURE. 106
FIGURE 5.9 THE POWER CONSUMPTION. 110
FIGURE 5.10 TOTAL POWER CONSUMPTION DISTRIBUTION 111
FIGURE 5.11 THE PROCESSING UTILISATION. 111
FIGURE 6.1 USER-MOBILITY AWARE COLLABORATIVE FOG UNITS OVER PON. 116
FIGURE 6.2 PROCESSING LOAD AMONG COLLABORATIVE FOG UNITS IN DIFFERENT TIME SLOTS 134
FIGURE 6.3 PLACEMENT OF VMS IN COLLABORATIVE FOG UNITS IN DIFFERENT TIME SLOTS. 134
FIGURE 6.4 POWER CONSUMPTION OF VMS PLACEMENT AND MIGRATION AMONG COLLABORATIVE FOG UNITS OVER AWGRS. 136
FIGURE 6.5 POWER CONSUMPTION OF VMS PLACEMENT AND MIGRATION AMONG COLLABORATIVE FOG UNITS OVER OLT..... 136
FIGURE 6.6 NUMBER OF ACTIVATED SERVERS OF JOINT MINIMISATION MODEL. 137
FIGURE 6.7 TOTAL NETWORKING POWER CONSUMPTION OF JOINT MINIMISATION MODEL. 137
FIGURE 6.8 PROPAGATION DELAY OF VMS MIGRATION AMONG COLLABORATIVE FOG UNITS OVER AWGRS IN THE JOINT MINIMISATION MODEL. 138

FIGURE 6.9 PROPAGATION DELAY OF VMS MIGRATION AMONG COLLABORATIVE FOG UNITS OVER OLT IN THE JOINT MINIMISATION MODEL. 139
FIGURE 6.10 AVERAGE PROPAGATION DELAY. 139
FIGURE 6.11 POWER CONSUMPTION WHEN MINIMISING ONLY THE PROCESSING POWER CONSUMPTION. 141
FIGURE 6.12 PROPAGATION DELAY WHEN MINIMISING ONLY THE PROCESSING POWER CONSUMPTION. 142
FIGURE 6.13 NUMBER OF ACTIVATED SEVERS WHEN CONSIDERING THE DIFFERENT OBJECTIVES. 142
FIGURE 6.14 POWER CONSUMPTION WHEN MINIMISING THE PROCESSING POWER CONSUMPTION ONLY. 143
FIGURE 6.15 PROPAGATION DELAY WHEN MINIMISING THE PROCESSING POWER CONSUMPTION ONLY. 144
FIGURE 6.16 POWER CONSUMPTION WHEN MINIMISING ONLY THE PROPAGATION DELAY. 145
FIGURE 6.17 PROPAGATION DELAY WHEN MINIMISING ONLY THE PROPAGATION DELAY. 145

List of Tables

TABLE 3.1 ROUTING MAP FOR INTER-FOG UNITS' COMMUNICATION.. 54
TABLE 3.2 POWER CONSUMPTION OF NETWORKING EQUIPMENT. ... 59
TABLE 4.1 THE INPUT DATA FOR THE VM PLACEMENT MODEL............ 72
TABLE 5.1 THE INPUT DATA FOR ENERGY EFFICIENT PLACEMENT FOR VMS OF END USERS. 100
TABLE 5.2 THE INPUT DATA FOR THE MILP MODEL IN A HETEROGENEOUS COLLABORATIVE-FOG COMPUTING ARCHITECTURE.. 107
TABLE 6.1 THE INPUT DATA FOR THE USER MOBILITY MODEL. 132

Abbreviations

ADMS: Add/drop multiplexers

ADSL: Asymmetric digital subscriber line

AON: Active optical network

ATM: Asynchronous transfer mode

AWG: Arrayed waveguide grating

AWGR: Arrayed waveguide grating router

BPON: Broadband PON

CE: Customers equipment

CPE: Customers premises equipment

CO: Central office

DACS: Digital access cross-connect system

DSL: Digital subscriber line

EPON: Ethernet PON

GPON: Gigabit PON

FAAS: Fog-as--a-service

HAAS: Hardware-as-a-service

HFC: Hybrid fibre-coaxial

IoT: Internet of things

LTE: Long term evolution

MEC: Mobile edge computing

MEN: Metro ethernet network

MILP: Mixed integer linear programming

NIC: Network interface card

ODN: Optical distribution network

OFDM-PON: Orthogonal frequency division multiplexing PON

OLT: Optical line terminal

ONT: Optical network terminal

ONU: Optical network unit

OXC: Optical cross connect

PAAS: Platform-as-a-service

PON: Passive optical network

RAN: Radio access network

SAAS: Software-as-a-service

SDH: Synchronous digital hierarchy

SDN: Software-defined networking

SONET: Synchronous optical networking

TDM-PON: Time division multiplexing PON

TOR: Top of rack

UNI: User-network interface

VDSL: Very high-speed digital subscriber line

VM: Virtual machine

VOD: Video on demand

WDM: Wavelength division multiplexing

WIFI: Wireless fidelity

WIMAX: Worldwide interoperability for microwave access

Chapter 1 Introduction

1.1 Motivation

The growth in the demand for next generation applications is accelerated by the need for IoT devices, smart cities, healthcare, and smart grids to name a few. This resulted in the generation of enormous volumes of data that is usually transported over multiple network domains towards remote cloud data centres for processing purposes. Processing all this data at the cloud will cause further bottlenecks in the already congested core networks and hence, this will have a detrimental impact on latency and power consumption. Alternatively, through the concept of fog computing, computational resources can be placed close to end-users, at the edge of the access network, to extend the capabilities of cloud computing. Fog computing units could be any device that can provide processing and storage capabilities such as routers, switches, accesses points or small racks of servers [1]–[7]. However, the processing capacity of fog units is limited compared to the cloud. This will often result in congestion or requests blockage under high demands. Therefore, the capacity of fog computing units should be addressed beside the power consumption to ensure that they are well-suited to the demands of delay-sensitive applications [8]–[10].

Due to its high capacity and passive components that lead to savings in the power consumption, optical networking technology is a good solution that can be utilised in different network domains to reduce the power consumption issues [15], [16]. Generally, there are essentially two types of systems that make fibre-to-the home network connections possible: the passive optical network (PON) and the active optical network (AON). Both systems provide multiple ways by which data can be separated and routed to their appropriate destinations [17]. PONs are widely utilised as an optimal technology in the access part of the network as well as the cloud data centres due to their energy efficiency and high bandwidths that are particularly suited to high bit-rate applications such as streaming, Video on Demand (VoD) and cloud gaming [15], [18]–[20]. The authors in [20] assessed wired and wireless network infrastructures in terms of their ability to support real-time applications. The study in [20] showed that PON is an energy efficient access technology due to using passive nodes, with the additional advantage of abundant bandwidth.

Virtualisation is currently one of the most effective techniques for achieving efficient fog and cloud computing systems. Virtualisation allows multiple VMs that represent independent applications to run on a single physical machine (server). Thus, a fog computing environment can host a set of distributed applications, each of which runs as a collection of VMs. The VMs are isolated from each other and each VM can utilise a portion of the physical server resources according to its CPU, memory, and bandwidth resources demands [21], [22]. However, some VMs need to communicate with other VMs to complete their tasks [23], [24]. Therefore, considering the inter-VMs traffic in the VMs placement optimisation is essential to achieve an energy-efficient fog computing environment [25], [26].

The fast growth in today's applications has also driven the network designers to improve the data centre' architectures to support current and upcoming applications [27]. To achieve an appropriate design of the data centre architecture, several aspects should be taken into consideration such as data centre performance, resilience, scalability, and power consumption. A data centre architecture consists of servers, storage, and network components, such as routers and switches, in charge of storing, transferring and computing data. Therefore, the data centre architecture is an important aspect in designing cloud and fog computing systems that impact the energy-efficiency and the computing and networking performance required to meet the requirements of delay-sensitive applications [27].

Moreover, billions of connected devices, each of which requires processing capacity, interact with their neighbouring computing systems which results in demand for more computational resources [28]. Due to the mobility of most of the connected devices, it is crucial for computing systems to be capable of dealing with the connected devices' mobility [28]. Allocating the nearest available resources for delay-sensitive application demands is highly affected by the user-mobility and location. Thus, fog computing systems should be aware of the users' mobility to optimally allocate the available nearest resources to minimise delay and power consumption. Furthermore, user mobility among multiple fog computing units imposes a number of challenges, such as resource managements, computation offloading, scheduling, and power consumption [29].

The access network is a critical segment of the network connecting the end-user devices to the Central Office (CO). The end-users as well as enterprise environments constantly require a reliable access network that can provide high bandwidth, low power consumption and low latency. The metro network collects the end users' traffic and provides an interface between the access network and the core network, while the core network comprises interconnected routers located in different cities or different metro networks [11]–[14]. Instead of transferring the delay-sensitive applications' demands to be processed at cloud computing units connected with in the core network, t fog computing offers a limited processing capabilities in the access networks that can reduce delay and power consumption. In this thesis, a collaborative fog computing units over PON is proposed to serve intensive demands of the delay sensitive applications close to the end users in the access network instead of serving them in the cloud.

This thesis considers the use of (WDM) PON technology to connect multiple distributed Fog Computing units as a collaborative architecture and determine the resultant power consumption reduction. We extended one of the PON-based data centre designs proposed in [30] that used Arrayed Waveguide Grating Routers (AWGRs) to include multiple PON cells, where each cell represents a fog computing unit. We proposed a MILP model to optimise the wavelength assignments in the proposed collaborative architecture to achieve full connectivity between the distributed fog computing units via the AWGRs. We also proposed a MILP model that optimises the placement of VMs while considering the inter-VMs traffic to achieve energy-efficient resource allocation in the proposed collaborative fog computing architecture. We then optimised the placement of VM demands originating from the end-users by formulating a MILP model to minimise the total power consumption by optimising the allocation of processing resources in the proposed architecture. Finally, we propose a MILP model to jointly minimise the total power consumption and delay while considering end-users mobility.

1.2 Objectives

The main research objectives of the work presented in this thesis are as follows:

1. To propose an energy efficient collaborative fog computing architecture containing multiple fog computing units connected using an AWGR-based PON.
2. To determine the wavelength assignment and routing in the proposed collaborative fog architecture to facilitate inter-fog communication and achieve all-to-all connectivity between the distributed fog computing units.
3. To benchmark the power consumption of the proposed architecture against a collaborative fog computing architecture connected using traditional data centre architectures.
4. To optimise the placement of VMs considering the inter-VMs traffic for the fog units' collaboration in serving delay sensitive application in the proposed architecture to achieve energy efficiency and to study the impact of the volume of the inter-VM traffic on the power consumption.
5. To extend the proposed model to consider customer-premises equipment (CPE) in the networking layer and then optimise the VM placement for end-users' demand in the extended proposed collaborative fog architecture where neighbouring fog cells can collaborate in processing intensive demands.
6. To investigate the impact of the heterogeneity of the fog cells in terms of the CPU capacity and power consumption on the performance of the extended proposed collaborative fog architecture.
7. To investigate user mobility across collaborative fog units in the access network and to optimise the VMs placement while considering user

mobility in different time slots while aim to minimise the total power consumption and propagation delay in the case where VMs migration is considered.

1.3 Thesis contributions

The key contributions of this thesis can be outlined as follows:

- We proposed a framework for collaborative fog computing architecture to serve the intensive delay sensitive application demands in the access network. To the best of our knowledge, no study has proposed collaboration among fog units close to the end users to serve the intensive demands in the access network. The proposed architecture contains several fog computing units interconnected by an AWGR-based PON. We proposed a MILP model to optimise the wavelength assignments and routing in the AWGR-based PON to achieve all-to-all connectivity between the collaborative fog computing units.
- We benchmarked the power consumption of the collaborative fog units over PON architecture against a collaborative fog units over a spine and leaf architecture.
- We developed a MILP model and a heuristic for energy efficient VMs placement over the proposed collaborative fog computing architecture considering the inter VMs traffic to facilitate the collaboration of distributed neighbouring fog units to serve delay sensitive application in the access network. Also, we deeply studied the impact of the inter-VMs traffic on the power consumption.

- We extend the previously proposed model to consider the end-users' sites, which are Customer Premises equipment (CPE) and we then developed a MILP model that optimises the VM placement for demands originating from the end-user, and hence, we studied the impact of the heterogeneity of the fog units on the VMs placement and the power consumption.
- We developed a MILP model to minimise the total power consumption and the propagation delay by optimising resource allocation in the collaborative fog computing architecture considering users mobility. Also, we studied the collaborative architecture with the consideration of a number of objectives; minimising the processing power consumption only, minimising the networking power consumption only, and minimising the propagation delay only.

1.4 Publications

The following journal and conference papers have been published / are to be submitted for publications:

1. A. M. Alqahtani, B. Yosuf, S. H. Mohamed, T. E. H. El-Gorashi, and J. M. H. Elmirghani, 'Energy Efficient Resource Allocation in Federated Fog Computing Networks', in 2021 IEEE Conference on Standards for Communications and Networking (CSCN), 2021, pp. 199–204, doi: 10.1109/CSCN53733.2021.9686117.

2. A. M. Alqahtani, S. H. Mohamed, T. E. H. El-Gorashi, and J. M. H. Elmirghani, 'PON-Based Connectivity for Fog Computing', in 2020 22nd International Conference on Transparent Optical Networks (ICTON), 2020, pp. 1–6, doi: 10.1109/ICTON51198.2020.9203425.

3. A. M. Alqahtani, B. Yosuf, S. H. Mohamed, T. E. H. El-Gorashi, and J. M. H. Elmirghani, ‘Energy Minimized Federated Fog Computing over Passive Optical Networks’, 2021 Int. Symp. Networks, Comput. Commun., pp. 1–6, Oct. 2021, doi: 10.1109/ISNCC52172.2021.9615749.

4. A. M. Alqahtani, B. Yosuf, S. H. Mohamed, T. E. H. El-Gorashi, and J. M. H. Elmirghani, ‘Energy Efficient-Fog Computing in Access Networks’ to be submitted to IEEE access.

5. A. M. Alqahtani, B. Yosuf, S. H. Mohamed, T. E. H. El-Gorashi, and J. M. H. Elmirghani, ‘User Mobility-Aware Collaborative Fog computing Units Architecture’ to be submitted to IEEE access.

6. A. M. Alqahtani, B. Yosuf, S. H. Mohamed, T. E. H. El-Gorashi, and J. M. H. Elmirghani, ‘Energy Efficient VM Placement in a Heterogeneous Fog Computing Architecture’ to be submitted to an IEEE ICTON 2023.

1.5 Thesis structure

Following this chapter, this thesis is organised as follows:

Chapter 2 provides an overview of the telecommunication network domains, the use of PON architectures in access networks and in data centres, cloud and fog computing architectures, and the end-user mobility models in access network.

Chapter 3 presents the collaborative fog units over an AWGR-based PON and discusses the advantage of using the PON architecture to connect collaborative fog computing units. It presents the routing and wavelength assignments MILP optimisation model and compares the power consumption of collaborative fog computing over the AWGR-based PON architecture with the power consumption of collaborative fog computing over a spine and leaf architecture.

Chapter 4 presents the MILP optimisation model for VMs placement in the proposed architecture presented in chapter 3 taking into consideration the inter-VMs traffic. Moreover, a heuristic is presented to provide real-time placement algorithm and verify and validate the results of the MILP model.

Chapter 5 extends the proposed model presented in chapter 3 by considering the end user's site CPE in the networking layer and provides the MILP optimisation model for placing VMs of demands originating from the end-user. In addition, it examines the impact of heterogeneous collaborative fog units in term of the power consumption and processing capacity.

Chapter 6 presents a MILP model developed to optimise VMs placement within different time slots in the extended proposed architecture presented in chapter 5 while considering the end users' mobility.

Finally, Chapter 7 provides the conclusions and future work direction.

Chapter 2 : Literature Review

This chapter reviews transport networks layers connecting users to data centres. Also, this chapter reviews in detail various PON architectures and their usage in access networks and in data centre networks. Moreover, this chapter provides an overview of cloud and fog computing architectures as options for processing user's data, followed by an overview of data centre architectures and virtualisation in cloud and fog computing. Finally, this chapter discusses the challenges of modelling user mobility in access networks and presents some of the proposed models in the literature.

2.1 Telecommunication Networks

Based on the geographical area covered by a network segment, telecommunication networks can be hierarchically classified into three types: core networks, metro networks, and access networks, as shown in Figure 2.1. The access networks are the last segments that connect the end-users to the service providers and can extend to tens of kilometres. The metro networks aggregate the traffic from different access networks and transport it to the core network and can extend to hundreds of kilometres. Finally, the core network interconnects metro networks covering a wide region (e.g. a country, a content), and can extend to several thousands of kilometres [15]. In this section, we describe the three types of telecommunication networks and introduce the most important network elements of each network.

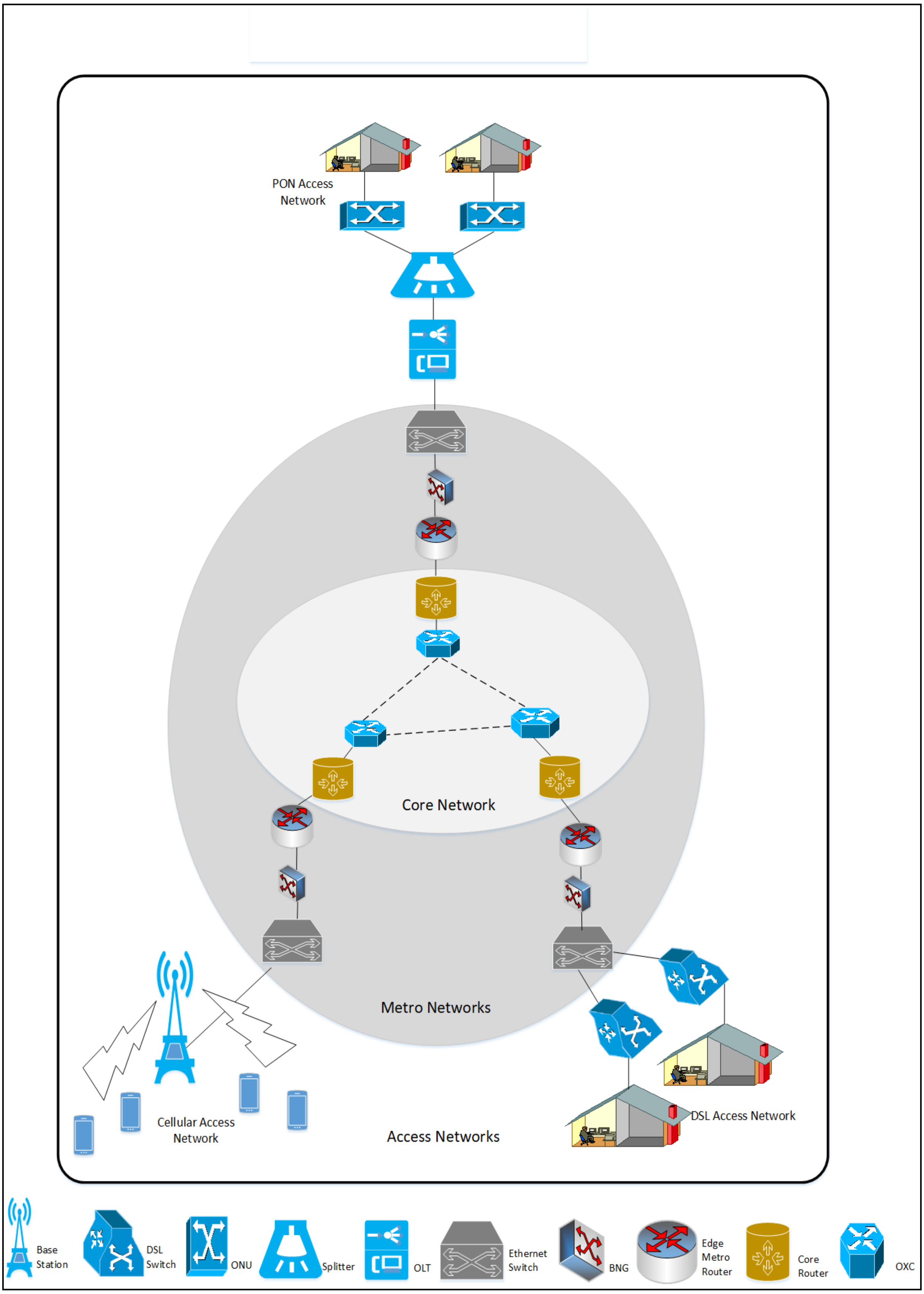

Figure 2.1 Telecommunication Networks.

2.1.1 Access network

The access network is the “last mile” of the network connecting the end-users to their service providers via various type of access technologies such as Digital Subscriber Line (DSL), Optical technologies, Hybrid Fibre-Coaxial (HFC), and wireless links [1]. Each of these technologies has different characteristics in term of bandwidth, reliability, and energy efficiency. Moreover, the distance covered by an access network scales up from a few metres (e.g., a wireless link) to up to tens of kilometres (e.g., Optical Technologies) [11].

DSL technology utilises twisted-pair copper wires in the telephone lines to connect the end-users to the central office. DSL is classified into two types: asymmetric digital subscriber line (ADSL), and very high-speed digital subscriber line (VDSL). ADSL supports asymmetrical transmission rate between the services provider and end-users in upstream and downstream. On the other hand, VDSL supports higher data rates but supports very limited distances [15], [31] .

HFC utilises a fibre cable and coaxial cable to provide broadband services such as Internet services, TV services, and video on demand services to the end-users. The fibre cables are utilised from the central office to the optical nodes placed in the end-users neighbourhood, while the coaxial cables deliver the services from the optical nodes into up to 2000 end-users [32].

Optical network technologies utilise either active (i.e., requires some electronic components to operate) or passive (i.e., do not require any electronic components to operate) devices for switching and routing the data. AON utilises powered devices such an Ethernet Switch or router while PON utilises passive devices such as AWGRs and splitters [4], [5]. Given the continuous growth in Internet services demand and the high bandwidth requirements, optical networks are a good technology in the access network due to their speed, large capacity, high bandwidth, and energy efficiency [4], [5].

Finally, wireless networking is widely utilised in the access network to address mobility requirements. Wireless Fidelity (WiFi) and Cellular networks (e.g., Long Term Evolution (LTE), 5G,etc.) are ubiquitous technologies in the access network [15].

2.1.2 Metro Network

The metro network is the mid segment of telecommunication networks that spans to metropolitan areas to aggregate the end-users' data traffic. It provides an interface to different access networks and connects to the Internet through the core network [15]. Synchronous Optical Networking (SONET), Optical WDM ring, and Ethernet Metro are the three predominant networking technologies in the metro network domain.

The metro Ethernet architecture is based on three network components; an edge router to connect the external networks (e.g., core network), a broadband network gateway which is the access point for the end-users in the access network [33], and Ethernet switches which are used to manage the flow of end user data traffic to connect the end-users to the core network [15]. Ethernet services are provided by the Metro Ethernet Network (MEN) providers and Customers Equipment (CE) that connect to the network using User-Network Interface (UNI), with different standards, and a 10Mbps, 100Mbps, 1Gbps or 10Gbps Ethernet interfaces [34]. The Metro Ethernet is capable of handling multiple subscribers UNIs attached to the MEN from a single building or a single location (site) [34]. There are two types of Ethernet services as illustrated in [34]: Ethernet line (E-line) which is a point-to-point service and Ethernet-LAN (E-LAN) which is a multipoint-to-multipoint service.

SONET and synchronous digital hierarchy (SDH) are standardized protocols used to carry various digital bit signals synchronously through optical fibres. The underlying reason behind the development of the SONET is the dissemination of the optical transmission signal interfaces to provide high speed transmission by using a single mode fibre interface which provides a direct optical interface on the terminal [35]. The two basic parts of the legacy SONET/SDH architecture are the metro-core and metro-access ring. These are interconnected by SONET/SDH add/drop multiplexers (ADMs) and a digital access cross-connect system (DACS) [35].

Metro WDM ring networks are designed to benefit from fibre optic technology characteristics, such as higher speed and massive bandwidth [15]. The substantive reason behind placing WDM in metro networks is its ability to send various data streams simultaneously over a single fibre, each of which uses a unique wavelength [36].

2.1.3 Core Network

The core network, or backbone infrastructure, represents the central part of the telecommunication networks segments that interconnects wide areas, such as cities over a country. Core networks are typically mesh topologies. Core networks collect massive data traffic from metro networks. Thus, a crucial step is to provide suitable interfaces that can handle, collect and distribute large amounts of data traffic aggregated from other telecommunication networks segments (e.g., metro network and access network) [15].

Deploying optical technologies in the core network, such as Internet Protocol (IP) over WDM is essential to achieve high speed data transmission, high capacity, and energy savings [15]. The IP over WDM network utilises multi-layer network architectures composed of an optical layer and an IP layer. The IP layer is composed of IP routers to collect the IP packets from access nodes to their destination nodes. The optical layer is composed of transponders and optical cross connect (OXC) to connect the IP and the optical layers [15].

2.2 Passive Optical Networks (PON)

The exponential growth in telecommunication applications and services and the demand for high-speed data processing that require low latency and low power consumption created a burden on traditional access networks. Therefore, data processing and energy efficiency are now becoming some of the most interesting research areas where several proposed technologies and techniques were introduced to overcome these issues in access networks. The access network is considered as the major consumer of power in communication networks due to the participation of massive numbers of active components [15], [37]. Optical networking such as PON in access network and in data centre has been considered recently as a candidate solution for energy saving. PON is a telecommunication technology that uses optical fibres to transfer multiple services to the end user in a point-to-multipoint form. It is composed of unpowered components [38]–[40] and is therefore more energy efficient compared to other access networking technologies [18] [41].

PON consists of three basic standards: The first is Broadband PON (BPON) which is based on Asynchronous Transfer Mode (ATM) as a transmission protocol and supports a data transfer rate of 622 Mbps for downlink and up to 155 Mbps for uplink. The second is Ethernet PON (EPON) which relies on Ethernet as a transmission protocol with a transmission speed of up to 1.25 Gbps for downlink and uplink. The third is Gigabit PON (GPON and XGPON) which is based on Ethernet, ATM, and TDM as transmission protocols with different transmission speeds. For GPON, the speeds are up to 2.5 Gbps for Optical downlink and 1.25 Gbps for uplink and for XG-PON the speeds are up to 10 Gbps for downlink and 2.5 Gbps for uplink [42].

The PON Architecture, as shown in Figure 2.2, consists of three essential parts: the Optical Line Terminal (OLT), Optical Network Units (ONU) or the Optical Network Terminal (ONT), and the Optical Distribution Network (ODN). The OLT is placed at CO of the service provider to control the flow of data traffic in both directions: to the end users, and to other external networks. The ONU or ONT are the devices near to the end devices that terminate the optical signal and convert it into electrical. The ODN consists of the fibres and splitters between the OLT and ONUs/ONTs that forms a point to multipoint architecture [43].

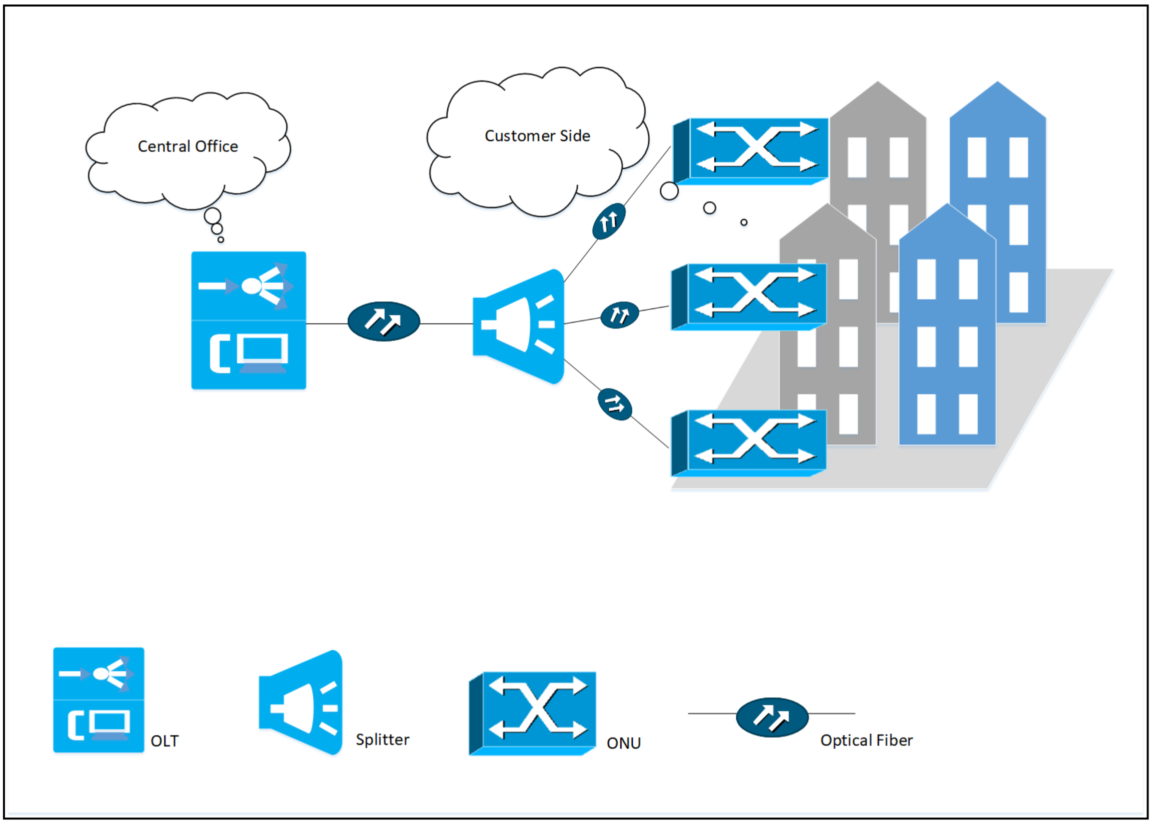

Figure 2.2 PON Architecture.

2.2.1 Passive Optical Network (PON) Devices

Typically, PON devices include AWGRs, coupler/splitter, and Fibre Bragg grating [43].

2.2.1.1 AWGs and AWGRs

An AWG is composed of two-star couplers, one is located at the input and the other is located at the output. The input and output ports are interconnected by an array of waveguides. AWG has various functions that use a cyclic wavelength routing property. One such function is, nx1 wavelength multiplexer, where n represents the number of input ports where each has a signal at a different wavelength. The signals at the input ports are combined onto one signal at the output port, as shown in Figure 2.3.(c). Also, the AWG can be used as 1xn wavelength demultiplexer, which represents the inverse function of the multiplexer, as shown in Figure 2.3(b). Moreover, a fully interconnect AWG is also known as an nxn AWGR, as shown in Figure 2.3(a). For example, if a wavelength, (e.g.,2) is sent to input port 1 and is assigned to output port 2 by design, that wavelength is blocked from reaching any output port except output port 2. Moreover, an AWG can be used as add-drop multiplexer. In an drop–add multiplexer, the data contained in a specified wavelength is extracted and replaced by different new data [43].

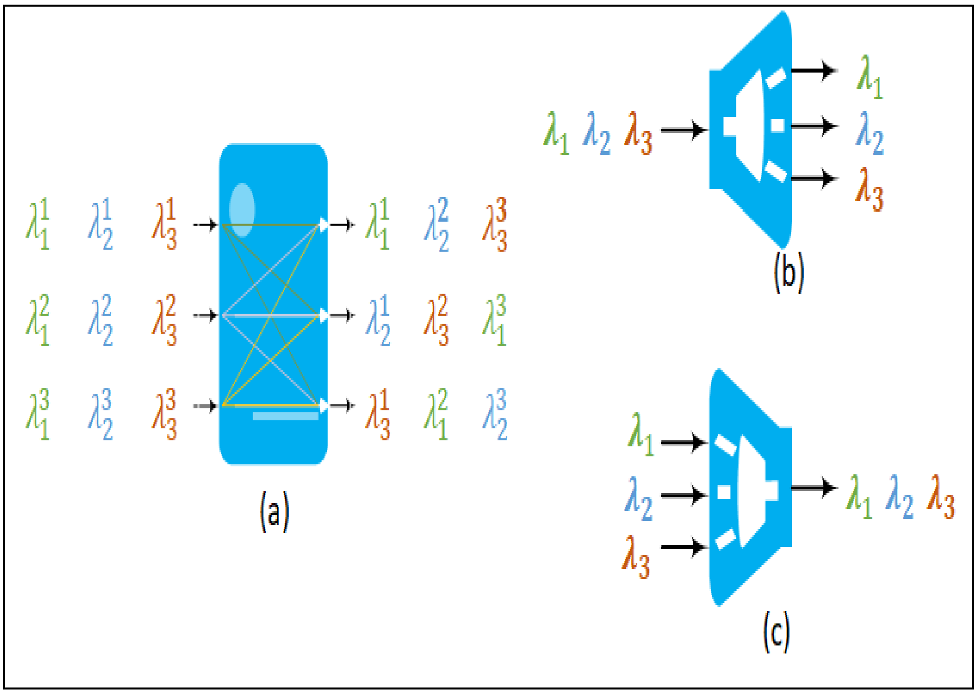

Figure 2.3 (a) AWGR ($\boldsymbol{n}$**x**$\boldsymbol{n}$), (b) AWG (**1x**$\boldsymbol{n}$), and (c) AWG ($\boldsymbol{n}$**x1**).

2.2.1.2 Fibre Bragg Gratings

The term grating describes the process involving the interference between optical signals initiating from the same source but having different phase shifts. Fibre Bragg Gratings can be used as a de-multiplexer to separate wavelengths, and can also be used as multiplexer to combine the wavelengths in WDM communication systems [43] .

2.2.1.3 Coupler/splitter

A coupler/splitter is a device implemented in many applications to allow splitting or combining signals in fibre networks. Most PON devices (for instance, couplers) are reciprocal devices in their functions, meaning that when the input signals and output signals are reversed, the devices work exactly in the same way. However, in many systems, nonreciprocal devices, such as isolators, which are used at the optical amplifiers and lasers, are required to prevent reflection from going through one of the directions [43] .

2.2.2 PONs Multiplexing Techniques

In PONs, multiplexing is classified into three techniques**:**

1) **Time Division Multiplexing PON (TDM-PON):** TDM-PON uses two wavelength signals; one for uplink (i.e., from ONUs to OLT); and a different one for the downlink (i.e., from OLT to ONUs). Each wavelength signal is shared by multiple end-users, where each is allocated certain time slots. Therefore, the sources should be synchronised to a common clock scheme [44].
2) **Wavelength Division Multiplexing PON (WDM-PON):** In WDM-PON, each wavelength in a single fibre can carry a data stream and it can be allocated for a single end-user or group of end-users [44] . WDM-PON and TDM-PON, however, have some limitations, such as the limited wavelength scalability and low bandwidth utilisation [45]. To overcome these limitations, hybrid WDM-TDM designs have been proposed. In

these designs, wavelengths are assigned and shared by multiple end-users [45].

3) **Orthogonal Frequency Division Multiplexing PON (OFDM-PON):** OFDM-PON also uses two wavelengths; one for uplink; the other for the downlink where the available bandwidth is divided by overlapped sub channels that are shared by the multiple end users, which leads to a high spectral efficiency [46].

2.2.3 Software-Defined Networking (SDN) for PON Networks

Software-defined networking (SDN) is considered an optimal technology in controlling the network traffic by separating the control plane and the user plane in its switches, which can enhance the overall network performance [47]. The control plane carries the signalling traffic, while the user plane, also known as data plane or forwarding plane, carries the user traffic. Separating the control plane from the data plane results in improved mobility, scalability, and flexibility in the networks [48], [49]. Enabling SDN over PONs or optical networks in general is important to provide flexibility in wavelength routing and assignment. Moreover, there were several studies that investigated the effectivity of using SDN-PON in data centres. The results of these studies revealed that the SDN-PON is a promising technique to facilitate inter-server communication in date centres [50].

2.2.4 Energy-Efficient Networking using PONs

The features of energy efficient PON devices that have been used in access networks have driven researchers to design energy efficient data centre architectures in the cloud computing based on PON [51], [52]. The authors in [52] proposed an energy efficient hybrid approach that uses Ethernet switches for intra-rack communication (between servers located within the same racks) using an Ethernet top of the rack (ToR) electronic switch and a wavelength division multiplexing WDM PON for inter-rack communication (between servers located in the different racks) using AWGRs. Based on the performance evaluation results, the design reduced the power consumption by 10%, with a slight increase in the average packets arrival delay.

Five novel designs were proposed in the data centres [30], [53]–[55] to support connectivity inside data centres and to facilitate inter-rack communications (i.e., the communication between servers in different racks) and intra-rack communications (i.e., the communication between the servers within the rack). These designs also aim to provide high energy-efficiency as these designs use mostly PON devices.

One of the designs in [30] showed that PON (option 3) data centre networks based on AWGRs have the capability of reducing the power consumption by 85% in comparison to the Fat-Tree architecture and by 93% in comparison to the BCube architecture. The work in [30] optimised the wavelength assignment and routing of the PON architecture and observed significant reduction in the energy consumption and the cost compared to the electrical data centres.

Also, One of the designs (PON option 5) [54] replaced the high cost tuneable ONU equipment by low cost passive optical backplane for intra-rack communication and utilised relay servers that have direct connection to other racks for inter-rack communication. The proposed MILP model optimised the wavelength routing of inter-rack traffic with the objective of minimising the power consumption. The results showed that the proposed architecture reduced the power consumption by 69% compared to the three-tier conventional data centre architecture. The author in [1] proposed MILP models to evaluate the energy efficiency of a server-centric PON-based data centre architecture PON (option 5) compared to legacy electronic server-centric data centre networking architecture utilised in fog computing. The results showed that the server-centric PON-based architecture in fog computing reduces the power consumption by 67% compared to the electronic data centre architecture with equivalent performance.

Another novel design in [55] addressed the oversubscription issues that are faced when using WDM PON without modification. This design used two-tiers of AWGRs to create multiple routes for inter-rack communication. The results showed that with SDN controller, the power consumption can be reduced by up to 90% with typical average data rates in the range of 250-2500Mb/s compared to the decentralised design. The idea behind using an SDN controller is its ability to manage and coordinate the route of inter-rack communication based on the wavelength between the OLT and PON groups, and the active OLT line cards [55].

The aforementioned work in [30], [53]–[55] has facilitated the inter-rack communication and intra-rack communication in the cloud computing data centres with the objective of minimising the power consumption . In our work, we aim to facilitate the connectivity among different computing racks in fog computing data centres by proposing an energy efficient collaborative fog units over a PON architecture presented in chapter 3 to support the connectivity between distributed neighbouring fog units to facilitate inter-rack communication and intra-rack communication.

2.3 Cloud computing

The US National Institute of Standards and Technology has defined cloud computing as a paradigm that allows sharing of computational resources (e.g., server, storage, and application) [56], [57]. Cloud computing provides pools of resources that are capable of provisioning the services to multiple users. It allows users to access, configure, and create applications online [58]. Cloud computing aims to use distributed resources, pool them to reach high throughput and provide a massive computing capability to provision the users' needs without their knowledge of the physical locations of resources.

Cloud computing can be classified into three service models: (i) Software-as-a-Service (SaaS) that enables the end-user to utilise the supplier's application and operates on remote servers through end-users' web browsers, (ii) Platform-as-a-Service (PaaS) accessed by end-users to create applications by using different sets of programming languages that can control this application, (iii) Infrastructure-as-a-Service (IaaS) which provisions clients with processors, networks, storage, and operating systems that the clients can deploy, manage, and run with different arbitrary software, including applications and operating systems. IaaS is also called Hardware-as-a-Service (HaaS) [56], [57].

Cloud computing is composed of four basic deployment models: Private cloud, public cloud, community cloud, and hybrid cloud. Private clouds were designed for exclusive single use by business organisations or companies containing multiple users. Public clouds were designed for open use by the public, while community clouds were designed for specific clients from several organisations or companies that share the same missions or the same policies. Finally, hybrid clouds were designed to use a mixture of two or more deployment models [56], [57].

2.4 Data Centres

The continuous growth in demand for data intensive applications has led to enhancing data centre networking architectures to be energy efficient with scalable computing and storage resources. Traditional data centre architectures, as shown in Figure 2.4, are usually composed of switches and routers in two or three layers, namely, an access layer, an aggregation layer, and a core layer. The three layers are in charge of managing the traffic going in and out the data centre [59]. However, the traditional data centre architectures cannot keep up with the growth in the traffic which has driven the industry to work on modifying the data centre architectures. Mainly, the architecture of data centres can be classified into three types: the electrical data centre, the optical data centre, and the hybrid electrical-optical data centre.

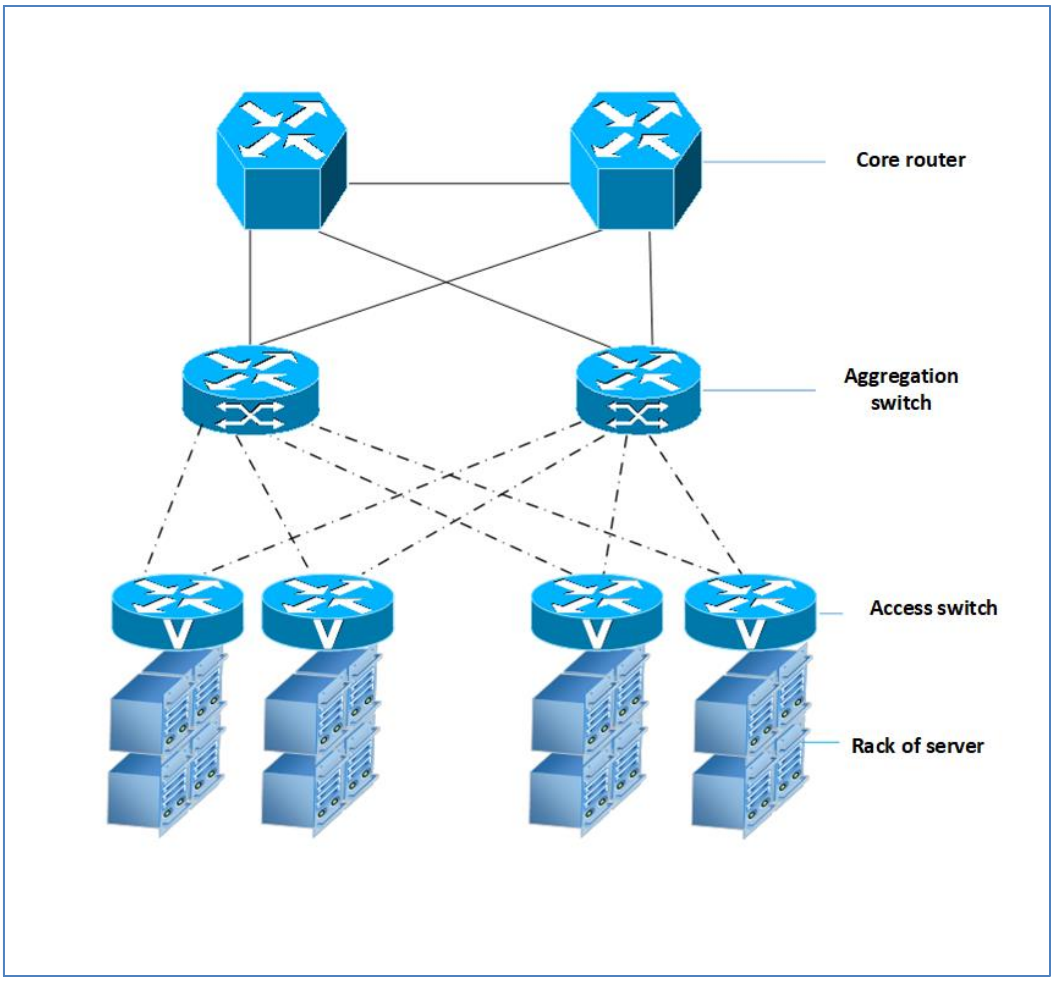

Figure 2.4 The traditional data centre.

2.4.1 Electronic Data centre

Based on where the interconnection intelligance is placed, electronic data centres architecture can be roughly classified as two types: switch-centric and server-centric.

2.4.1.1 Switch-Centric Architecture

This is a type of data centre architecture that uses the switches as the major component for data centres' routing and interconnection. In this architecture, the switches are the responsible nodes for packet forwarding. The switch-centric architecture can be expanded by increasing the number of switches. The common examples of switch-centric data centres include the Fat-tree [60], Portland [61], VL2 [59], and spine and leaf architecture [62]. These examples of switch-centric data centres are designrd to overcome the challenges that were present in the traditional data centre, such as the power consumption, the oversubscriptions ratio, agility and load balancing [59].

2.4.1.2 Server-Centric Architecture

This is a type of data centre architecture that uses servers that have a network interface card (NIC) to forward packets and perform routing activity. In this architecture, servers are considered not only as the end hosts, but also as relay nodes that forward traffic to each other. The interconnection intelligence in this architecture is placed in the server, in addition to the switches, to make a rational decision in the communication. Common examples of server-centric architecture are BCube, Ficonn, and DCell [63]. The server-centric architecture is designed to avoid the existence of a single point of failure as well as to support all types of traffic at high capacity, which is important for intensive computing applications that require low delay [59].

2.4.2 Hybrid Data Centre Architectures

Hybrid data centre architectures are proposed to utilise the high-capacity fibres and the electrical switches. Combining the optical network advantages, such as high bandwidth, low latency, and low power consumption, with electrical network advantages, such as low-cost switches, in one architecture, is the underlying reason behind proposing this architecture. Helios and c-Through are the best known examples of Hybrid optical-electrical data centre architectures [59].

2.4.3 Optical Data Centre Architecture

Optical Components are the optimal solution to provide high capacity, low power consumption, and low latency data centre architecture. Optical data centre architecture contains active or passive optical devices responsible for switching, routing, and interconnecting, such as Optical Amplifiers (used as optical switches), AWGRs, and Couplers and Splitters [59].

2.4.4 Traffic Patterns in Data centre

To improve the data centre architecture, the traffic characteristics should be taken into consideration. Traffic in data centres depends on the type of applications. For instance, flows generated just by the browsers search queries, are commonly smaller than some applications that require more computing. Some of these applications are regarded as delay-sensitive applications, while others demand more capacity for data transfer between multiple servers that might be in the same cluster or in different ones [64]. The traffic in data centres can be classified into two types: East-West traffic and the South-North traffic [64].

2.4.4.1 The East-West Traffic

East-West traffic refers to the traffic that stays within the data centre to transfer the data packets from one server to another server, also known by the term server-to-server traffic, depicted horizontally to illustrate the traffic that stays within the data centre. Typically, some software layers for some applications might lie in multiple virtual machines on multiple physical servers. Therefore, the virtual machines are one of the underlying reasons behind the increase in east west traffic beside storage and replications. The conventional data centres' architectures are not well-designed to deal with this kind of traffic but on the other hand, the data centre architectures developed in this thesis overcome this issue. For example, the Spine and leaf architecture is capable of managing the traffic by relying on the SDN control [64]. The East-West traffic can be classified into one-to-one, one-to-many, one-to-all, and all-to-all traffic patterns [65]. On the other hand, there are other classifications for East-West traffic based on the location of the server. The flows in the data centre can be categorised as intra-rack communication and inter-rack communication. Intra-rack communication flow is the flow when the source and the destination are within the same rack. Inter-rack communication flow is the flow when the source and the destination are in different racks.

2.4.4.2 The South-North Traffic

The South-North traffic refers to the traffic that transfers from the data centre to the outside world, known also as client-server traffic. South-North traffic is typically depicted vertically, to demonstrate the fact that the traffic is coming into or out of the data centre. Explanatorily, the South-North traffic is the client-server traffic that occurs between end users and the servers that host the user application in the data centre [64].

2.5 Fog Computing

Fog computing, also known as edge computing, represents the intermediate tier between conventional cloud computing and the user device, as shown in Figure 2.5. It provides the real time responses required by delay-sensitive applications [4]. Edge computing consists of three computing implementations known as, Mobile Edge Computing (MEC), Fog Computing and Cloudlet Computing [4]. MEC can store and process data within the Radio Access Network (RAN) in a base station by deploying intermediate nodes. The servers of MEC are in charge of providing real time information on their networks, including the capacities and loads. These servers also provide information to users, including network information and the user's location [4]. Cloudlet Computing relies on specific devices that have the same capabilities of data centres and are placed close to users. Cloudlet Computing can be considered as a “data centre in a box“ and is able to provide resources to users over a Wireless Local Area Network (WLAN) [4]–[6], [66]. Fog Computing is designed as an intermediate virtualised layer based on a decentralised architecture between the devices and conventional cloud computing. It utilises many nodes placed close to end-users but distributed geographically to provide computing, storing, and processing data to provide the real time interaction required by some applications, such as augmented reality applications. In addition, it also supports mobility by means of location awareness that allows the distributed fog nodes inferring their location and tracking end user devices [4]–[6], [66].

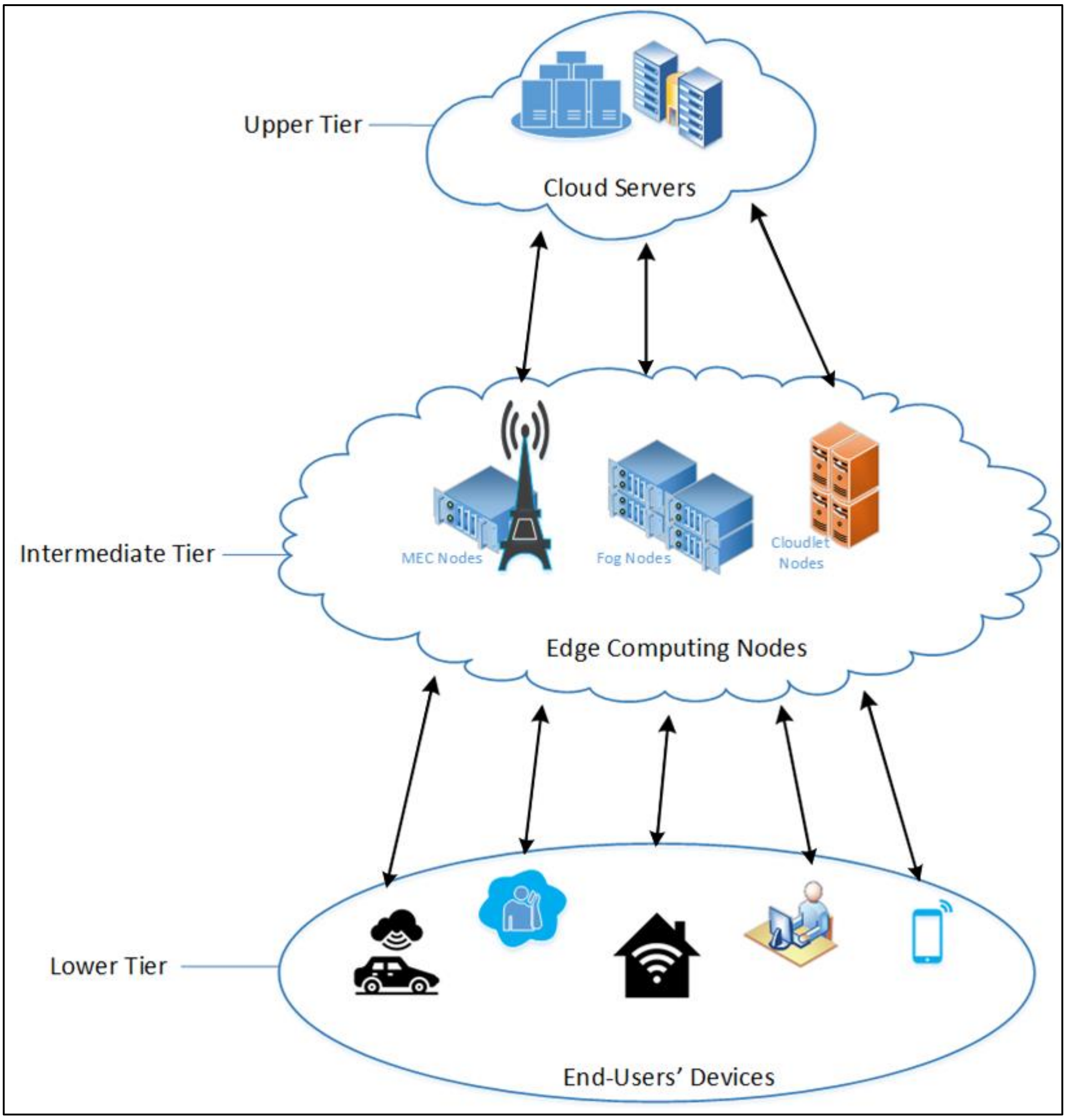

Figure 2.5 Edge Computing Architecture.

The Open Fog Consortium defined fog computing in [67] as a paradigm that uses distrusted units close to the end-users with computation capabilities, to meet the user demands [67]. Fog Computing is considered as a complementary element and not as a replacement for conventional cloud computing as the fog computing nodes have less computing and storage capacity compared to the cloud nodes [66].

2.5.1 Fog Computing Architectures

Because fog computing can provide lower latency and lower power consumption compared to cloud computing, designing and optimising computing architectures with fog computing is becoming a significant research area. Most of proposed architectures have used the essential three layers structure where the layers are the end-user layer which consists of user devices, fog layer that includes fog nodes (e.g., Router, Gateway, Switchers, Access Point, Base stations, Specific Fog servers), and the cloud layer that includes the conventional nodes of cloud computing as shown in Figure 2.5 [68]. The Open Fog Consortium refers to the infrastructure of fog computing as Fog-as-a-Service (FaaS), which consist of "IaaS, PaaS, and SaaS" [67].

2.5.2 Characteristic and Challenges of Fog Computing

The goals behind designing a fog computing system consist of:

1) Reduced latency, which is an essential goal to provision the users' applications that require low latency.
2) High efficiency, which is providing efficient resource utilisation and high energy efficiency since some of nodes have limited computing resources and power sources.
3) Generality, which aims to use the application programming interfaces (APIs) to cover different applications layer and end-users' services due to the fact that the fog nodes and user devices are heterogeneous [5].

With the services of fog computing, the new generation of applications that requires real time response, will be processed and stored at the edge of networks, while traditional applications that are not latency-sensitive can be processed and stored at the cloud computing layer [66] . However, there have been some challenges that encountered fog computing including:

1) The selection of the type of virtualisation technique, as the performance of a node depends on the chosen type of virtualisation technique.
2) Data aggregation can cause delay if it is uncompleted before the start of date processing.
3) And the optimisation of resources provisioning is challenging since some resources are limited, so fog computing is in need of optimal ways to overcome this challenges [5].

2.5.3 Energy-efficiency in Fog Computing

Fog computing offer solutions to the challenges experienced in cloud computing with the massive growth in data traffic. In comparison to cloud computing, fog computing has three features: (i) carrying out data storage near or at the end users location instead of placing them only in faraway data centre; (ii) placing control and computing functions near end users instead of faraway cloud data centres; and (iii) networking and communication occurs at or near the end users instead of through core networks [69]. The above three features significantly enable low latency and obtain real time interactions that are required in delay-sensitive applications.

Moreover, power saving is considered one of the substantial characteristics that fog computing aimed to provide since its resources are places close to the end-users [70]-[71]. The authors in [70] proposed a fog computing architecture and tested its performance in the case of serving delay-sensitive applications such

IoT applications. The results clearly show that for a system with delay-sensitive applications, it is preferable to place the data processing in fog computing rather than cloud computing to reduce latency and power consumption. Unlike the work in [70], in our work, we aim to serve intensive demand of delay sensitive application by proposing collaborative fog computing over PON capable of borrowing data processing from neighbouring fog units to serve intensive demand .

Furthermore, the authors in [71] investigated the power consumption in fog computing using distributed servers namely Nano Data Centres capable of hosting and distributing content to users in a peer-to-peer mode. To study the power consumption in Nano data centres, they proposed and used two power consumptions models: a time-based model for unshared network equipment, and a flow-based model for shared network equipment, such as routers and switches. The results in [71] showed the reasons behind consuming less power by the decentralised servers compared to centralised servers, such as the type of access networks linked to fog computing, fog server’s time utilisation (proportion of the idle times to active times), and the type of applications operating on fog computing. The results indicated that the Nano data centres can operate as a complement to centralised servers to serve certain delay-sensitive applications, most of which require real-time response. Also, off-loading the delay-sensitive application from centralised servers to decentralised servers has led to energy savings.

2.6 Virtualisation in cloud and fog Computing.

Virtualisation, which is a promising technique for enhancing the scalability and the efficiency of data centres, has been proposed for cloud and fog computing environments to realise energy-efficient resource allocation by consolidating the workloads in few servers. This is achieved by running multiple VMs that use different applications in a single physical machine (e.g., server). Each of which has its allocated CPU, memory, and storage capacities that are isolated from other VMs while sharing the same physical machine. Therefore, the main advantage of virtualisation towards energy efficient computing systems is to allow multiple heterogeneous virtual entities, each running a different application serving end-users, to coexist in a smaller number of activated physical machines [25]. Furthermore, virtualisation generates several advantages beside energy efficiency. First, VMs migration among different hardware system enhances the service availability and load balancing. Second, the existence of different operating systems on the same physical machine (each running in an isolated VM), and the optimisation of resources utilisation used in computing environments reduces the resources used and hence, the costs [72]. Virtualisation in fog and cloud systems is typically orchestrated by a VM monitor (VMM), also known as a hypervisor, which is a software to create and run one or multiple VMs in a single physical machine. It also has the authorisation to control all the VMs' operating system and the server resources.

Placing VM requests by attempting to locate the appropriate physical machine to host the VMs has a critical influence on the efficiency of the computing system's performance, its power consumption, and latency. The exponential increase in demands in both cloud and fog computing imposed limits on computing nodes such as exceeding the bandwidth capacity, the CPU capacity and the memory capacity [41]. Additionally, inter-VM traffic should be taken into consideration since it has a critical influence on networking power consumption [25]. Therefore, an optimal VMs placement approach requires an appropriate consolidation of the VMs that frequently communicate with each other.

Several recent papers have investigated the energy efficiency of resource allocation by optimising the VMs placement in the cloud computing system [25], [73]. In [25], the influence of inter-VM communication on power consumption in the cloud data centres was investigated. The developed MILP model focused on the cooperation and synchronisation between VM pairs to optimise the energy efficiency of cloud computing. The results show a substantial increase in power consumption in cases that do not consider the inter-VMs traffic in the optimisation. In [73], VMs placement has been investigated to achieve energy-efficient cloud data centre. The result showed a substantial impact of inter-VM traffic in the data centre on the power consumption.

The works in [25], [73] have investigated the impact of inter-VMs traffic when placing VMs in cloud computing with the objective of minimising the power consumption. In our work, we developed a MILP model, in chapter 4, to optimise the VMs placement in the proposed collaborative fog units' architecture with the objective of minimising the total power consumption while taking into the consideration the inter-VMs traffic.

In data centre environments, the traffic between VMs placed in different servers can be considered an east-west traffic [23]. VMs might cooperate with other VMs in order to satisfy some application requests or they might be migrated or copied to a different server in order to guarantee synchronisation and also to provide service reliability [24]. The east-west traffic is expected to take over majority of the traffic and networking power consumption in data centres when compared to the south-north traffic [25]. Therefore, optimising the routing of the east-west traffic is highly desired to achieve energy-efficient resource allocation in fog computing.

2.7 User Mobility

User-Mobility models have been studied widely to enhance the performance of routing protocols in mobile networks. This means that the users' mobility plays a critical role in the networking and computing' performance. Mobility models are designed to describe the pattern of the mobile users' movements, as well as their current and future anticipated positions, their speed and time. Due to the critical role of user mobility in networking and computing performance, designing models that are capable of simulating real user movement patterns is crucial to determine the access network's and computing system's capabilities [74]–[76]. Several mobility models have been proposed for mobile networks, and different classifications of mobility models have been illustrated based on several aspects as detailed in [76]–[85].

In this section, we classify mobility models into three main categories, as shown in Figure 2.6, namely: individual-mobility models, group-mobility models, and vehicular-mobility models. Entity mobility models are designated to the nodes which are characterised by independent mobility, and do not rely on other nodes for their movements. On the other hand, group mobility models are designated to nodes that are characterised by dependent mobility, relying on the other nodes for their movements. Vehicular mobility models are designated to the mobility of high-speed nodes that have restricted movement patterns [76]–[85].

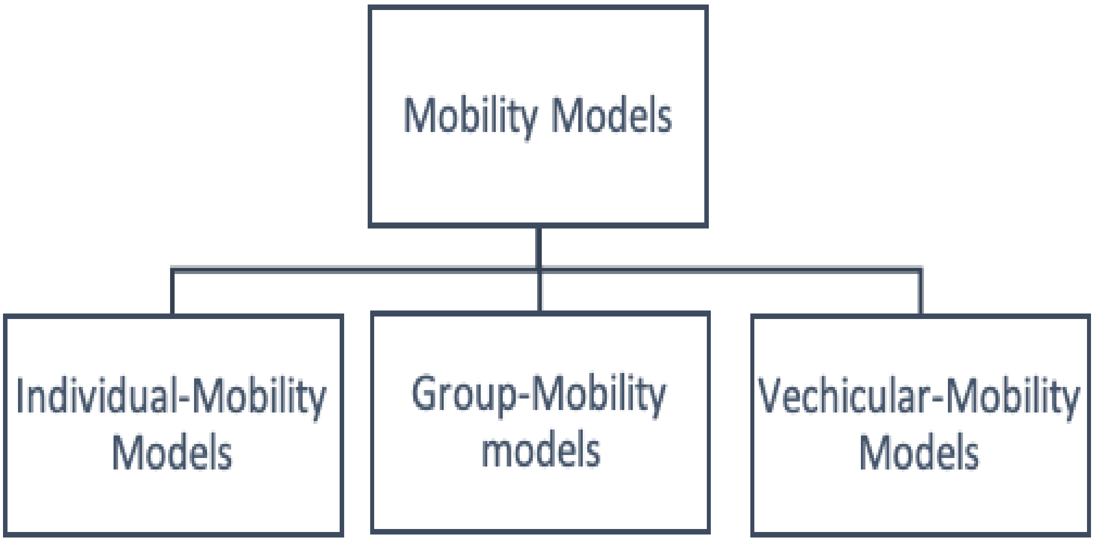

Figure 2.6 Classification of User-Mobility Models.

2.7.1 Individual-Mobility Model

Individual mobility models are independent, implying that each mobile node relies on itself for its movement. In this section, we have classified individual mobility models into three main classes: random mobility models, temporal or spatial dependency models, and geographic dependency models. Random mobility model denotes the unconstrained mobility of mobile nodes. Temporal or Spatial Dependency Models represent cases when the current movement of the mobile nodes depends on its movement history. Geographical Dependency Models are characterised by a restriction in the node movement to a particular area [80].

2.7.1.1 Random Mobility Model.

In this class, the dimensions of the mobility models, such the direction of the mobile nodes and the speed of the mobile nodes, are randomly selected. It is noteworthy that the random selection of directions and speeds is the reason that random mobility models are memoryless [80]. These mobility models are further divided into three models, random walk model, random waypoint model, and random direction model.

2.7.1.1.1 Random Walk Model

The random walk model was initially introduced by the Brownian motion [86], and was proposed to simulate the random movement of certain particles in a fluid. Due to the random movements of some mobile nodes, this mobility model was designed to simulate their random movements. It is a highly used model by researchers, as it can be used to model the impact of mobility on the networking and computing system under individual movements [87]. The random walk model uses the same behaviour as the random waypoint model in terms of random movements of the mobile nodes. However, the mobile nodes shift to new random locations with a random choice for the velocity and destination for each movement. The new velocity and direction are selected from ranges that have been pre-defined. This model is considered as a memoryless model because it does not retain the past velocity values and locations [76], [88].

2.7.1.1.2 Random Waypoint Model

The random waypoint model was initially proposed in [89]. One of this model features is that it provides a standard model to enhance the networking protocols, especially in networking system, due to its simplicity and availability [87]. This model uses the same random parameters used in the random walk model, such as random destination and random velocity, however, a pause time is included in the random waypoint model between the random changes in the destination or velocity [80]. The mobile nodes in the random waypoint model select a destination randomly and a velocity that is uniformly distributed between a min-velocity, and a max-velocity. It then moves at the chosen speed towards the selected destination. When it arrives at the selected destination, the node pauses for a stated period and then chooses a random velocity and destination again and continues with the process. Several flaws have however appeared in this model. For instance, the lack of providing a solid system that adjusts the pause time with the maximum velocity since both are considered significant factors in this model [91]. Moreover, the non-uniform change in the behaviour in choosing the spatial distribution for mobile nodes is considered to be a flaw in this model, known as non-uniform spatial distribution [80].

2.7.1.1.3 Random Direction Model

This model was introduced in [92] in an effort to eliminate the non-uniform spatial distribution that appears in the random waypoint model, as well as to provide a solution for the density wave issue. In this model, the mobile nodes select the velocity and direction randomly and uniformly which determines its movement until it reaches the borderline. After a pause, it then randomly and uniformly selects another direction on which to travel. This ensures that the nodes are distributed uniformly within the designated area [80].

2.8 Summary

In this chapter, we have provided a review of access network, metro network, and core network including the most important network elements. This chapter also discussed the use of PONs in access networks starting by giving an overview and then describing the architecture, PON devices, multiplexing techniques and SDN for PONs. Attention was then given to energy efficiency approaches in data centre network designs that were proposed to use PON. Cloud and fog computing systems were discussed in this chapter including the data centre architectures and energy-efficient networking approaches. Also, virtualisation was introduced in this chapter in addition to the VMs placements to review their role in achieving efficient use of cloud and fog resources in term of capacity and power consumption. Finally, the user mobility models in the access network were introduced and discussed.

Chapter 3 PON-Based Connectivity for Collaborative Fog Computing units

3.1 Introduction

As explained in Chapter 2, compared to the centralised cloud computing units in the core network, the distributed fog computing units in the access networks have limited processing capacity that can be under or over utilised depending on the instantaneous demands [1]–[7]. This chapter extends the available processing capacity for serving intensive demand of delay sensitive applications in the access network by proposing a collaborative fog computing architecture based on SDN-enabled PON. In terms of aiming for low latency and low power consumption, it is preferable to place the data processing of delay sensitive application in fog computing rather than cloud computing.

This chapter also presents a MILP model to optimise the connectivity among distributed fog computing units in the proposed architecture.

3.1 PON-Based Collaborative Fog Computing units

Fog computing architectures have gained increased attention in recent years. Several studies have proposed feasible solutions to optimise their energy efficiency and minimise their delay [70], [71]. However, there are still areas that require further attention such as resolving the challenges that are related to the limited capacity of the distributed fog computing units. Typically, fog computing units are equipped with limited resources that can be excessively demanded [93]. This chapter proposes an energy efficient collaborative fog computing architecture that can extend the capacity of distributed fog computing units by connecting them through an AWGR-based PON network that also eases moving the processing demands between connected neighbouring fog units according to the instantaneous needs and availability. Moving processing capability mostly occurs when one of the fog computing systems is fully occupied and there is no processing capacity to serve additional incoming demands. However, instead of moving the data to be processed in the cloud through a backbone network, the data is moved to a neighbouring fog computing unit through the PON network. This reduces the networking power consumption and satisfies the application requirements through fog computing. To achieve this, PONs can be utilised as an energy efficient technology capable of connecting the distributed fogs. First, the PON connects the computing units (i.e., servers) within a fog computing unit as intra-rack connection. Second, the PON can connect the servers within different fog computing units as inter rack connections. To clarify, intra-rack communication occurs when the source and the destination are in the same rack while inter-rack communication occurs when the source and the destination are in different racks [94].

PONs enable full connectivity between multiple distributed fog units while being energy efficient as they utilise passive components such as AWGRs and splitters. Compared to electronic switching data centre networks such as the spine and leaf architecture [30], [62], [95], PONs do not require powered components in the network fabric. Figure 3.1 shows a PON used to connect three neighbouring fog computing systems in the access network. This PON is composed of a powered OLT switch and three passive AWGRs to achieve full connectivity between the servers in the three fog units. In the spine and leaf electronic architecture, several powered leaf switches and spine switches are required. Figure 3.2 shows a spine and leaf-based fog computing system where the leaf switches are responsible for connecting the servers and storage, while the spine switches are responsible for connecting all access (leaf) switches [96]. On the other hand, in the proposed PON architecture, only components at the edge of the fabric (i.e., the OLT and several ONUs) are powered to connect the three neighbouring fog computing systems while fully connecting different computing units passively via the PON architecture. Therefore, the PON architecture is generally more energy-efficient and cost-effective compared to the spine and leaf architecture when connecting multiple fog computing systems.

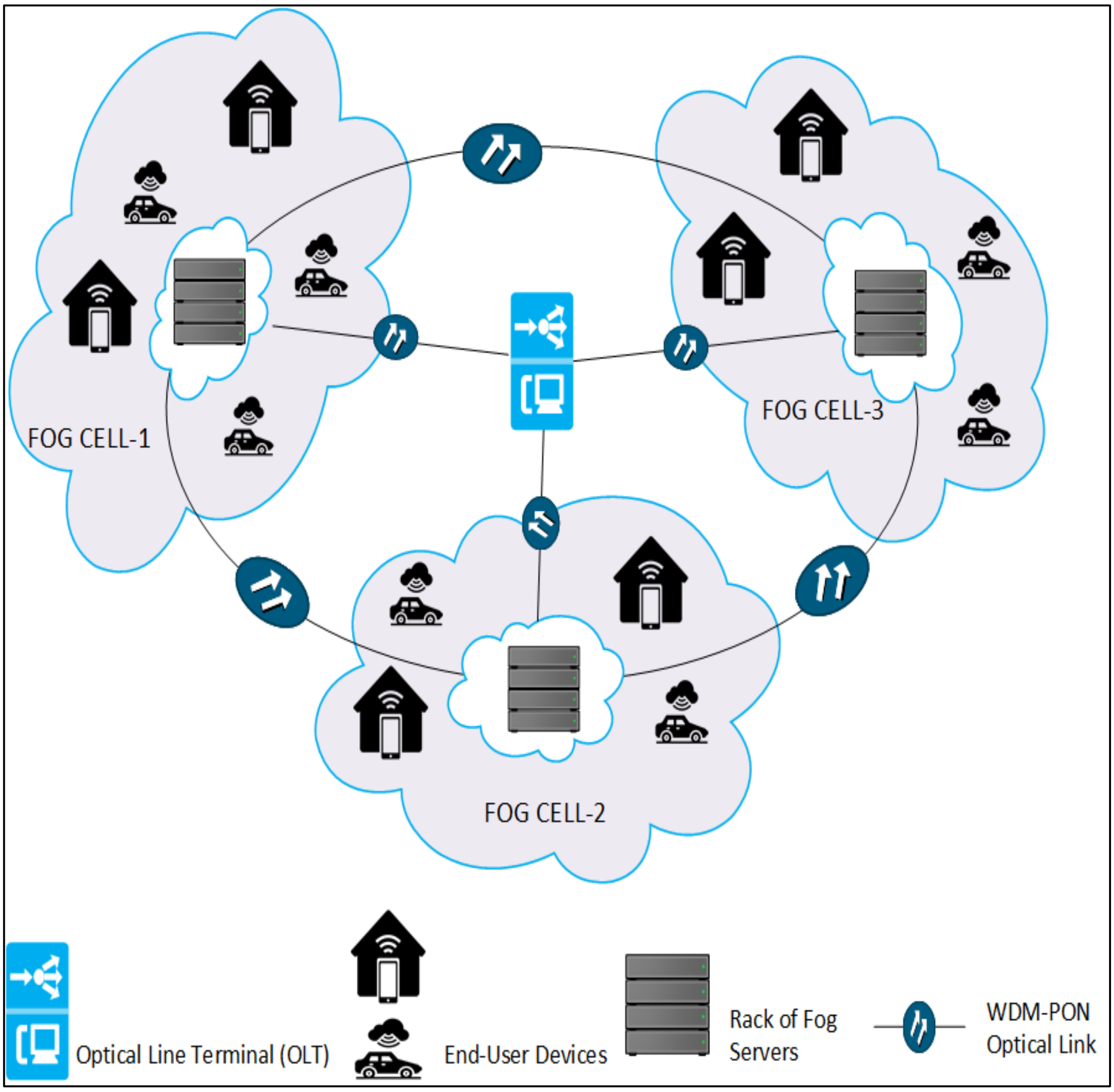

Figure 3.1 PON-based collaborative fog computing.

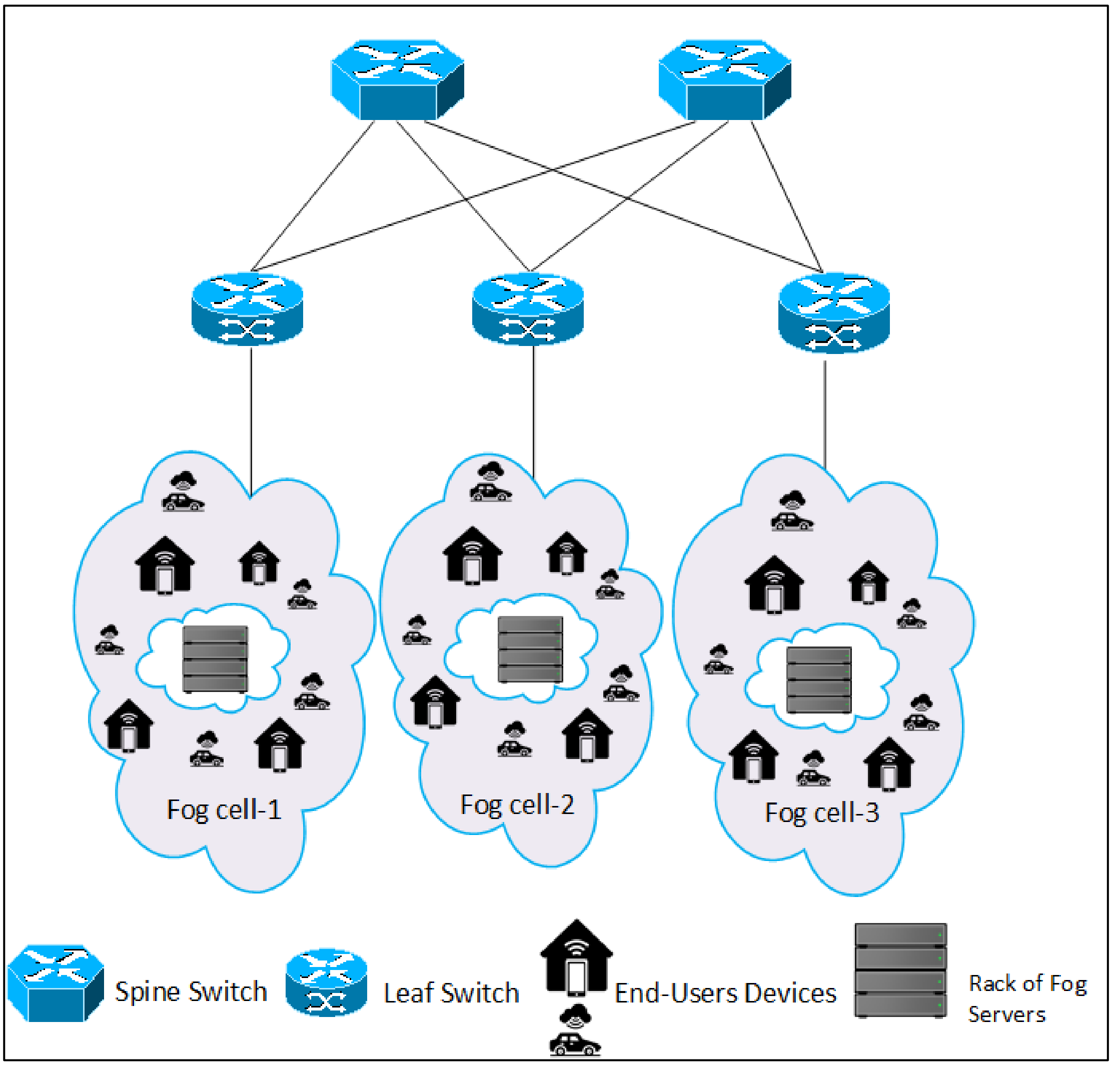

Figure 3.2 Spine and Leaf-based collaborative fog computing.

Several studies have demonstrated a reduction in the power consumption and delay in the cloud date centre by using a PON to facilitate inter-rack and intra-rack communication [30], [53], [54], [97]. The authors in [53] proposed five novel designs based on PON technology to facilitate the inter-rack and intra-rack communication between servers to provide high speed links and energy efficiency in cloud computing data centres.

Different from aforementioned work, we aim in this chapter to propose a collaborative fog architecture by connecting multiple fog units through PON architecture to facilitate the inter-fog and intra-fog communication to meet the delay sensitive application requirements in term of delay and power consumption. We proposed an AWGR-based PON connectivity for multiple fog units as shown in Figure 3.3. This creates collaborative fog computing environment where the AWGRs facilitate inter-fog computing communication if it becomes necessary to borrow data processing capability from a neighbouring cell (i.e., fog computing unit). Moreover, SDN-enabled PON is a promising technique that can be used to facilitate inter-server communication (i.e. servers in different racks) or intra-server communication (i.e. between the servers within the rack) in PON-based data centres [50] . We consider utilising an SDN controller to manage the routing and wavelength assignments for inter-rack communication as will be described in the following section.

3.2 Collaborative Fog Computing units based on the SDN-PON Architecture

We describe in this section the fog commuting units of the collaborative fog computing architecture. As shown in Figure 3.3, each fog unit, also known as a fog cell, consists of two racks of servers, where each rack is also known as a PON group, and an AWGR. In Figure 3.3, the three fog cells are interconnected by three intermediate AWGRs.

Each PON group contains one rack capable of hosting 16 servers due to the small space of the racks in fog computing environments [99]. Each server is connected to a wavelength tuneable ONU for the purpose of tuning to the appropriate assigned wavelength. The AWGRs achieve connectivity between the PON groups located in different PON cells and between the PON groups and the SDN-enabled OLT (SD-OLT). To facilitate inter-cell communication and to achieve full connectivity between the PON cells, as shown in Figure 3.3, each

AWGR should be connected to all other intermediate AWGRs located in different PON cells. In addition, each AWGR should be connected with the centralised SD-OLT. This will enable servers to send request massages via the AWGRs to the SDN controller, to connect with servers in other PON groups and to receive the wavelength tuning instructions. The SDN-enabled OLT is connected with an SDN controller to receive requests and send instructions relating to the routing and wavelength assignment and tuning and to provide information about the collaborative fog units and the status of servers.

The servers in the racks in this architecture are responsible for any processing required in the fog computing layer. Each server in this architecture is equipped with a tuneable ONU device [30] to terminate the AWGR-based PON at the servers. The main function of the ONU attached to a server is to receive the traffic destined to this server and to send the traffic destined to other servers (in case of VM migration as we will study in Chapter 6) or to the OLT. The tuning of the transmit and receive wavelengths in this architecture is controlled by the SDN controller. The servers are assumed to have on-off power profile. When the servers are switched off, the equipped ONUs are also switched off for power saving [30].

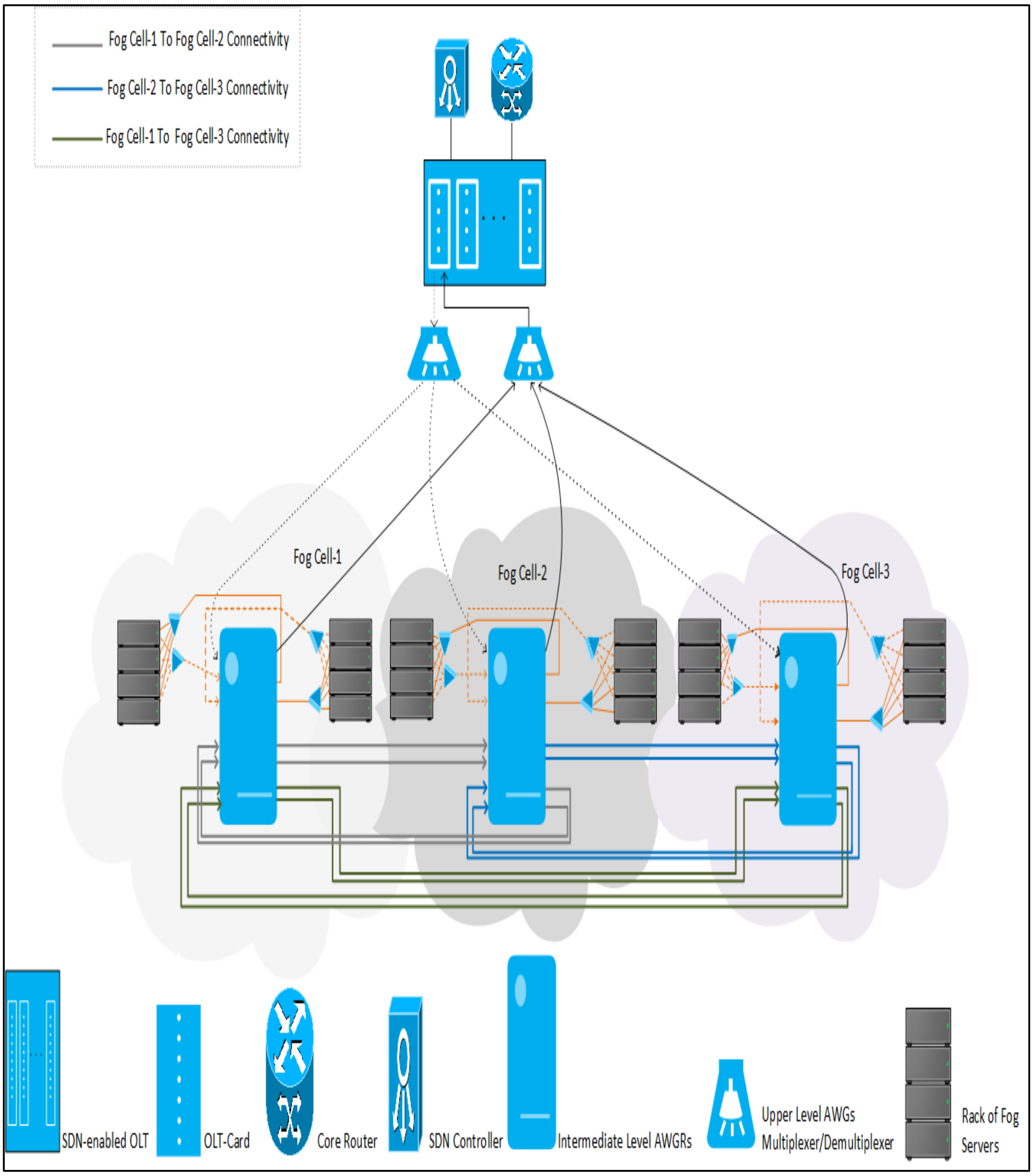

Figure 3.3 Collaborative fog computing cells based on PON connectivity.

In the proposed architecture, as shown in Figure 3.3, the connection between the SDN-enabled OLT and PON groups is given by $1xn$ AWG in the downstream links, and $nx1$ AWG in the upstream links, while the connection between different PON group is given by three nxn AWGRs.

Intra-communication between servers located within the same PON group (i.e., rack) occurs passively via fibre Bragg grating or a star reflector as in [41], both of which can be used to reflect particular wavelengths assigned to the servers within same PON group while passing the others [100]. Inter-PON group communication in the same or different PON cell (i.e., in different fog processing unit) occurs via the OLT switch or directly through the intermediate AWGRs. To achieve this, multiple links between each set of two AWGRs are used to achieve full connectivity, as shown in Figure 3.3. The ability to avoid the OLT switch for inter-communication between the PON groups is crucial to reduce the delay because the OLT introduces additional queueing delays as it handles the requests of all the cells. The SDN-enabled OLT manages the inter-communication between the PON groups, so a server in any PON cell should first communicate with the SDN-enabled OLT, using the appropriate assigned wavelength, to send a message requesting communication with a server in any cell. The OLT sends, via appropriate wavelengths, control messages to both servers to instruct them on the wavelength tuning. Moreover, the number of wavelengths used for inter-communication between servers should be equal to $PON\ \ groups + OLT - 1$ if the nodes do not connect to themselves through the intermediate AWGRs. and otherwise, it should be equal to $PON\ \ groups + OLT$. In this work, we consider that each node (i.e., each PON group) does not use the intermediate AWGRs for intra rack communication and instead we utilise fibre Bragg grating or a star reflector for intra-rack communication. Thus, the number of wavelengths used for inter-communication between servers equal $PON\ \ groups + OLT - 1$.

It can be assumed that the distances between the SDN-enabled OLT and the PON cells do not exceed 20 km, as it is the typical reach for a PON without amplification [101]. The OLT chassis typically hosts up to 18 cards, 2 of which are reserved for the switching matrix [102] . Each card can contain 16 ports, where each port has a split ratio of up to 128. Hence, one port can serve up to 128 servers and one card can serve up to 2048 servers [102].

3.3 The MILP Model for the Connectivity

We develop a MILP model to maximise the connectivity through the AWGRs between the fog computing units in the proposed fog computing architecture.

The parameters for the MILP model are as follows:

N	Set of all nodes (i.e., the PON groups, all input and output ports of intermediate AWGRs and AWGs, and the SD-OLT).
N_m	Set of all the neighbour nodes of node $m \in N$.
A	Set of intermediate AWGRs.
B	Set of upper-level AWGs.
P	Set of PON groups in all PON cells and the SD-OLT.
I_a	Set of input ports of intermediate AWGR $a, a \in A$.
O_a	Set of output ports of intermediate AWGR$a, a \in A$.
I_b	Set of input ports of upper-level AWG $b, b \in B$..

O_b Set of output ports of upper-level AWG $b, b \in B$.

W Set of wavelengths.

The variables for the MILP model are as follows:

λ_{sd}^{i} A binary variable that is equal to 1 (λ_{sd}^{i}= 1) if wavelength i is used to connect PON group s with PON group d; otherwise, it is equal to zero (λ_{sd}^{i} = 0), $s, d \in P,\ i \in W$.

λ_{sd}^{imn} A binary variable that is equal to 1 ($\lambda_{sd}^{imn} = 1$) if wavelength i is used to connect PON group at s with PON group d through link (m, n); otherwise it is equal to zero, λ_{sd}^{imn} = 0, $s, d\ \in P,\ m \in N, n\ \in N_m, i \in W$.

The MILP model is defined as follows:

The Objective: Maximise the AWGR connections established through the AWGR to connect the PON groups to each other and to the SDN-enabled OLT.

$$max \sum_{s \in P} \sum_{\substack{d \in P \\ s \neq d}} \sum_{i \in W} \lambda_{sd}^{i} \qquad (3.1)$$

Subject to the following constraints:

$$\sum_{i \in W} \lambda_{sd}^{i} \leq 1 \tag{3.2}$$

$$\forall\ s, d\ \in P, s \neq d$$

Constraint (3.2) ensures a single wavelength is used to establish a connection between any two PON groups or a connection between a PON group and the SDN-enabled OLT.

$$\sum_{\substack{s \in P \\ s \neq d}} \lambda_{sd}^{i} \leq 1 \tag{3.3}$$

$$\forall\ d \in P, \forall\ \ i \in W$$

Constraint (3.3) ensures that each destination in P (i.e., a PON group or the SDN-enabled OLT) receives a unique wavelength from each source in P (i.e., a PON group or the SDN-enabled OLT).

$$\sum_{\substack{d \in P \\ s \neq d}} \lambda_{sd}^{i} \leq 1 \tag{3.4}$$

$$\forall\ s \in P, \forall\ i\ \in W$$

Constraint (3.4) ensures that each source node uses a unique wavelength, to connect to the desired destination.

$$\sum_{\substack{n \in N_m \\ m \neq n}} \lambda_{sd}^{imn} - \sum_{\substack{n \in N_m \\ m \neq n}} \lambda_{sd}^{inm} = \begin{cases} \lambda_{sd}^{i} & m = s \\ -\lambda_{sd}^{i} & m = d \\ 0 & otherwise \end{cases} \tag{3.5}$$

$$\forall\ s, d \in P, \forall m \in N\ \ \forall\ i\ \in W$$

Constraint (3.5) ensures that the flow conservation law is obeyed which guarantees that any flow that enters a node (except for the source and destination nodes) leaves it with the same amount of data using the same wavelength (no wavelength conversion is used) [103].

$$\sum_{s \in P} \sum_{\substack{d \in P \\ s \neq d}} \lambda_{sd}^{imn} \leq 1 \qquad (3.6)$$

$$\forall m \in N,\ \forall n \in N_m,\ \forall\ i\ \in W$$

Constraint (3.6) ensures that in each physical link a unique wavelength is used to establish a connection.

$$\sum_{i \in W} \lambda_{sd}^{inm} \leq 0 \qquad (3.7)$$

$$\forall\ s \in P,\ \forall\ d \in P, s \neq d\ ,\ \forall\ m \in I_A,\ \forall\ n \in O_A$$

Constraint (3.7) ensures the flow direction inside the intermediate AWGRs; the flow direction is only from the input ports to the output ports.

$$\sum_{s \in P} \sum_{\substack{d \in P \\ s \neq d}} \sum_{i \in W} \lambda_{sd}^{imn} \leq 1 \qquad (3.8)$$

$$\forall m \in I_A,\ \forall n \in O_A$$

Constraint (3.8) ensures the correct flow direction inside the intermediate AWGRs. Each input port should forward a single wavelength to an output port.

$$\sum_{i \in W} \lambda_{sd}^{inm} \leq 0 \quad (3.9)$$

$$\forall\ s \in P,\ \forall\ d \in P, s \neq d\ ,\ \forall\ m \in I_B,\ \forall\ n \in O_B$$

Constraint (3.9) ensures that the flow direction inside the upper-level AWGs is correct. The flow direction is only from the input ports to the output ports and is not in the opposite direction.

$$\sum_{s \in P} \sum_{\substack{d \in P \\ s \neq d}} \sum_{i \in W} \lambda_{sd}^{imn} \leq 1 \quad (3.10)$$

$$\forall\ m \in I_B, \forall\ n \in O_B$$

Constraint (3.10) ensures the correct flow direction inside the upper level AWGRs. The input port should forward a single wavelength to an output port.

$$\sum_{\substack{u \in P, n \in N_u \\ u \neq s}} \lambda_{sd}^{iun} \leq 0 \quad (3.11)$$

$$\forall\ s, d\ \in P, i \in W.$$

Constraint (3.11) is used to stop PON groups from forwarding the traffic of other PON groups and thus it reduces the number of intermediate points or hops needed between the source and destination.

3.4 Results and discussion

In this section, we present and discuss the connectivity optimisation MILP model results. Table 3.1 shows the optimal wavelength assignments for inter-communication between the fog computing units and OLT. The optimal wavelength assignments and routing through the intermediate and upper' levels AWGRs are shown in Figure 3.4.

Table 3.1 Routing map for inter-fog units' communication.

	PON Group-1	PON Group-2	PON Group-3	PON Group-4	PON Group-5	PON Group-6	OLT
PON Group-1		λ_3	λ_2	λ_5	λ_4	λ_1	λ_6
PON Group-2	λ_3		λ_1	λ_4	λ_2	λ_6	λ_5
PON Group-3	λ_2	λ_5		λ_1	λ_6	λ_3	λ_4
PON Group-4	λ_4	λ_1	λ_6		λ_5	λ_2	λ_3
PON Group-5	λ_1	λ_6	λ_5	λ_3		λ_4	λ_2
PON Group-6	λ_5	λ_2	λ_4	λ_6	λ_3		λ_1
OLT	λ_6	λ_4	λ_3	λ_2	λ_1	λ_5	

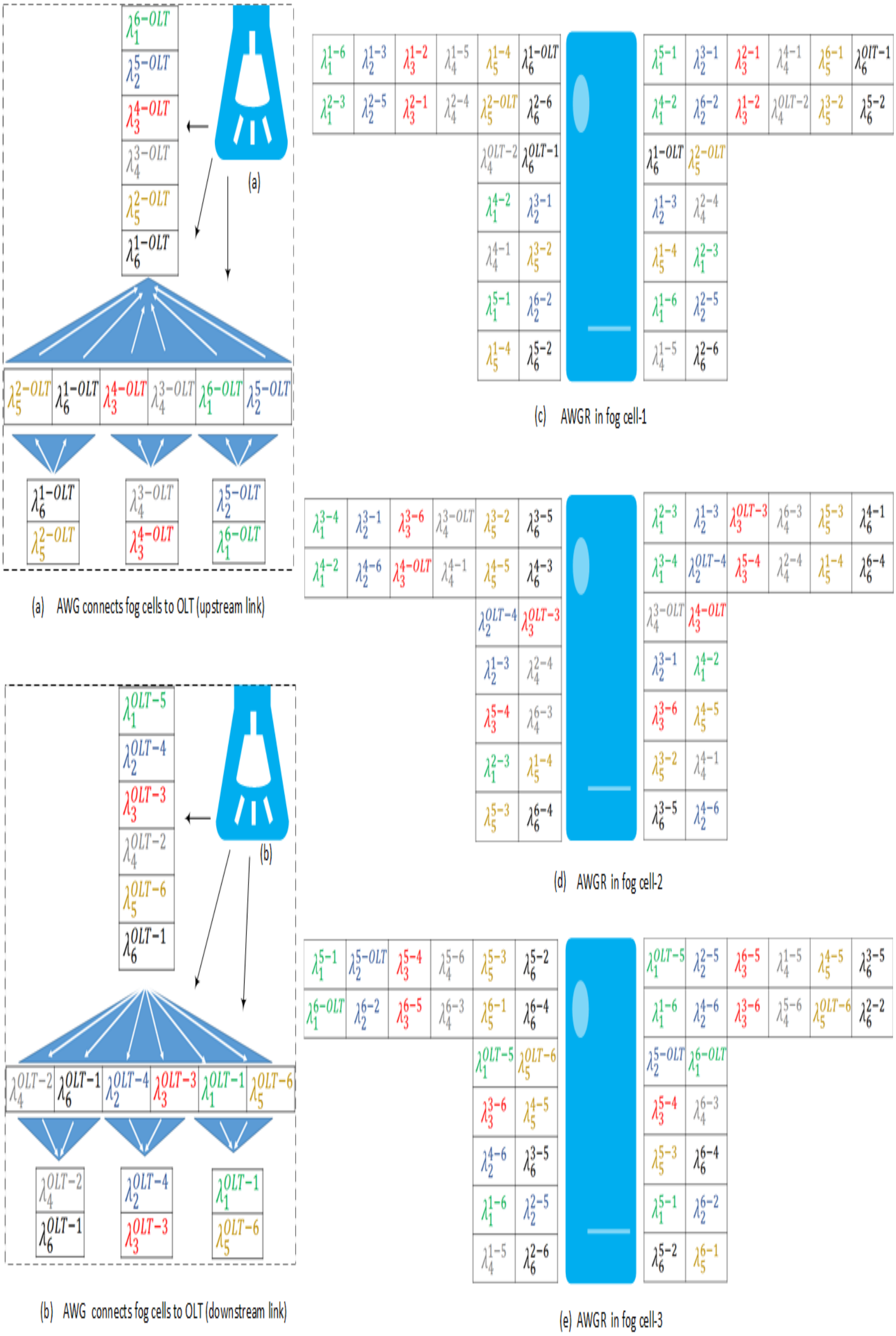

Figure 3.4 Wavelength Assignments and Routing.

The servers located in different PON groups can communicate with each other (i.e., inter-rack communication between the cells of the collaborative fog computing architecture) after gaining permission from the SDN-enabled OLT. For example, as illustrated in the routing map shown in Table 3.1, if a server in PON group 2 needs to communicate with a server in PON group 4, the process is as follows. First, the server in PON group 2 sends a request message (control message) to the SDN-enabled OLT using $\boldsymbol{\lambda}_5$ directed firstly through the intermediate AWGR in PON cell-1 from input port 2 to output port 3, as shown in Figure 3.4 (c). Then, $\boldsymbol{\lambda}_5$ passes through the upper layer AWG (in the upstream direction), as shown in Figure 3.4.(a) to the OLT.

When the SDN-enabled OLT authorises the communication, it sends a control message containing the wavelength assignment to the servers in PON group 2 and PON group 4 so that they can communicate with each other, using $\boldsymbol{\lambda}_4$ and $\boldsymbol{\lambda}_2$, respectively. $\boldsymbol{\lambda}_4$ and $\boldsymbol{\lambda}_2$ are then directed through the upper layer AWG (in the downstream direction), as shown in Figure 3.4 (b), then through the intermediate AWGRs in PON cell-1 and PON cell-2, as shown in Figure 3.4 (c) and (d), then to PON group 2 and 4, respectively. Based on the wavelength assignment sent by the SDN-enabled OLT, the two servers are able to communicate with each other by tuning their transceivers to $\boldsymbol{\lambda}_4$. This wavelength is routed firstly from the server located in PON group 2, which carries the data stream through the intermediate AWGR in PON cell-1 from input port 2 to output port 4. Then the data stream is directed through the intermediate AWGR in PON cell-2 from input port 4 to output port 1 to reach the desired destination, which is the server in PON group 4, as shown in Figure 3.4 (c) and (e). This process reduces the delay and power consumption because it avoids the queuing involved in processing the data stream in the SDN-enabled OLT.

3.5 Benchmarking the Power Consumption

This section compares the power consumption of the proposed fog computing connectivity against the power consumption of a spine and leaf architecture used to connect the fog computing units. In the spine and leaf architecture, all servers in the rack are connected to the leaf switches (Also known as Top-of-the-Rack (ToR) switch) and all leaf switches are connected with all the spine switches creating a full mesh topology [62]. For inter-rack communication, the data stream is routed from the server's leaf switch to one of the spine switches. The spine switch then directs the data stream to the destination server's leaf switch to reach the desired server [62]. The networking power consumption of leaf-spine architecture is [93]:

$$P_{T=}\ (P_S\, N_S) + (P_L N_L) + (P_{CS}\ \ N_{CS}) \qquad (3.11)$$

where P_S is the spine switch power consumption, N_S is the number of spine switches used in the architecture, P_L is the leaf switch's power consumption, N_L is the number of leaf switches used in the architecture, P_{CS} is the server transceiver's power consumption and N_{CS} is the number of transceivers (equal to the number of servers) used in the architecture.

Examples of the power consumption of the equipment used in leaf-spine architecture is shown in Table 3.2. This table also shows the power consumption values for the equipment that can be used in the proposed PON-based connectivity. Each PON cell in the proposed architecture comprises two PON groups. Each PON group consists of servers connected to a wavelength tuneable ONUs and are interconnected to a single OLT switch via the AWGR existing in that cell. The networking power consumption of the proposed architecture is:

$$P_{T=} (P_{LC}^{OLT} N_{LC}) + (P_{F}^{OLT}) + (P_{M}^{OLT}) + (P_{ONU} N_{CS}) + (P_{CS} N_{CS}) \qquad (3.12)$$

where P_{LC}^{OLT} is the OLT line card's power consumption, N_{LC} is the number of line cards used in the architecture, P_{F}^{OLT} is the OLT fan's power consumption, P_{M}^{OLT} is the OLT switching matrix's power consumption, P_{ONU} is the tuneable ONU's power consumption, P_{CS} is the server transceiver's power consumption, and N_{CS} is the number of servers used in the architecture. Please note that the tuneable ONUs are attached to the servers for inter-rack communication and the transceivers are attached to the servers for the intra rack communication through the FBGs or the star couplers.

Table 3.2 Power Consumption of networking Equipment.

Equipment	Power consumption
Cisco ME 4620 OLT, GPON line card [102].	90W
Cisco ME 4620 OLT, Chassis fan [102].	55W
Cisco ME 4620 OLT, Switching matrix [102].	180W
Tuneable ONU [104]	2.5W
Spine Switch, Cisco Nexus 9332C [96]	700W
Spine Switch, Cisco Nexus 9364C [96]	1245W
Leaf Switch [105]	475W
Server's Transceivers [106]	3W

The proposed design has lower power consumption compared to the spine and leaf architecture as shown in Figure 3.5. In the proposed architecture, the electronic switches are replaced by passive devices such as AWGRs, couplers and FBGs to reduce the power consumption. Using AWGRs to route traffic instead of electronic switches is the key to reducing power consumption due to the passive nature of AWGRs. The power consumption of the proposed architecture when using 96 servers, 128 servers and 2048 servers is reduced by 81%, 77% and 66%, respectively compared to the case when the same number of servers are considered in the spine and leaf architecture as shown in Figure 3.6. It is worth noting that we used Cisco Nexus 9332C as a spine switch to accommodate 96 servers and 128 servers and Cisco Nexus 9364C as a spine switch to accommodate 2048 servers.

As the number of servers increases, the power consumption saved by the proposed architecture is slightly reduced compared to spine and leaf architecture as shown in Figure 3.6. This is because the power consumption of the switches used to build the leaf and spine layers does not increase linearly as the number of ports increases. On the other hand, the power consumption of the proposed architecture increases linearly as the number of servers increases because the servers are equipped with tuneable ONUs. However, this power consumption is still less than that of the spine and leaf architecture for the fog computing units scale considered in this work (i.e., up to 2048 servers).

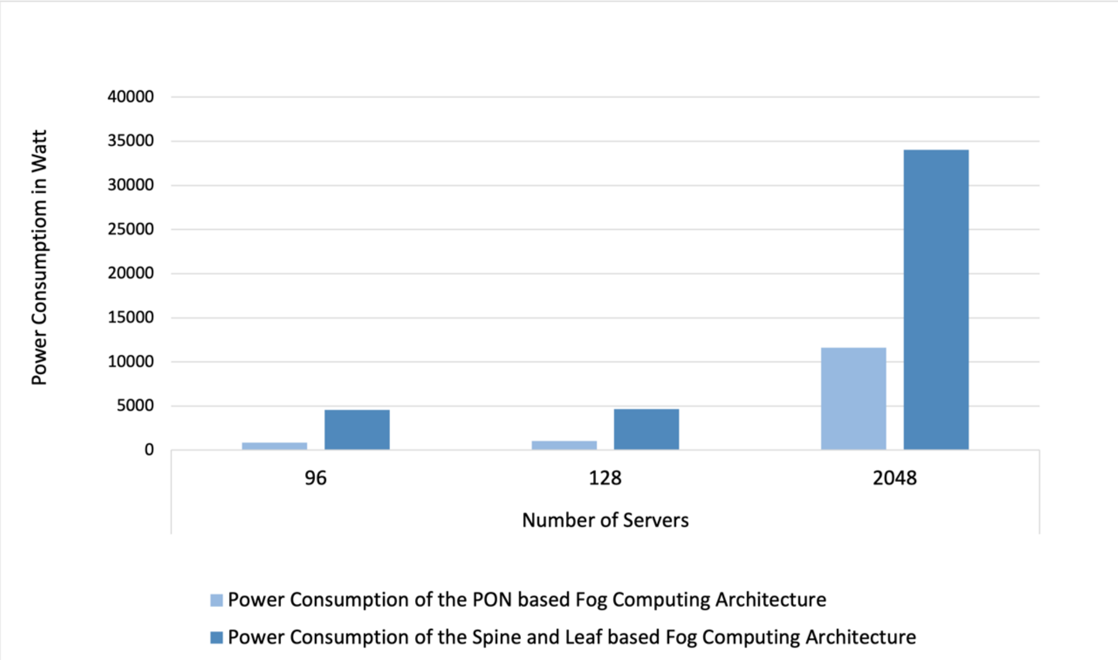

Figure 3.5 The power consumption of the proposed architecture vs spine and leaf architecture.

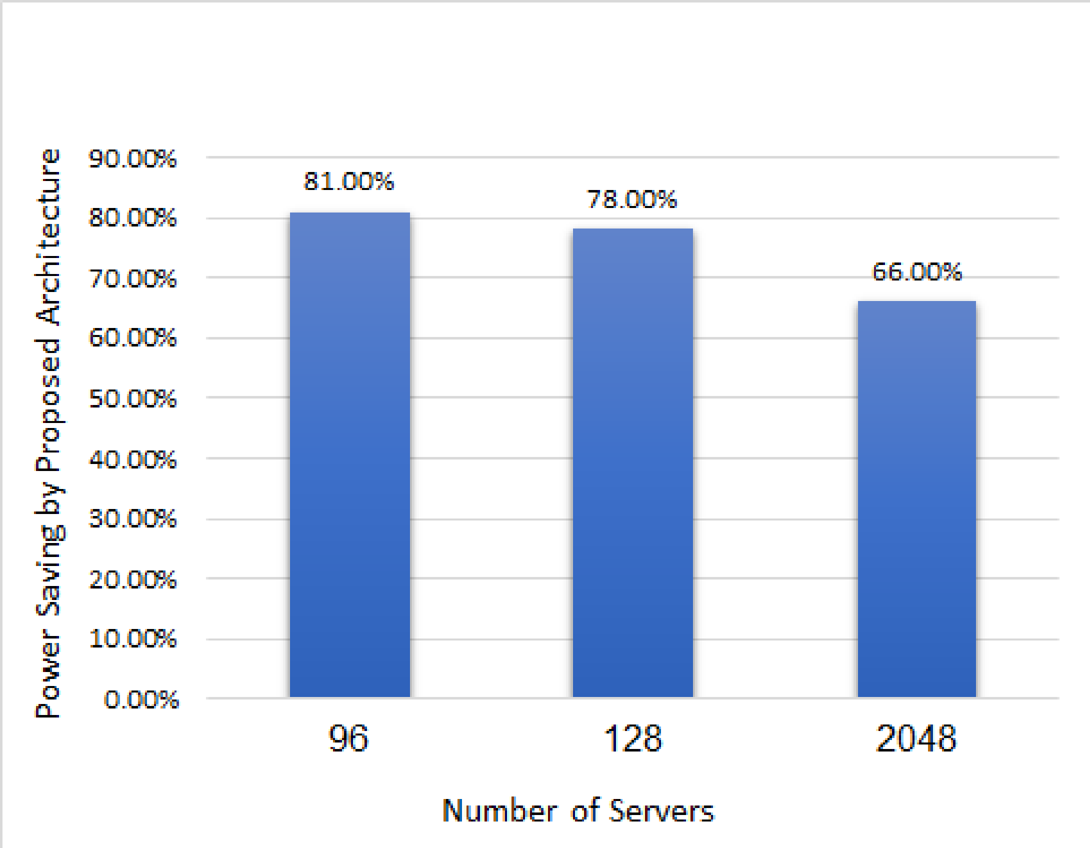

Figure 3.6 Power saving by the proposed architecture compared to spine and leaf.

3.6 Summary.

In this chapter, a PON architecture that relies on energy efficient PON components such as AWGRs, couplers and FBGs have been designed to connect distributed fog computing units. The inter-fog units communication is facilitated by optimising the interconnection of the AWGRs that exist in each PON cell. The power consumption of the proposed architecture accommodating 96, 128 and 2048 servers is lower by 81%, 77% and 66% respectively, compared to a spine and leaf architecture.

Chapter 4 Energy Efficient VM Placement in the Collaborative Fog Computing Architecture

4.1 Introduction

Virtualisation plays a significant role in achieving energy efficient resource allocation in the fog computing systems by consolidating diverse application requests into a fewer number of physical machines [107]. Therefore, virtualisation is widely used for resource allocation in the fog by slicing the resources of a single physical server to accommodate multiple VMs to achieve an energy efficient environment. The VMs are isolated from each other and each VM can use a part of the physical server resources according to the application need by being allocated its own CPU, memory, and bandwidth resources. Consequently, optimal resource utilisation and power saving by turning off unused physical machines can be achieved through virtualisation. However, some VMs might need to communicate with other VMs. Resulting in traffic traversing the network if VMs are placed in different servers. [23], [107].

In data centre environments, the inter-VMs traffic between VMs placed in different servers can be considered as an east-west traffic [23]. The east-west traffic is expected to account for the majority of the traffic and networking power consumption in data centres compared to the south-north traffic [25]. Therefore, optimising the routing of the east-west traffic is crucial to achieve an energy efficient resource allocation in fog computing environments.

Placing VMs requests by attempting to select the appropriate physical machines to host the VMs is crucial. Virtual machine placement has a critical influence on the efficiency of the computing system's performance, its power consumption and latency [41]. Additionally, inter-VM traffic should be taken into consideration since it has a critical influence on the networking power consumption [25].

The work in this chapter optimises VMs placement in the proposed collaborative fog computing units over PON architecture presented in chapter 3. We develop a MILP model for VM placement that minimises the power consumption. Also, this chapter investigates the impact of the volume of inter-VM traffic demand on VM placement in the proposed architecture. In addition, we propose a heuristic model for real-time energy efficient VM placement.

Note that the MILP model is developed to provide optimal results of VMs placement while considering the inter-VMs traffic by using mathematical programming model, while the heuristic model provides simplified algorithm that's comprises of simplified steps that can provide fast solution in real time implementation and hence it runs faster than MILP. The heuristic model could not guarantee the optimal results. Moreover, the heuristic is developed to verify and validate the results of the MILP model.

4.2 Related Work.

Several recent papers have investigated the energy efficiency of resource allocation by optimising the VM placement in computing systems [25], [73]. In [25], the influence of inter-VM communication on the power consumption was investigated. The developed MILP model considered the cooperation and synchronisation traffic between VM pairs to optimise the energy efficiency of cloud computing. The results show a substantial increase in the networking power consumption when not considering the inter-VM traffic in the optimisation. In [73], VM placement has been investigated to achieve energy efficiency in a PON based cloud data centre. The result showed a substantial impact of inter-VM traffic on the power consumption of data centres.

4.3 MILP Optimisation Model

In this section, we develop a MILP model to optimise the VM placement in the PON-based fog computing architecture shown in Figure 3.3 with three fog cells, each with two PON groups. This model optimises the placement of VMs in the fog servers under the objective of minimising the power consumption of the system while considering the capacity constraints of the physical machines and the networking equipment. In this work, we assume that the AWGR connections between the fog cells are sufficient to handle all required communication, and hence we ignored the modelling of the OLT and the consideration of its power consumption.

The sets, parameters, and variables used in the MILP model are as the following:

Sets:

S Set of servers.

PG Set of PON groups (i.e., racks).

S_g Set of servers within PON group $g, g \in PG$.

VM Set of VM requests.

Parameters:

I Idle power consumption of a server in Watts.

M Maximum power consumption of a server in Watts.

C CPU capacity of a server in Million instructions per second (MIPS).

R Memory capacity of a server in GB.

C_v CPU demand of VM request $v, v \in VM$ in MIPS.

R_v Memory demand of VM request $v, v \in VM$ in GB.

T_{if} The traffic demand between VM i and VM f, $i, f \in VM$ in Gbps.

PO Maximum Power Consumption of an ONU in Watt.

DO ONU data rate in Gbps.

W Capacity of WDM-PON links used to connect the PON groups.

Δ The maximum number of servers that are allowed to serve a VM.

L Large positive number.

O Defines as M- I, (The proportional power of servers, which is the difference between the Maximum power of a server and its idle power).

The variables:

A_s A_s = 1, if server $s \in S$ is activated, otherwise A_s = 0.

δ_s^i δ_s^i = 1, if request $i \in$ VM is processed by server s $\in$ S, otherwise δ_s^i= 0.

V_{if} V_{if} = 1, if requests i and f $\in VM$ are placed in the same server, otherwise $V_{if} = 0$.

U_s The uplink traffic for server s , $s \in S$.

D_s The downlink traffic for server $s, s \in S$.

N_s Number of VM served by server $s, s \in S$.

Q_{sd}^{if} Q_{sd}^{if} is the multiplication of two binary variables δ_s^i and δ_d^f,i.e., $Q_{sd}^{if} = \delta_s^i \, \delta_d^f$, where s and $d \in S$, and $s \neq d$. Q_{sd}^{if} is used to calculate the uplink and downlink traffic

B_s^{if} B_s^{if} is the multiplication of two binary variables δ_s^i and δ_s^f,i.g. $B_s^{if} = \delta_s^i \, \delta_s^f$, where $s \in S$ and $i, f \in VM$ B_s^{if} is used to identify the VMs placed in the same server.

TS_{sd} The total traffic between two servers s and d, $s, d \in S$.

P_s^i The processing resources used to serve VM i, $i \in VM$ in server $s, s \in S$.

The power consumption of the servers and the ONUs are as the following:

1. The power consumption of the fog servers (PC_S) is expressed as an idle power plus proportional power profile as [108]:

$$PC_S = \sum_{s \in S} \left(I \;\; A_s + \frac{O}{C} \sum_{i \in VM} P_s^i \right) \qquad (4.1)$$

where P_s^i is calculated as:

$$P_s^i = C_i \, \delta_s^i. \tag{4.2}$$

2. The power consumption of the ONUs attached to the servers (PC_{ONU}) [108] (These ONUs operate as transceivers as explained in Chapter 3), which are calculated based on a proportional power profile (no idle power):

$$PC_{ONU} = \frac{PO}{DO}\left(\sum_{s \in S} (U_s + D_s) \right). \tag{4.3}$$

The MILP model is defined as follows:

The Objective: Minimise the total power consumption of the fog units, including the fog servers and the ONUs attached with the fog servers.

$$\text{Min} \quad PC_S + PC_{ONU} \tag{4.4}$$

Subject to the following constraints:

$$U_s = \sum_{i \in VM} \sum_{\substack{f \in VM \\ i \neq f}} \sum_{d \in S} T_{if} \; Q_{sd}^{if} \tag{4.5}$$

$$\forall s \in S$$

$$D_s = \sum_{i \in VM} \sum_{\substack{f \in VM \\ i \neq f}} \sum_{s \in S} T_{if} \quad Q_{sd}^{if} \tag{4.6}$$

$$\forall\, d \in S$$

Constraints (4.5) and (4.6) are used to calculate the uplink and downlink traffic, respectively, for each server traffic that results due to the communication between two VMs placed in two different servers, where Q_{sd}^{if} is calculated by the following constraint.

$$Q_{sd}^{if} = \delta_s^i\, \delta_d^f \tag{4.7}$$

$$\forall\, s, d \in S\,, \forall\, i, f \in VM, i \neq f, and\ s \neq d$$

Constraints (4.7) is used to calculate the variable Q_{sd}^{if}, which consist of a multiplication of two variables δ_s^i , and δ_d^f which makes the model nonlinear. To linearise it, it is replaced by the following constraints (4.8, 4.9, and 4.10):

$$Q_{sd}^{if} \leq \delta_s^i \tag{4.8}$$

$$\forall\, s, d \in S\,, \forall\, i, f \in VM, i \neq f, and\ s \neq d$$

$$Q_{sd}^{if} \leq \delta_d^f \tag{4.9}$$

$$\forall\, s, d \in S\,, \forall\, i, f \in VM, i \neq f, and\ s \neq d$$

$$Q_{\ sd}^{\ if} \geq \delta_s^i + \delta_d^f - 1 \tag{4.10}$$

$$\forall\, s, d \in S\,, \forall\, i, f \in VM, i \neq f, and\ s \neq d$$

$$V_{if} = \sum_{s \in S} B_s^{if} \tag{4.11}$$

$$\forall\, i, f \in VM \text{ and } i \neq f$$

Constraint (4.11) is used to indicate whether two VMs are placed in the same server or not. The variable B_s^{if} is given as the multiplication of two variables δ_s^i, and δ_S^f , which makes this constraint nonlinear. Therefore, the three following constraints (4.12, 4.13, and 4.14) have been used to linearise the constraint (4.11).

$$B_s^{if} \leq \delta_s^i \tag{4.12}$$

$$\forall\, s \in S \text{ and } \forall\, i, f \in VM$$

$$B_s^{if} \leq \delta_s^f \tag{4.13}$$

$$\forall\, s \in S \text{ and } \forall\, i, f \in VM$$

$$B_s^{if} \geq \delta_s^i + \delta_s^f - 1 \tag{4.14}$$

$$\forall\, s \in S, \forall\, i, f \in VM \text{ and } i \neq f$$

$$\sum_{i \in VM} R_i\, \delta_s^i \leq R \tag{4.15}$$

$$\forall\, s \in S$$

Constraint (4.15) guarantees that the memory capacity of the VM requests assigned to server s, $s \in S$ does not exceed the memory capacity of the server.

$$\sum_{i \in VM} C_i\, \delta_s^i \leq C \tag{4.16}$$

$$\forall\, s \in S$$

Constraint (4.16) guarantees that the processing capacity of the VMs requests assigned to server $s, s \in S$ does not exceed its processing capacity.

$$U_s \leq DO \qquad (4.17)$$

$$\forall s \in S$$

$$D_s \leq DO \qquad (4.18)$$

$$\forall s \in S$$

Constraint (4.17) and (4.18) guarantee that the uplink traffic and downlink traffic passing through each server, respectively, does not exceed the data rate of the ONU attached with the fog servers.

$$\sum_{s \in S} \delta_s^i \leq \Delta \qquad (4.19)$$

$$\forall i \in VM$$

Constraint (4.19) guarantees that the number of servers that serve each VM request do not exceed the maximum allowed split of the VM.

$$N_s = \sum_{i \in VM} \delta_s^i \qquad (4.20)$$

$$\forall s \in S$$

Constraint (4.20) calculates the number of VM request that are assigned to server $s, s \in S$.

$$A_s \leq N_s \qquad (4.21)$$

$$\forall s \in S$$

$$LA_s \geq N_s \qquad (4.22)$$

$$\forall s \in S$$

Constraints (4.21) and (4.22) are used to relate the status of the server (binary variable A_s), to the number of VMs in the server N_s (non-binary variable) where *L* represents a large number.

$$TS_{sd} = \sum_{i \in VM} \sum_{\substack{f \in VM \\ i \neq f}} T_{if} \quad Q_{sd}^{if} \qquad (4.23)$$

$$\forall\ s, d \in S \ and\ s \neq d$$

Constraint (4.23) calculate the traffic between servers that result from inter-VM communication assigned to different servers.

$$\sum_{s \in S_g} \sum_{d \in S_g} TS_{sd} \ \leq W \qquad (4.24)$$

$$\forall\ s, d \in PG \ and\ s \neq d$$

Constraints (4.24) is added to guarantee that the traffic demand between two VMs requests placed in two different servers in two PON groups does not exceed the shared physical link wavelength capacity.

4.4 Results and Discussion

In this section, we evaluate the power savings of the proposed VM placement MILP model. We investigated four different scenarios which consist of 1) 5 VMs, 2) 10 VMs, 3) 15 VMs, and 4) 20 VMs. In these scenarios, we assume random distributed values for inter-VM traffic data rates generated using a uniform random generator as illustrated in Table 4.1. The VMs memory and processing requirements are generated randomly to take values of 10%, 50% and 100% of the server's memory and CPU capacity. The inter-VM traffic demand data rates are distributed uniformly between 100 Mbps to 10 Gbps, where each VM can communicate randomly with up to 4 VMs.

In the examined system, we consider that each rack contains 4 servers, and hence, we consider a total of 24 fog servers. Each server possesses the same specifications in terms of the power consumption (i.e., the idle power consumption and the maximum power consumption), the memory capacity and the CPU capacity.

The computational capacity of the servers is defined as instructions per second (I_{PS}). However, the datasheet of the servers does not give the capacity of servers in I_{PS} [109]. Therefore, the value is estimated in [110] using equation 4.25:

$$I_{PS} = Core_N \; C_P \; I_{PC} \tag{4.25}$$

where, $Core_N$ is the number of cores in the processor of fog server, C_P is the processor clock rate in GHz. Both value can be founded in [72] . I_{PC} is the value of instruction per cycle , and it is estimated that a fog server can execute four instructions per second [110].

The input data that is used in the MILP model is presented in Table 4.1.

Table 4.1 The Input Data for the VM placement model.

Maximum power consumption of a server [109].	457W.
Idle power consumption of a server (Assumed to be 66% of the maximum power consumption) [109].	301.6W.
Processing capacity of a server [109].	2.5 GHz, (280k MIPS).

Processing demand of the VMs.	(10%, 50% and 100%) of servers' CPU.
Memory capacity (RAM) of the server [109].	16 GB.
Memory demand of the VMs.	100-500 MB.
ONU power consumption [104].	2.5W.
ONU data rate [104].	10 Gbps.
Inter-VM traffic demand.	100Mbps-10Gbps.
Capacity of a physical link.	6 wavelengths per fibre at 10 Gbps per wavelength
Large Number (L).	1000.

We have compared the power consumption of the proposed system based on the VM assignment resulting from the optimisation model proposed in Section 4.3 with the power consumption of the system as a result of a baseline model that places VMs and meets their demands without consideration of power consumption. Figure 4.1 presents the total power consumption of the system when serving four sets of VMs (5VMs, 10VMs, 15VMs and 20VMs) and Figure 4.2 presents the number of activated servers needed for hosting these VMs.

Figure 4.1 indicates that the total power consumption of the system based on the proposed optimisation model has been reduced in comparison to the baseline model. This is due to the lower number of servers activated to place the VMs, as shown in Figure 4.2, under the proposed model. Accordingly, the proposed model with the objective of minimising the total power consumption has reduced the power consumption of 5VMs, 10VMs, 15VMs and 20 VMs by 40%, 41%, 44% and 38%, respectively in comparison to the baseline model. The proposed model places the VMs that communicate with each other in the same server as much as possible in order to reduce the number of activated servers and also to reduce the amount of the traffic traversing the network. This results in a reduction in the total power consumption. On the other hand, the baseline model places the VMs randomly without focusing on reducing the power consumption by reducing the inter-VM traffic or placing the VMs in fewer servers.

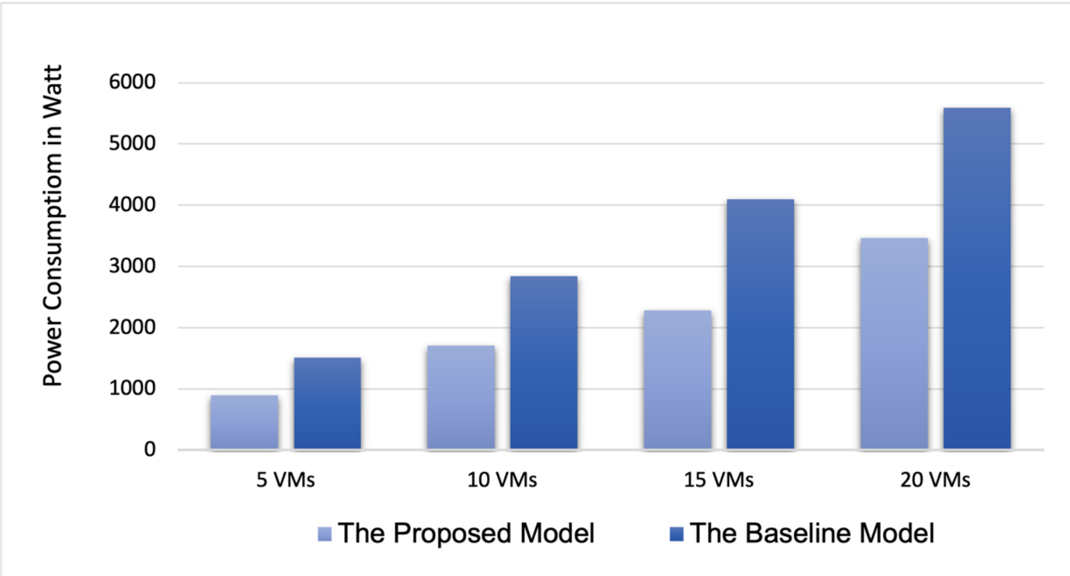

Figure 4.1 The power consumption of system of the proposed model and the baseline model.

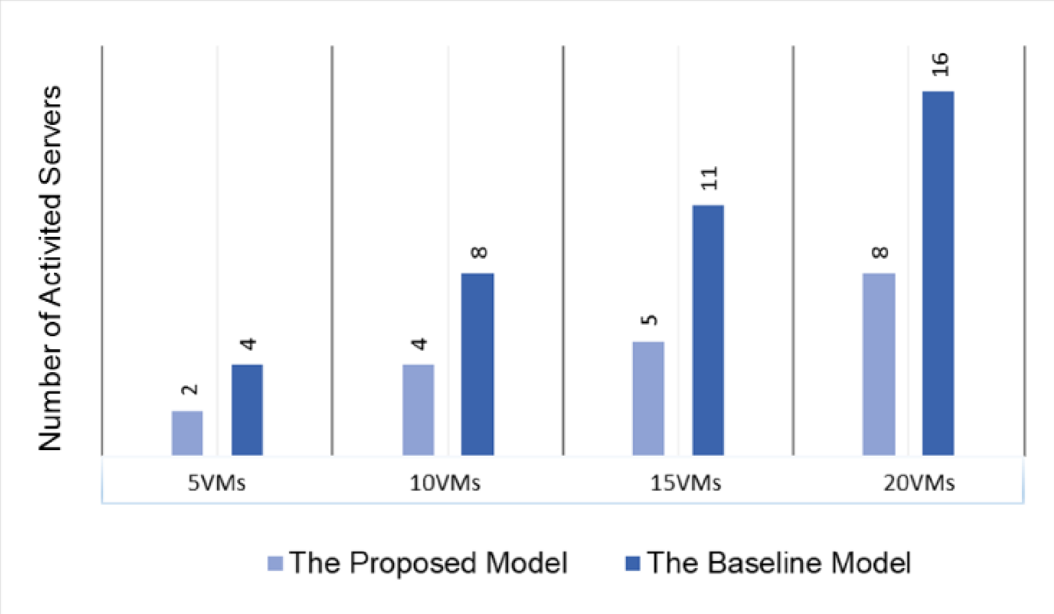

Figure 4.2 Numbers of Activated Servers of the proposed model and the baseline model.

4.5 Impact of Inter-VM Traffic on The Power Consumption.

In this section, we compare energy efficient placement of VMs; with and without inter-VM traffic. We performed the comparison using identical VMs workload at 15% of server CPU capacity with diverse sets of inter-VM traffic demand data rate (100Mbps, 500Mbps, 1Gbps and 2Gbps). In these scenarios, we also assume random distributed values for inter-VM traffic data rates generated using a uniform random generator as given in Table 4.1.

Figure 4.3 and Figure 4.4 present the total power consumption and the number of activated servers, respectively. The power consumption of the system under the proposed model when placing 5 VMs ,10 VMs, 20 VMs, and 30 VMs slightly increased by 1%, 0.8%, 0.7 %, and 10%, respectively compared to the case with no-inter-VM traffic demand as shown in Figure 4.3. Although the number of activated servers for placing 5VMs, 10VMs and 15VMs has not increased as shown in Figure 4.4, an increase in power consumption occurred due to activating additional ONUs to handle the inter-VM traffic demand. As shown in Figure 4.3.

and Figure 4.4, the increase in the number of activated servers for placing 20 VMs besides the power consumption of ONUs, were the reasons behind the 10% increase in the power consumption.

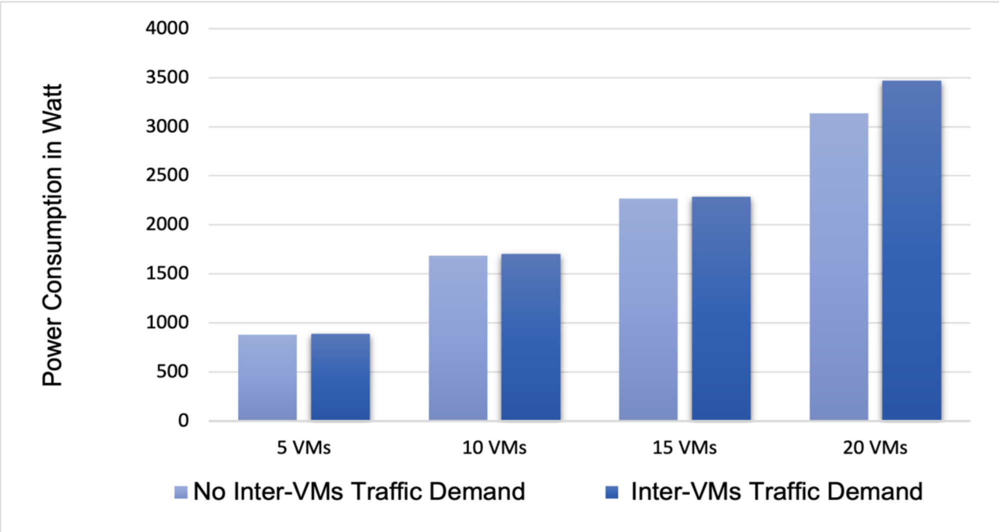

Figure 4.3 The power consumption of proposed model with inter-VM traffic demand versus no-inter-VM traffic demand.

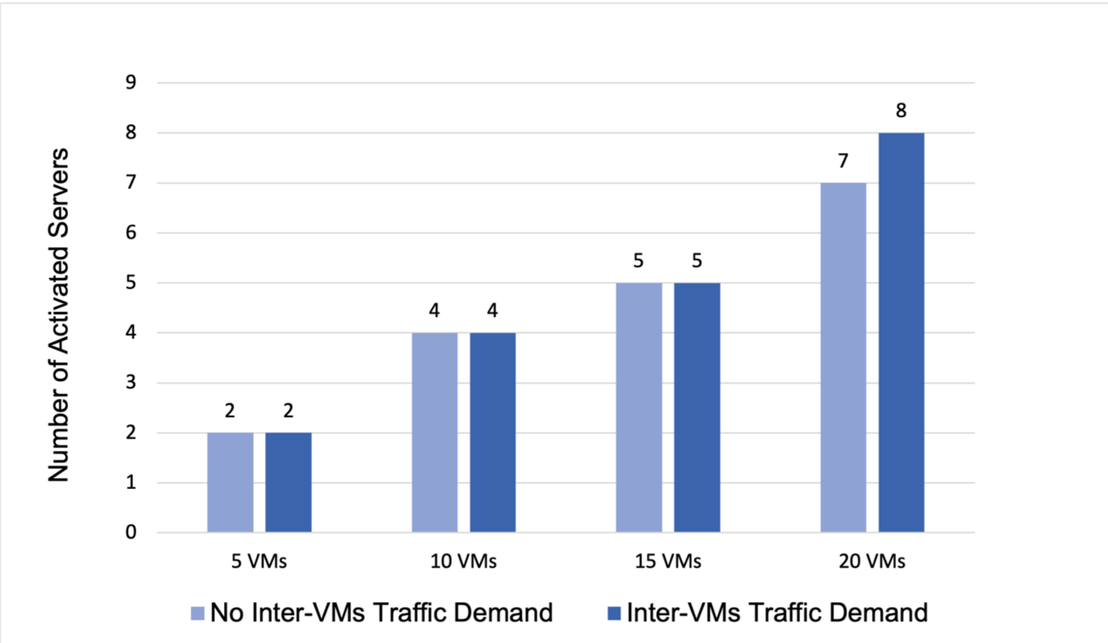

Figure 4.4 Numbers of activated servers of no inter-VMs traffic demand versus varied inter-VMs traffic demand.

Figure 4.5 and Figure 4.6 present the total power consumption of the proposed model and the number of activated servers with diverse sets of inter-VM traffic demand data (100Mbps, 500Mbps, 1Gbps and 2Gbps), each value evaluated separately. In the case where the VM requests were placed in one server (which was the case for the scenario of 5 VMs) as shown in Figure 4.6, inter-VM traffic demand has no impact on the power consumption, as shown in Figure 4.5. On the other hand, the impact of inter-VMs traffic can be observed when the VMs are distributed among multiple servers such as the scenarios with 10 VMs, 15VMs and 20VMs. Accordingly, the power consumption of the proposed model using different sets of data rate increases with the increase of the inter-VM traffic volume, as shown in Figure 4.5.

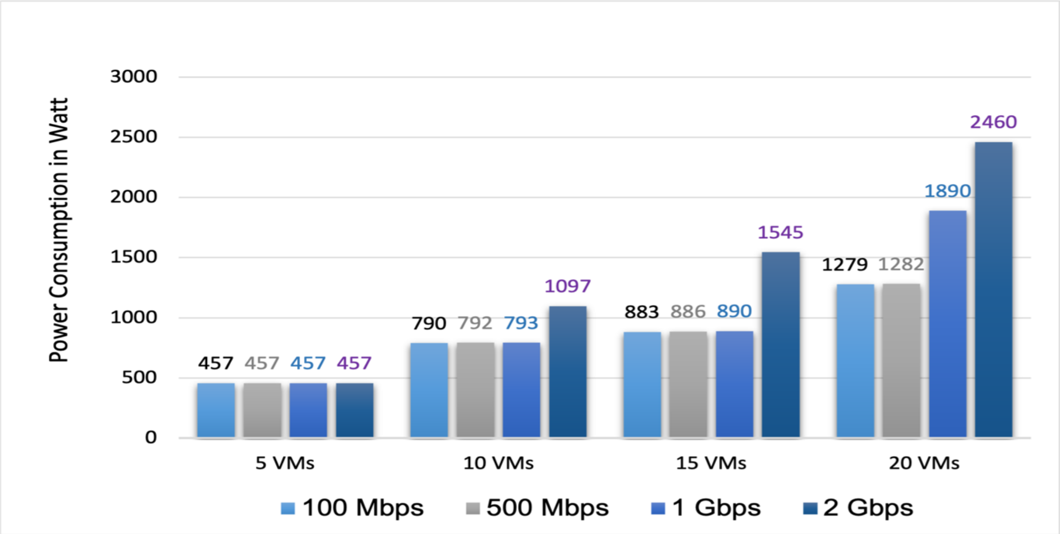

Figure 4.5 The power consumption of different sets of inter-VM traffic demand.

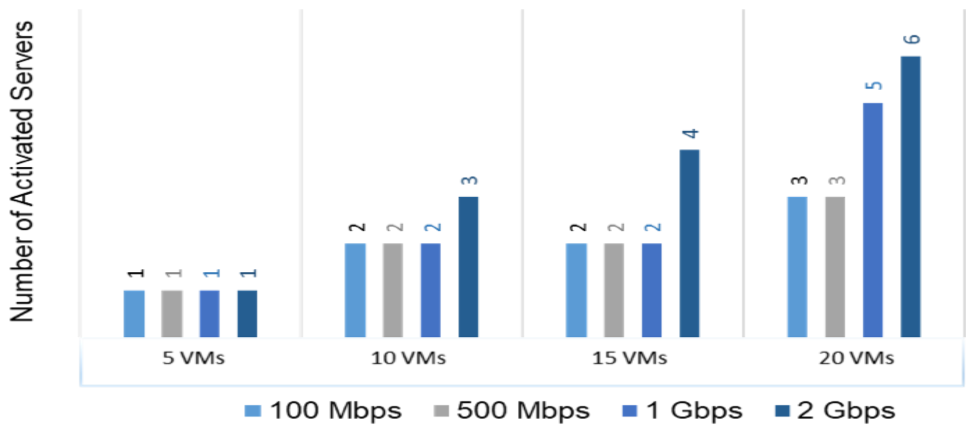

Figure 4.6 The number of activated servers of different sets of inter-VM traffic demand.

The power consumption increases as the data rates increase due to the load on the ONUs and the need to activate more servers to handle the inter-VM traffic demand. Note that the number of VMs placed in a server is limited by the data rate of the ONUs. Figure 4.7 total traffic between the servers. presents the total traffic between the activated servers. The higher the data rate of inter-VM traffic demand, the more activated servers are needed.

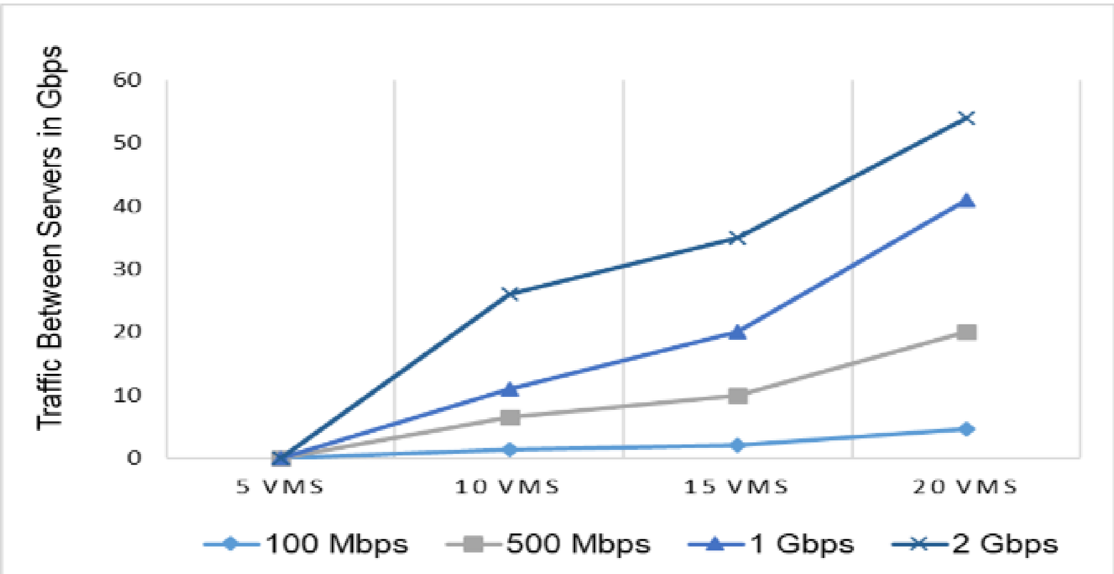

Figure 4.7 total traffic between the servers.

4.6 Heuristic Approach to Energy Efficient Virtual Machines (VM) Placement in PON-based Fog Computing

In this section, we propose a real-time energy efficient heuristic model to optimally place the VM while taking into consideration the inter-VM traffic demands. The proposed heuristic model is based on a greedy algorithm designed to solve the bin packing problem which is the Best Fit Decreasing (BFD) algorithm [112]. Minimising the total power consumption by reducing the number of activated servers, while considering the impact of inter-VM traffic is the objective of the proposed algorithm. In general, algorithms for the bin packing problem are used to pack multiple entities efficiently, for instance into a minimal number of servers [112]–[114]. BFD algorithms use the same constraints approach of bin packing (BP) algorithms, which are modelled to pack as many VMs as possible into a server given the server capacity. If the VM cannot be fitted into any of the activated servers, the algorithm will activate a new server. However, BFD algorithms sort VMs by the size of their CPU utilisations, traffic demand or RAM utilisation, from the largest to the smallest before implementing the Best Fit (BF) algorithms [115], [116].

The flow chart of the heuristic approach is shown in Figure 4.8. First, the heuristic lists all fog servers, VMs demands, and the inter-VMs demand. Second, it sorts all the VMs based on inter VMs traffic in decreasing order to create new list of VMs. This is done to place them according to the BFD algorithm. Then, for each VM in the new list, it checks the processing and memory requirements for the VMs to be sure that the available servers' capacity enables hosting the VMs. The optimal energy efficient placement is achieved as the algorithm searches for the available servers to optimally pack as many VMs as possible, so that VMs demand do not exceed available server resources in terms of CPU, and RAM memory capacity. In addition, the algorithm searches for servers that still have available capacity and uses them to place the remaining VMs in the sorted list instead of packing into new servers. Next, and after having an initial placement for all the VMs, the algorithm calculates the inter-traffic between different fog servers to ensure that the traffic does not exceed the capacity of the shared link and ONUs equipped with servers. If this is exceeded, some VMs are re-assigned to a new server. After placing all the VMs, the total power consumption is calculated. The uplink and downlink traffic for server resulting from inter-VM traffic demand is calculated to obtain the networking power consumption. The number of activated servers and their CPU utilisation are calculated to obtain the power consumption of servers.

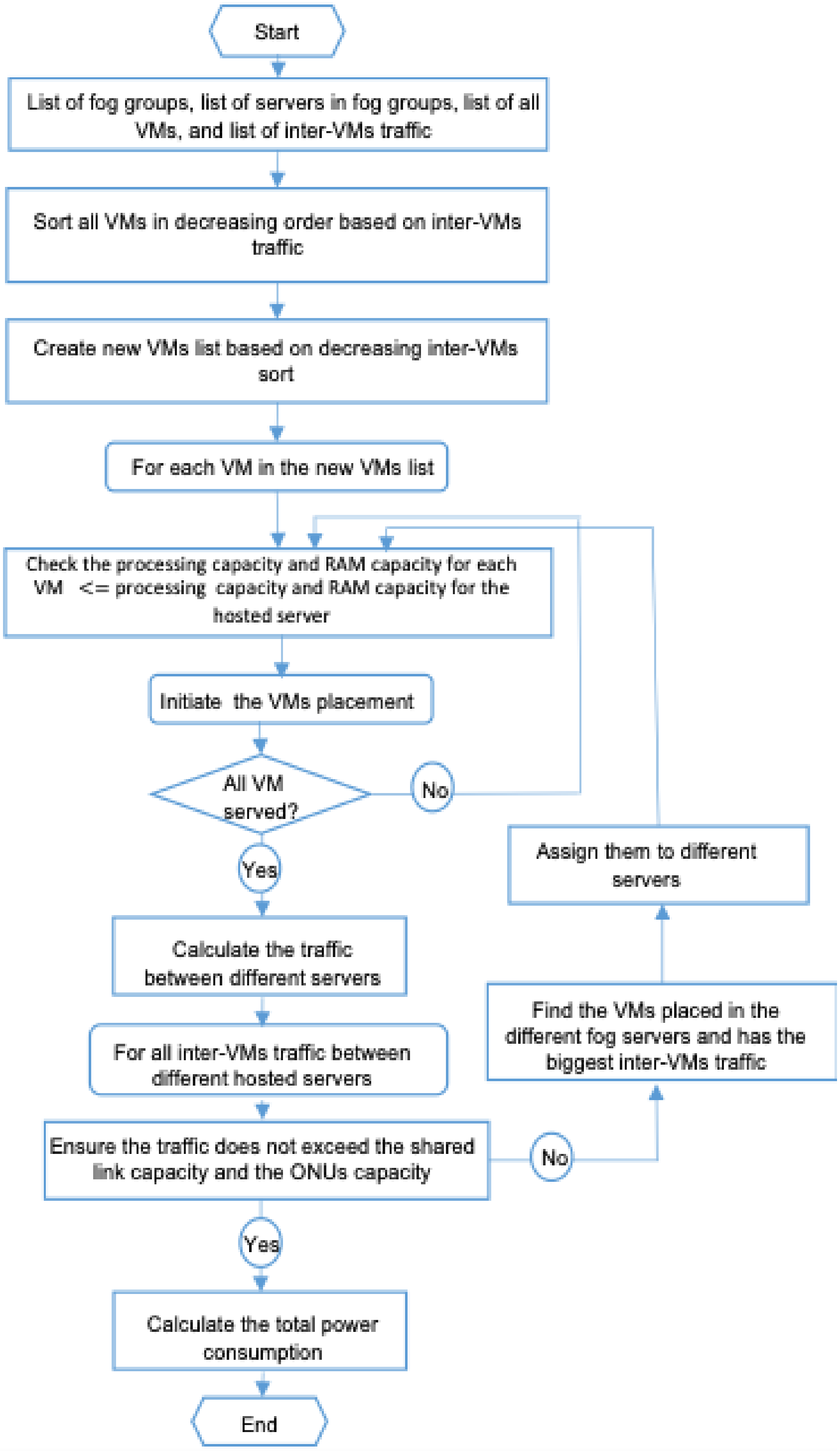

.

Figure 4.8 Flowchart of the heuristic model.

Figure 4.9 and Figure 4.10 show the total power consumption and the number of activated servers, respectively resulting from placing VMs using the heuristic and the MILP model.

The input data used to evaluate the heuristic model is presented in Table 4.1.

Figure 4.9 shows that performance gap between the heuristic and the MILP model is limited to 1%, 11%, 12%, and 14% increase in the power consumption. The heuristic algorithm utilised the same number of activated servers compared the MILP model to optimally place 5VMs and one extra server to place 10VMs and 15 VMs while utilised two extra servers to place 20 VMs as shown in Figure 4.10.

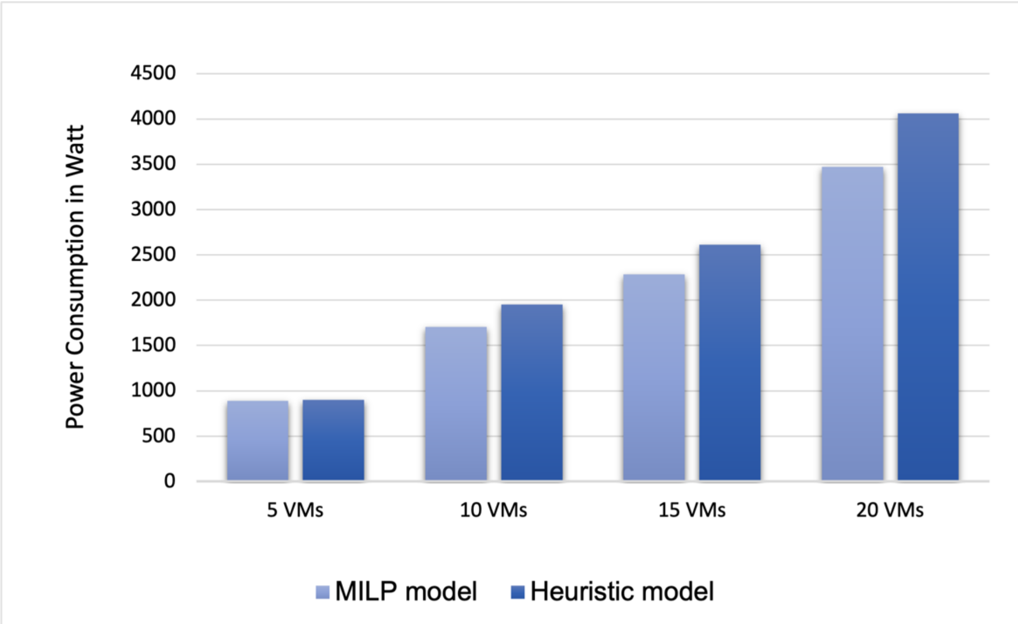

Figure 4.9 The power consumption results of the MILP optimisation model versus the heuristic model.

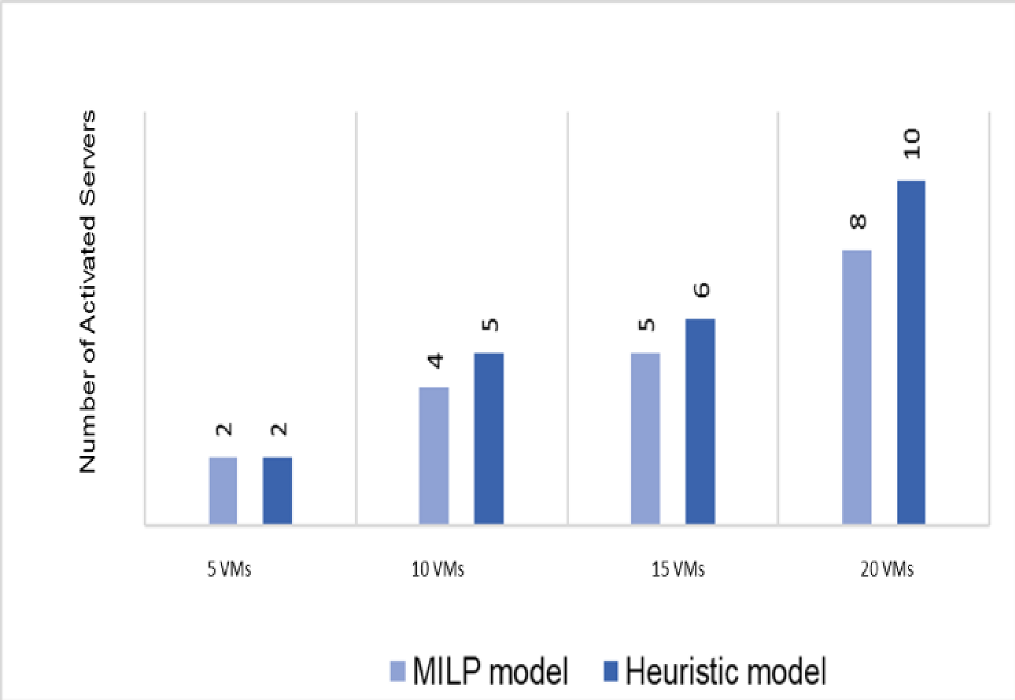

Figure 4.10 The Number of activated servers to place the VMs in the MILP optimisation model and the heuristic model.

It is worth mentioning that the heuristic model produces the results in a time scale of seconds for all VMs sets while the MILP model produces the results in seconds for 5 VMs set, in at least 2 minutes for 10 VMs set, in at least 1 hour for 15 VMs set, and in at least 24 hours for 20VMs set. However, the heuristic results are suboptimal compared to the MILP model because the heuristic comprises of a set of simplified steps and hence it only approximates the MILP. The heuristic was executed in an Intel Core i5, 2.7 GHz processor with 32 GB RAM. All MILP models were run on high-performance Intel(R) Xeon(R), 3.5GHz processor with 64 GB RAM.

Summary

This chapter developed a MILP model and a heuristic algorithm to optimise the placement of VMs in the collaborative fog computing architecture considering the inter-VM traffic demand to minimise power consumption. The results show that the power consumption is reduced by up to 52% compared to placing VM with no consideration of power consumption.

This chapter has also studied the impact of inter-VM traffic demand on the total power consumption. The results show that the impact of inter-VM traffic in total power consumption is governed by the data rate of the traffic demand between VMs placed in different servers. As the data rate increases, the power consumption increases, and the number of activated servers might increase to accommodate the inter-VMs traffic demand. The results of different data rates for inter-VM traffic demand based on the VM placement MILP model were compared to the results obtained by a real-time heuristic algorithm. The results show that the heuristic algorithm performance approaches that of the MILP model with an average gap of 15%.

Chapter 5 Energy Efficient Placement for End Users' demands in a Collaborative Fog Computing Architecture

5.1 Introduction

Delay-sensitive applications should be processed in the nearest fog computing units close to the end-devices to meet the low-latency requirements of these applications. Fog computing units can be any device with computing capabilities such as routers, switches, accesses points or servers [1]–[7]. However, the processing capacity of such fog units is limited compared to the cloud which will often result in congestion or VM request blockage under high demands. Therefore, the capacity of fog computing units should be addressed to ensure that they are well-suited to the demands of delay-sensitive applications.

The collaborative fog computing architecture, presented in Chapter 3, realises a collaborative fog approach in which fog cells are connected through a dedicated PON.

This chapter extends the proposed architecture in chapter 3 to consider the end users' site in the networking layer where neighbouring fog cells can collaborate in processing intensive demands. In addition, this chapter evaluates the energy efficiency improvement obtained by this collaborative approach. Also, this chapter investigates the impact of the heterogeneity of the fog units' capacity and energy-efficiency on the overall energy-efficiency of the fog system. We optimise the VM placement considering VM requests representing delay-sensitive application initiated by users at the access network as opposed to the model in Chapter 4 where VMs requests are initiated by a central entity.

5.1 Related Work

Several research studies investigated the processing capacity of various fog units to provide the required capacity of processing intensive demands [8], [9]. The authors in [8] optimised the service allocation problem using an integer programming model in a cloud-fog architecture. The goal of the work was to minimise the latency experienced by IoT services while meeting resource constraints. Two modes of service allocation were considered which the authors refer to as serial and parallel allocation. With the former approach, higher delays are experienced by the services, whilst with the latter approach, lower service delays are observed. The study in [9] reported on the work of a consortium called RECAP that aims to advance cloud and edge technologies and to develop mechanisms for reliable capacity provisioning as well as making application placement and infrastructure orchestration autonomous, predictable, and optimised. This automation is achieved by intelligent profiling of workloads.

In a heterogeneous fog computing environment, due to equipment being manufactured by different vendors, computational resources that are placed in different locations may be of different efficiencies in terms of power consumption [117]. Several research studies investigated different optimisation models to improve the performance of heterogeneous computing systems in term of data processing speed and the power consumption [118]–[120]. The authors in [118] investigated the optimal placement of IoT applications in a heterogeneous architecture supported by edge and cloud computing. They proposed a model that utilises a weighted objective function to optimise the latency and power consumption. In a similar study, the authors in [119] tackled the balance of power consumption and delay when optimally placing end-users requests in a three-layer heterogeneous cloudlet environment. Based on the end-user applications' type, the appropriate cloudlet layer is selected to process the request to minimise the power consumption and delay. The authors in [120] proposed an optimisation model for end-user requests' placement taking into account the processing provided by the cloud and the access network. Their proposed model utilised a weighted objective function to optimise the power consumption and delay.

5.2 The Proposed PON-based collaborative FOG architecture

Figure 5.1 shows the fog based PON architecture with connectivity between the end user and access points ONUs in the access layer. The proposed architecture, as shown in 5.1 , comprised of a networking layer and a processing layer. In the following, we elaborate these layers.

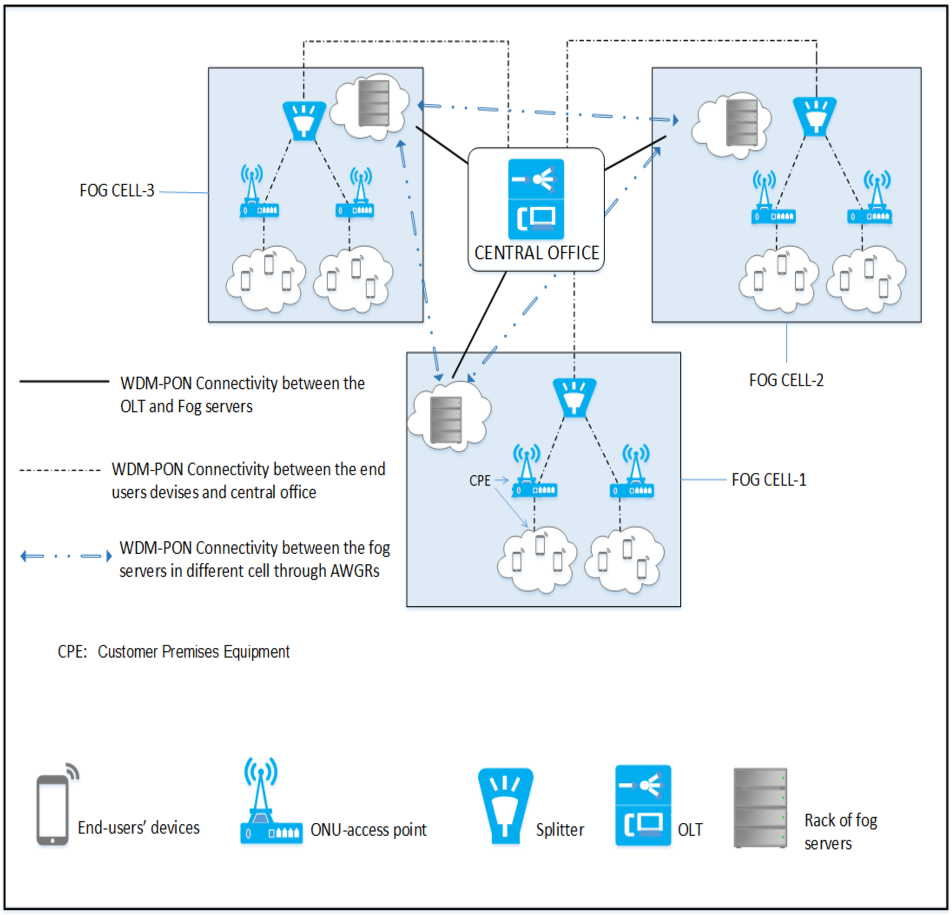

Figure 5.1 The collaborative Fog Architecture over PON.

5.2.1 The Networking Layer

The networking layer is responsible for aggregating the data from the end-user's equipment and forwarding it to the processing units. In the proposed architecture, the networking layer is composed of energy efficient devices within the PON architecture that are comprised of the ONU, that represent the Customer Premises Equipment (CPE). These devices are in charge of collecting data from end-users. In addition, an OLT at the Central Office, and a passive splitter between the ONUs and OLT. The OLT provides a point-to-multipoint fibre optical connectivity.

The VM requests are initially assembled in the ONU-Access points, and then forwarded to the OLT, as shown in Figure 5.1. The OLT later forward the user data to the assigned server in one of the fog cells via a WDM-PON composed of AWGRs.

5.2.2 The Processing Layer

The processing layer is responsible for hosting the virtual machines requests generated from the end-user's devices and processing the data in efficient ways to meet the delay-sensitive applications requirements. In the proposed architecture, the processing layer is comprised of fog servers, where each fog cell has multiple fog servers. Each server is equipped with an ONU device. The OLT optimally allocates the VMs requests to the appropriate fog servers based on the available capacity and the power consumption reduction goals via the WDM-PON. Moreover, the servers within different cells, as shown in 5.1, can communicate with each other directly via the passive PON component (the AWGRs) to avoid consuming high amount of power by communicating via the OLT as explained in Chapter 3.

In this collaborative fog computing system, multiple fog cells can collaborate to host the user demands and this can subsequently reduce the total power consumption as the passive connectivity through the AWGR- facilitates "the borrowing" of data processing capabilities.

We compare the collaborative fog architecture to a fog architecture where there is no PON connectivity among fog cells. AWGRs are used to provide connectivity among racks of servers in a fog cell and to connect the racks to the OLT, i.e., connections between PON cells have to go through the OLT. Due to the high-power consumption of the OLT and the delay resulting from routing through the OLT, the fog cells do not collaborate in this architecture, referred to as a non-collaborative fog architecture.

5.3 MILP Optimisation Model for Energy Efficient Placement of End Users' demands

This MILP model aims to minimise the total power consumption jointly with minimising the number of blocked VMs. The model optimises the allocation of the demands among the neighbouring fog computing cells so that VM requests that no longer fit in one of the fog cells can be processed in other connected available fog cells. The proposed MILP model minimises the networking and processing power consumption of VM requests. Each VM request consists of a CPU processing demand which is the amount of processing required in MIPS, the VMs' traffic demand, which is the amount of data required in Gbps, and the RAM workload which is the amount of memory allocated to each VM request in MB.

The following notations are the sets, parameters and variables used in the optimisation model:

Sets:

N	Set of all nodes in the proposed architecture including ONUs, OLT fog servers and VM source nodes.
N_m	Set of all neighbouring nodes to node $m,\ m \in N$.
ONU	Set of ONUs in the networking layer, where $ONU \subset N$.
OLT	Set of OLTs in the networking layer, where $\mathrm{OLT} \subset N$.
S	Set of fog servers in the processing layer, where $S \subset N$.
γ	Set of VM source nodes, where $\gamma \subset N$.

Networking Layer Parameters:

$\mathcal{MU}$	Maximum power consumption of the *ONU*.
$\mathcal{IU}$	Idle power consumption of the *ONU*.
$\mathcal{DU}$	Maximum data rate of the *ONU*.
$\mathcal{EU}$	Energy per bit of the *ONU*, where:

$$\mathcal{EU} = \left(\frac{\mathcal{MU} - \mathcal{IU}}{\mathcal{DU}}\right) \tag{5.1}$$

$\mathcal{MO}$ Maximum power consumption of *OLT*.

$\mathcal{IO}$ Idle power consumption of *OLT*.

$\mathcal{DO}$ Maximum data rate of *OLT*.

$\mathcal{EO}$ Energy per bit of OLT, where:

$$\mathcal{EO} = \left(\frac{\mathcal{MO} - \mathcal{IO}}{\mathcal{DO}}\right) \tag{5.2}$$

$\mathcal{C}_{mn}$ Capacity of the physical link (m, n), where $m, n \in N$.

Processing Layer Parameters:

$\mathcal{M}$ Maximum power consumption of the server.

I Idle power consumption of the server.

C CPU capacity of the the server.

R RAM memory capacity of the server.

O The proportional power consumption of the servers, where:

$$O = \mathcal{M} - I \tag{5.3}$$

Δ Number of servers permitted to serve one VM request.

ρ Maximum power consumption of *the ONU* attached to the server.

σ Data rate of the *ONU* attached to the server.

VM Requests Parameters:

C_s	CPU demand of the VM at source node $s,\ s \in \gamma$ In MIPS.
R_s	RAM memory demand of the VM at source node $s,\ s \in \gamma$ in GB.
T_s	Traffic demand of the VM at source node $s,\ s \in \gamma$ in Gbps.
$\mathcal{L}$	A large enough number.

Variables:

L_{sd}	Traffic demand between the VM source s, and the fog server d, where $s \in \gamma$ and $d \in S$.
L_{sd}^{mn}	Traffic demand between the VM source s, and the fog server d, traversing link (m, n) where $s \in \gamma$, $d \in S$, $m \in N$ and $n \in N_m$.
P_{sd}	The amount of processing demand of the VM from source node $s \in \gamma$ that is assigned to fog server $d \in S$.
R_{sd}	The amount of RAM memory demand of the VM from source node $s \in \gamma$ that is assigned to fog server $d \in S$.
$Þ_{sd}$	$Þ_{sd} = 1$, if the processing and memory demand of the VM from source node $s \in \gamma$ is allocated to fog server $d \in S$, otherwise $Þ_{sd} = 0$
L_m	Amount of traffic that passes through node $m \in N$.

B_m B_m = 1 if the node $m \in N$ is activated, otherwise B_m = 0.

D_m Defined as the AND of two variables B_m and L_m, $m \in N$.

$\hat{A}_s$ $\hat{A}_s$ = 1 if the server $s, s \in S$ is activated, otherwise $\hat{A}_s = 0$.

The networking layer power consumption $(\mathbb{N})$, is composed of:

a) The power consumption of the ONUs in the Networking Layer $(\mathbf{ONU}_{PC})$ which is expressed based on idle power plus proportional power profile, and is given as:

$$(ONU_{PC} = \sum_{m \in ONU} \mathcal{EU}\ L_m \quad + \sum_{m \in ONU} \mathcal{IU}\ \ B_m \qquad (5.4)$$

.

b) Power consumption of OLTs in the Networking Layer $(\mathbf{OLT}_{PC})$ which is expressed based on an idle power plus proportional power profile is given as:

$$OLT_{PC} = \sum_{m \in OLT} \mathcal{EO}\, L_m \quad + \sum_{m \in OLT} \mathcal{IO}\ \frac{D_m}{\mathcal{DO}} \qquad (5.5)$$

It is important to note that since the OLT is shared by many users and applications, the idle power consumption of this device should be divided among the applications running at a given point in time. Thus, only a fraction of the maximum idle power consumption is used based on the VMs traffic given by variable L_m [121].

The Processing power consumption, ($\mathbb{P}$), is composed of:

a) The power consumption of the servers ($\boldsymbol{S_{PC}}$), (we considered the CPU power consumption as it is the most significant contributor to the server's power consumption) which is expressed based on an idle power plus proportional power profile as:

$$S_{PC} = \sum_{d \in S} \left(I \; \hat{\text{A}}_s + \frac{O}{C} \sum_{s \,\in\, \gamma} P_{sd} \right) \tag{5.6}$$

where

$$P_{sd} = \text{C}_s \; \text{Þ}_{sd}. \qquad \forall \; s \in \; \gamma, d \in S \tag{5.7}$$

b) The power consumption of the ONUs attached to each server ($\boldsymbol{S\_ONU_{PC}}$) is expressed as a proportional power profile, and is given as:

$$S\_ONU_{PC} = \frac{\rho}{\sigma} \sum_{s \in \mathbf{S}} L_s \;, \tag{5.8}$$

.

Note that the power consumption of the ONU devices in this work is of two types:

1) The ONUs attached to the processing servers which work as transceivers and have a proportional power consumption profile. This power adds up to the processing power consumption.

2) The ONUs used as CPE. These have a proportional plus an idle power consumption profile [41], [121]. This power adds up to the networking power consumption.

The MILP model is defined as follows:

The objective: Minimise the total networking and processing power consumption of the proposed architecture:

$$\mathbb{N} + \mathbb{P} \tag{5.9}$$

$$\mathbb{N} = \mathrm{ONU}_{PC} + \mathrm{OLT}_{PC} \tag{5.10}$$

$$\mathbb{P} = S_{PC} + S\_ONU_{PC} \tag{5.11}$$

Subject to the following constraints:

$$\sum_{\substack{n \in N_m \\ m \neq n}} L_{sd}^{mn} - \sum_{\substack{n \in N_m \\ m \neq n}} L_{sd}^{nm} = \begin{cases} L_{sd} & m = s \\ -L_{sd} & m = d \\ 0 & otherwise \end{cases} \tag{5.12}$$

$$\forall\ s \in \gamma, d \in S, \forall\ m \in \mathrm{N}$$

Constraint (5.12) is a traffic flow conservation constraint to ensure that the traffic demand for each VM that enters a node leaves it (except for the source and destination nodes).

$$P_{sd} = Þ_{sd}\, C_s$$

$$\forall\, s \in \gamma \tag{5.13}$$

Constraint (5.13) ensures that the processing demand for each VM is met by fog servers. This constraint holds as a VM is served by a single server as given in constraint (5.30).

$$\mathcal{L}\ \ P_{sd} \geq \text{Þ}_{sd} \tag{5.14}$$

$$\forall\, s \in \gamma, d \in S$$

$$P_{sd} \leq \mathcal{L}\ \ \text{Þ}_{sd} \tag{5.15}$$

$$\forall\, s \in \gamma, d \in S$$

Constraints (5.14) and (5.15) are given to relate the binary variable Þ_{sd} with the non-binary variable P_{sd}.

$$R_{sd} = \text{Þ}_{sd}\, R_s$$

$$\forall\, s \in \gamma, d \in S \tag{5.16}$$

Constraint (5.16) ensures that the RAM memory demand for each VM source node s $\in \gamma$ is met by a fog server. This constraint holds as a VM is served by a single server as given in constraint (5.30).

$$\mathcal{L}\ R_{sd} \geq \text{Þ}_{sd} \tag{5.17}$$

$$\forall\, s \in \gamma, d \in S$$

$$R_{sd} \leq \mathcal{L}\ \text{Þ}_{sd} \tag{5.18}$$

$$\forall\, s \in \gamma, \quad d \in S$$

Constraints (5.17) and (5.18) relate the binary variable Þ_{sd} to the non-binary variable R_{sd}.

$$L_{sd} = Þ_{sd} \quad T_s \qquad (5.19)$$
$$\forall \; s \in \gamma, \qquad d \in S$$

Constraint (5.19) ensures that the traffic demand for each VM source node s $\in \gamma$ is met at a given destination node. This constraint holds as a VM is served by a single server as given in constraint (5.30). Note that the same binary variable, $Þ_{sd}$, is used in constraints (5.13), (5.16) and (5.19) which ensures that all the demands of a VM are served in one server.

$$L_m = \sum_{s \in \gamma} \sum_{d \in S} \sum_{\substack{n \in N_m \\ m \neq n}} L_{sd}^{mn} + \sum_{s \in \gamma} \sum_{d \in S} \sum_{\substack{n \in N_m \\ m \neq n}} L_{sd}^{nm} \qquad (5.20)$$
$$\forall \; m \in N$$

Constraint (5.20) gives the amount of traffic traversing each node in the proposed architecture to calculate the power consumption.

$$D_m \leq \mathcal{L} \, B_m \qquad (5.21)$$
$$\forall \; m \in \mathrm{N}$$

$$D_m \leq \mathcal{L} \, L_m \qquad (5.22)$$
$$\forall \; m \in \mathrm{N}$$

$$D_m \geq L_m - (1 - B_m) M \qquad (5.23)$$
$$\forall \; m \in \mathrm{N}$$

$$D_m \geq 0 \qquad (5.24)$$
$$\forall \; m \in \mathrm{N}$$

Constraints (5.21), (5.22), (5.23) and (5.24) are used to linearise the multiplication of two variables B_m, L_m .

$$\sum_{s \in \gamma} C_s \, Þ_{sd} \leq C \qquad \forall\, d \in S \tag{5.25}$$

Constraint (5.25) ensures that the processing capacity of the VM requests served by a server does not exceed the processing capacity of the server.

$$\sum_{s \in \gamma} R_s \, Ñ_{sd} \leq R \qquad \forall\, d \in S \tag{5.26}$$

Constraint (5.26) ensures that the memory of the VM requests served by a server does not exceed the memory capacity of the server.

$$L_m \leq \mathcal{DU} \qquad \forall\, m \in ONU \tag{5.27}$$

Constraint (5.27) ensures that the total traffic load on the ONU does not exceed the data rate of the ONU.

$$L_s \leq \sigma \qquad \forall\, s \in S \tag{5.28}$$

Constraint (5.28) ensures that the total traffic flow to a server does not exceed the data rate of the ONU attached to the server.

$$\sum_{s\in\gamma}\sum_{d\in S} L_{sd}^{mn} \leq \mathcal{C}_{mn} \tag{5.29}$$

$$\forall\, n \in N, m \in N_m$$

Constraint (5.29) ensures that the total traffic passing through the physical link m, n does not exceed the capacity of the link.

$$\sum_{d\in S} Þ_{sd} \leq 1 \tag{5.30}$$

$$s \in \gamma$$

Constraint (5.30) ensures the number of servers that host each VM request is a single server.

$$L_m \geq B_m \tag{5.31}$$

$$\forall\; m \in \mathrm{N}$$

$$L_m \leq \mathcal{L}\, B_m \tag{5.32}$$

$$\forall\; m \in \mathrm{N}$$

Constraint (5.31) and (5.32) relate the binary variable B_m to the non-binary variable L_m.

$$\sum_{s\in\gamma} Þ_{sd} \geq \hat{\mathrm{A}}_s \tag{5.33}$$

$$\forall\; d \in S$$

$$\sum_{s\in\gamma} Þ_{sd} \leq \mathcal{L}\, \hat{\mathrm{A}}_s \tag{5.34}$$

$$\forall\; d \in S$$

Constraint (5.33) and (5.34) relate the binary variable $\hat{A}_s$ to the non-bianry variable $Þ_{sd}$

5.4 MILP MODEL RESULT

In this section, we evaluate the energy efficiency of the collaborative-fog over PON compared to the non-collaborative fog under three different scenarios of VMs requests (i.e., 10, 15, and 20 VMs). This was performed with uniform random distribution for the CPU, memory and traffic demands as shown in Table 5.1. The VMs' processing requirements are uniformly distributed between 160k MIPS and 280k MIPS in one cell, and 10k MIPS to 56k MIPS in the other cells. This results in one fog cell being highly loaded to show the proposed architecture's ability of collaborating in serving high demands. The VMs memory requirements are uniformly distributed between 100MB and 500MB. Moreover, The VMs' traffic demands (i.e., the traffic between end-users and fog servers hosting VMs) are uniformly distributed between 1 Gbps and 5 Gbps.

The input data used in the MILP model is presented in Table 5.1.

Table 5.1 The Input Data for Energy Efficient Placement for VMs of End Users.

Server's maximum power consumption [109].	457 W
Server's idle power consumption (66% of Maximum power) [109].	301 W
Processing capacity of the server [109].	280k MIPS

Cores in the processor of fog server [109] [110].	28
Processing capacity of the VMs.	10k MIPS - 280k MIPS
Memory capacity (RAM) of the server [109].	16 GB
Memory capacity (RAM) of the VMs [41].	100 MB - 500 MB
OLT Maximum power consumption [102].	1940 W
OLT idle power consumption (90% of Maximum power).	1746 W
OLT data rate [102].	8600 Gbps
ONU Maximum power consumption [104].	2.5 W
ONU idle power consumption (60% of Maximum power) [104].	1.5 W
ONU data rate [104].	10 Gbps
VMs Traffic Demands [41].	1 Gbps – 5 Gbps
Capacity of Optical physical link.	6 wavelengths per fibre at 10 Gbps per wavelength

We have evaluated the server utilisation of both architectures by comparing the number of VM requests processed and the number of VM requests blocked. Figure 5. shows that with the non-collaborative fog approach, 1 VM is blocked when 15 VMs are requested and 2 VMs are blocked when 20 VMs are requested due to the limited local processing resources available to each fog cell. Figure 5., on the other hand, shows that as each cell in the collaborative Fog architecture is capable of borrowing data processing from neighbouring fog cells, no VMs are blocked with this approach for all the scenarios. At 10 VMs, both architectures have processed all the VM demands, as shown in Figure 5. and Figure 5.. Moreover, we have compared the total power consumption of both approaches. As can be seen in Figure 5. , although more VMs are served by the collaborative fog architecture, its power consumption is lower than the non-collaborative fog architecture. The processing power consumption reduction (Figure 5.) resulting from activating fewer servers, as shown in Figure 5.**,** is the main contributing factor to the power savings. In the collaborative-fog architecture, the model is able to pack VMs in servers across all the fog cells due to the collaboration facilitated by the PON connectivity and hence use fewer processing servers. When considering the placement of 20 VMs, the non-collaborative fog has used 7 servers to accommodate 18 VMs out of 20 VMs while the collaborative Fog has used 6 servers to accommodate all of the VMs, as shown in Figure 5..

As PON devices are used in the networking layer, both architectures are highly energy efficient in networking power consumption as shown in Figure 5.. The collaborative fog architecture shows a slight increse in networking power consumption for 20 VMs while utlising 6 servers due to processing all 20 VMs compared to the non collabortive architecture.

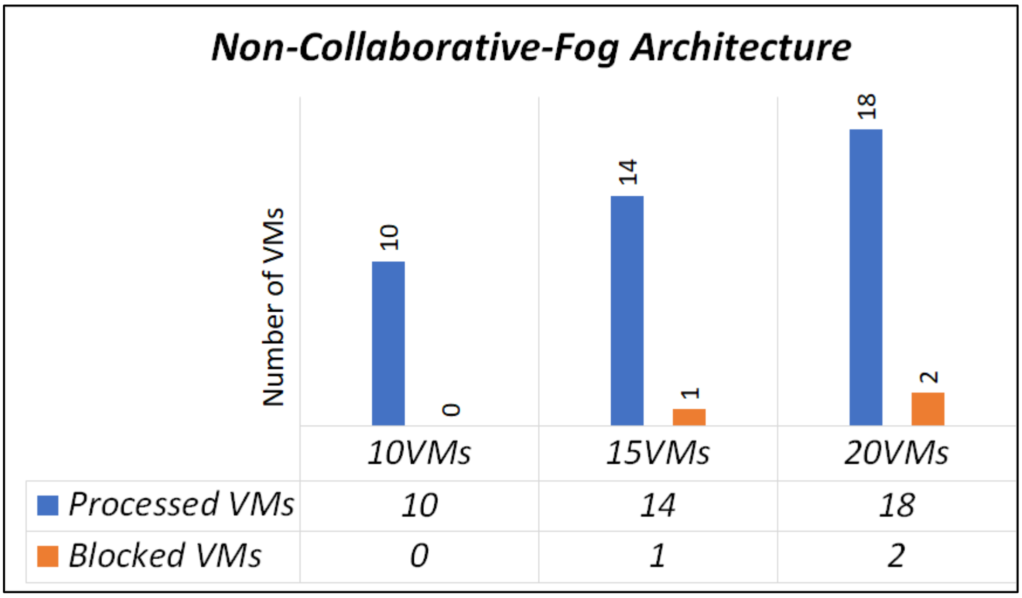

Figure 5.2 Number of processed versus blocked VMs in the non-collaborative Fog.

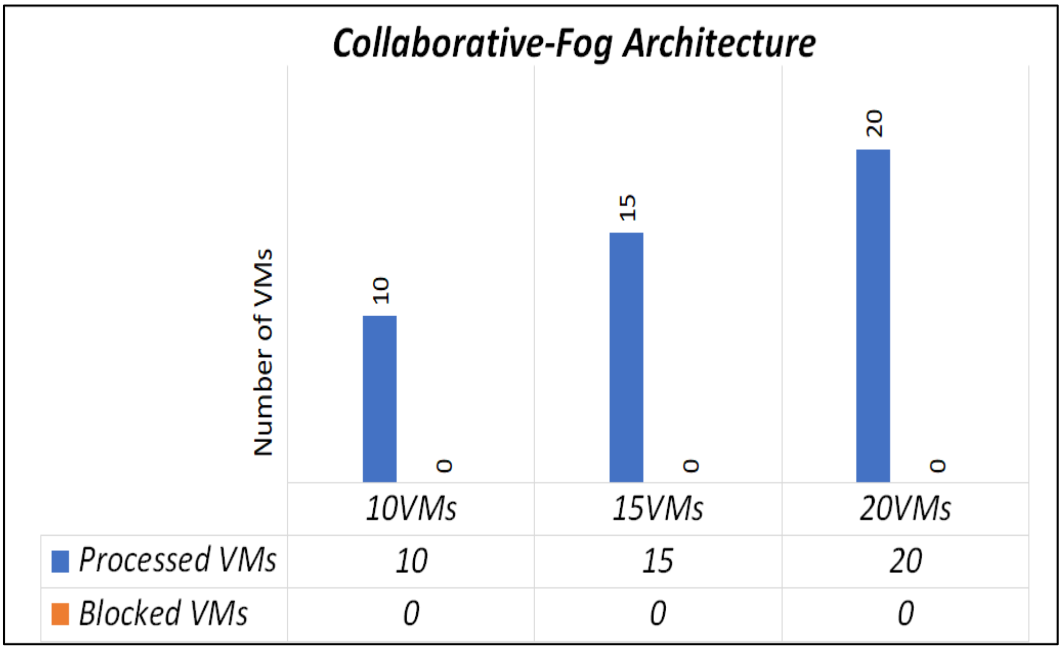

Figure 5.3 Number of processed versus blocked VMs in the collaborative Fog.

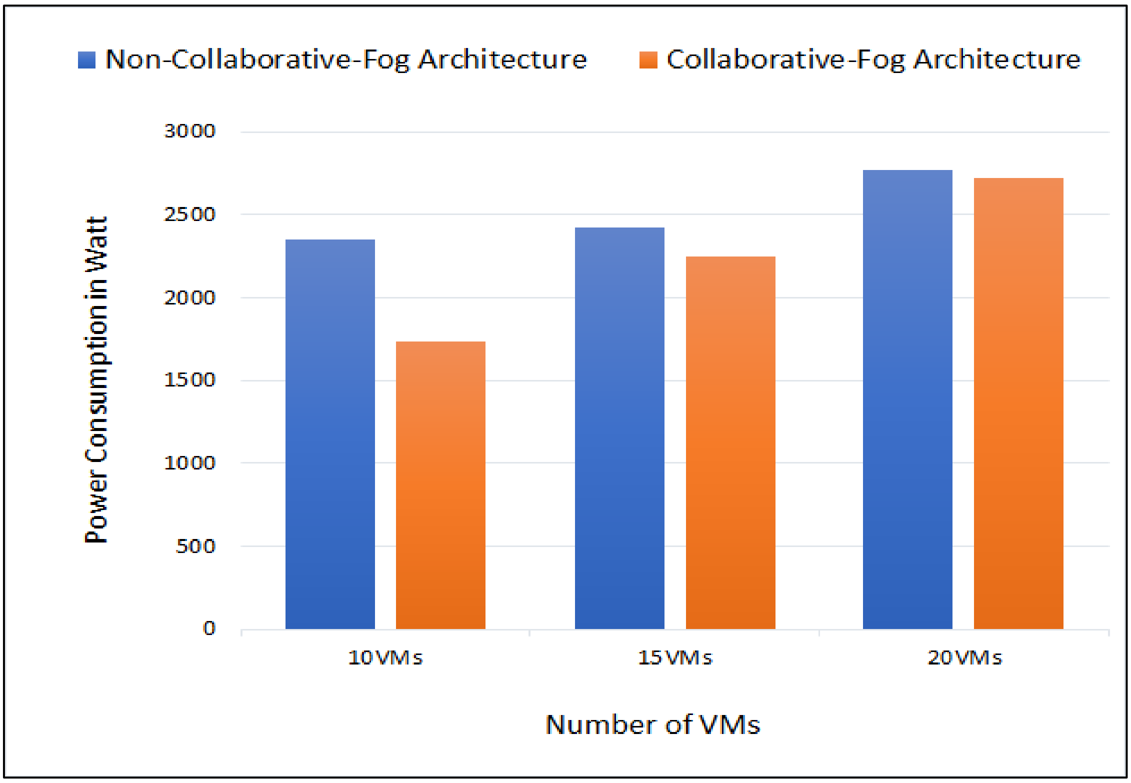

Figure 5.4 Total power consumption (i.e., networking and processing) of both fog architectures.

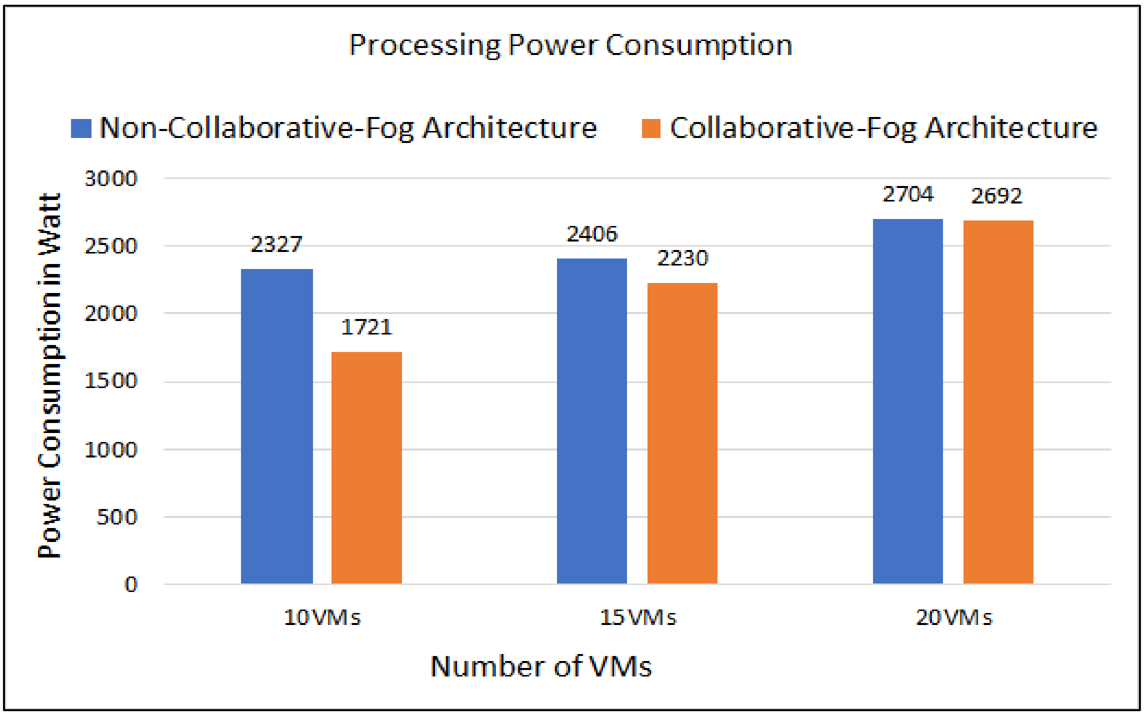

Figure 5.5 Processing power consumption in both fog architectures.

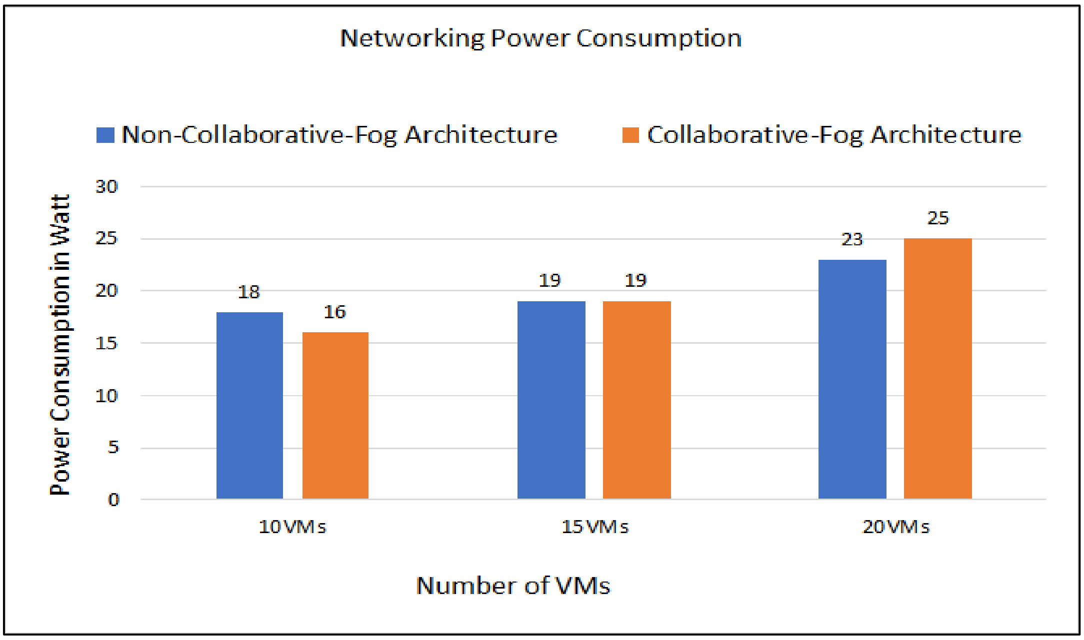

Figure 5.6 Networking power consumption in both fog architectures.

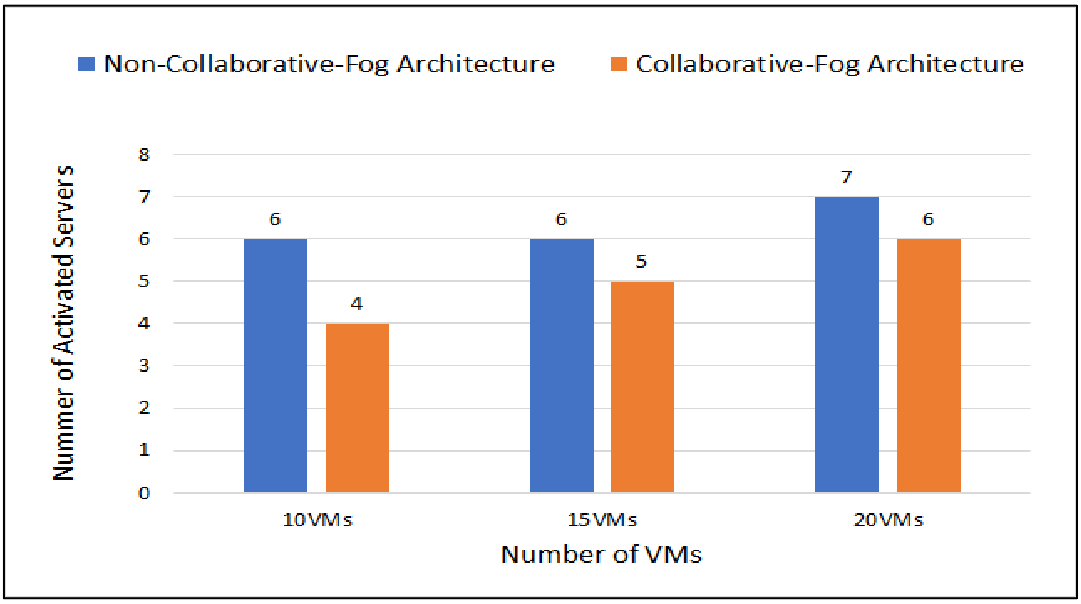

Figure 5.7 Number of used servers in both fog architectures.

5.5 Energy Efficient VM Placement in a Heterogeneous Collaborative-Fog Computing Architecture

The power consumption optimisation framework in this section considers a heterogeneous collaborative-fog computing environment that consists of three fog cells. In practical environments fog cells may belong to different organisations, therefore, it is likely that such fog cells may deploy servers of different specifications such as processing capabilities and energy efficiency. In the following, we address the impact of the heterogeneity of the fog cells on the energy efficiency of the proposed collaborative architecture.

5.5.1 The Proposed Architecture

The proposed architecture, as shown in Figure 5., is composed of three heterogeneous collaborative-fog computing cells. We have differentiated between the servers' power consumption efficiencies in the fog cells as shown in Figure 5.. We considered the MILP model in Section 5.5 to optimise the placement of VMs in this architecture.

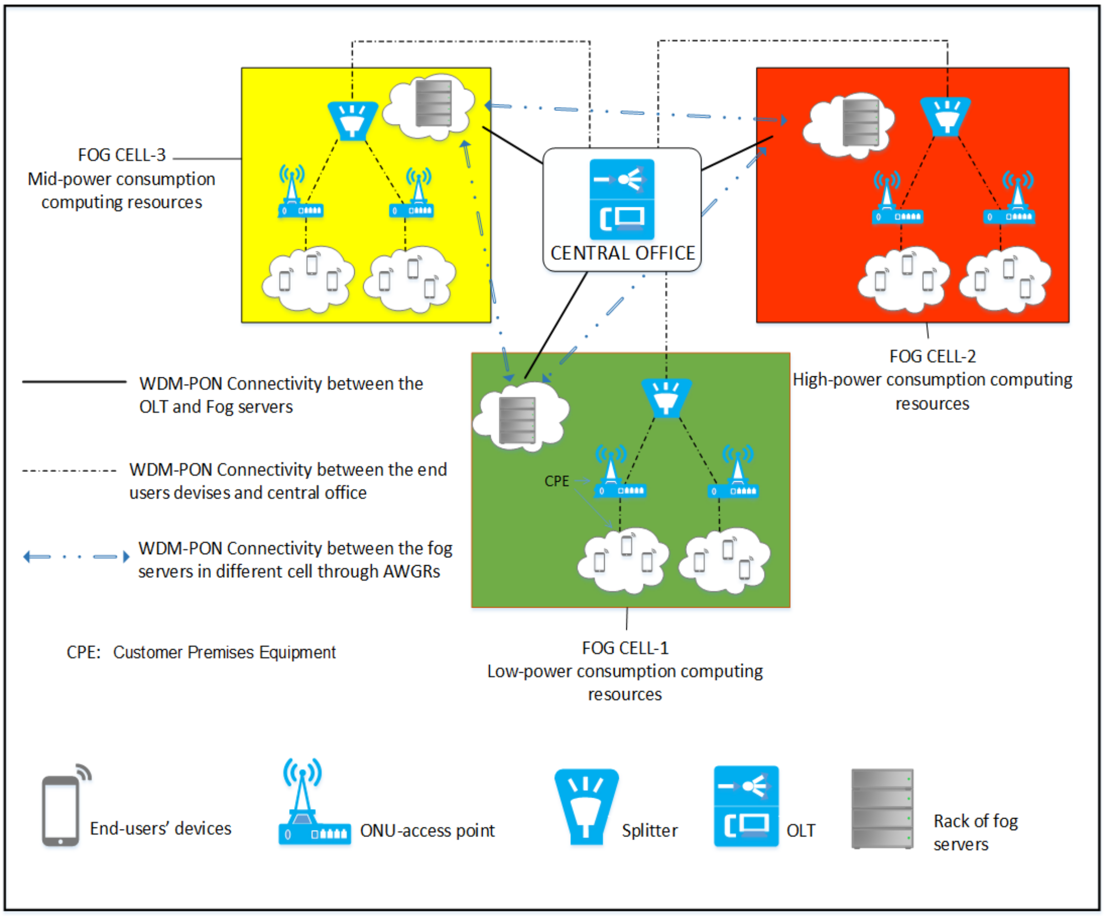

Figure 5.8 The evaluated heterogeneous collaborative-fog computing architecture.

5.5.2 Results

In this section, we evaluate the energy efficiency of the proposed heterogeneous collaborative-fog computing model. The evaluation considered the same objectives in Section 5.5 under three different sets of VMs which are 10 VMs, 15 VMs, and 20 VMs. We considered randomly distributed values for the CPU capacity requested (between 10k MIPS and 280k MIPS), memory capacity (between 100MB and 500MB) and data traffic (between 0.1 Gbps and 10 Gbps), as illustrated in Table 5.2. Fog cell1 which is highlighted in green in Figure 5. contains high energy efficient servers with CPU capacity of 290k MIPS and power consumption of 243 W (maximum) and 160.38 1 W (idle). In fog cell2, highlighted in red, we considered low energy efficiency servers with CPU capacity of 280k MIPS and power consumption of 457 W (maximum) and 301 W (idle). Fog cell3, highlighted in yellow, comprised of servers with mid-range energy efficiency with CPU capacity of 270k MIPS and power consumption of 325 W (maximum) and 214.5 W (idle). The input data used in the MILP model is shown in Table 5.2.

Table 5.2 The Input Data for the MILP model in a Heterogeneous Collaborative-Fog Computing Architecture.

Fog Cell-1 Server's maximum power consumption (Dell PowerEdge R620) [122].	243 W
Fog Cell-1 Server's idle power consumption [122].	160 W
The cores number of Fog Cell-1 Server's processor[122].	8
Fog Cell-1 Server's Processing capacity (CPU)[122] [110].	83.2k MIPS

Fog Cell-1 Server's Memory capacity (RAM) [122].	16 GB
Fog Cell-2 Server's maximum power consumption (Dell PowerEdge R740) [109].	457 W
Fog Cell-2 Server's idle power consumption[109].	301 W
The cores number of Fog Cell-2 Server's processor[109].	28
Fog Cell-2 Server's Processing capacity [109] [110].	280k MIPS
Fog Cell-2 Server's Memory capacity (RAM)[109]	16 GB
Fog Cell-3 Server's maximum power consumption Hitachi, Ltd. HA8000/RS220-hHM)[123].	325 W
Fog Cell-3 Server's idle power consumption[123].	214W
The cores number of Fog Cell-3 Server's processor[123] [110].	8
Fog Cell-3 Server's Processing capacity [123]	80k MIPS
Fog Cell-3 Server's Memory capacity [123]	8 GB
Memory capacity (RAM) of the VMs [41].	100MB – 500MB
OLT Maximum power consumption [102].	1940 W

OLT idle power consumption	1746 W
OLT data rate [102].	8600 Gbps
ONU Maximum power consumption [104].	2.5 W
ONU idle power consumption [104].	1.5 W
ONU data rate [104].	10 Gbps
VMs Traffic Demands [41].	1Gbps–5 Gbps
Capacity of Optical physical link.	6 wavelengths per fibre at 10 Gbps per wavelength

We have evaluated the total power consumption of the heterogeneous collaborative-fog architecture. Figure 5. presents the total power consumption and its breakdown into the networking power consumption and processing power consumption under different number of VMs. Figure 5. shows the fact that the processing power consumption contribution to the total power consumption is much greater than that of the networking power consumption due to the higher power consumption of servers compared to the PON networking equipment. Hence, VMs are assigned to more efficient servers. The networking power consumption remains constant due to the passive nature of the AWGR-based

PON connecting the fog cells and its low power consumption allowing the placement of the VMs in the most efficient servers.

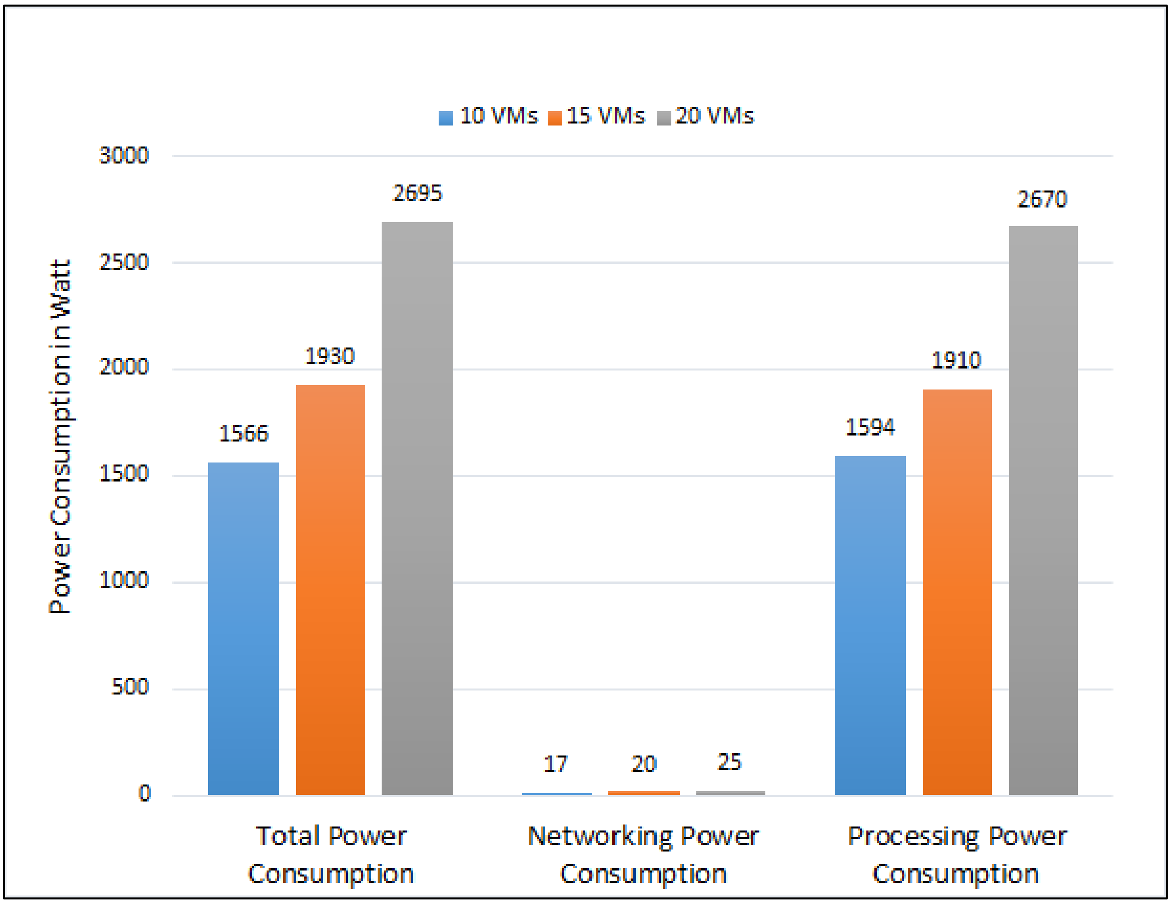

Figure 5.9 The Power Consumption.

Figure 5.10 presents the distribution of the total power consumption among the fog cells and Figure 5.11 presents the server utilisation of the three fog cells under different VM workloads. It can be clearly seen that the model favours fog cell 1 during the VM allocation, due to the processing efficiency of the servers in that cell. The VMs were only allocated to the servers in fog cell 2, the least energy efficient, due to capacity limitations at 20 VMs test case.

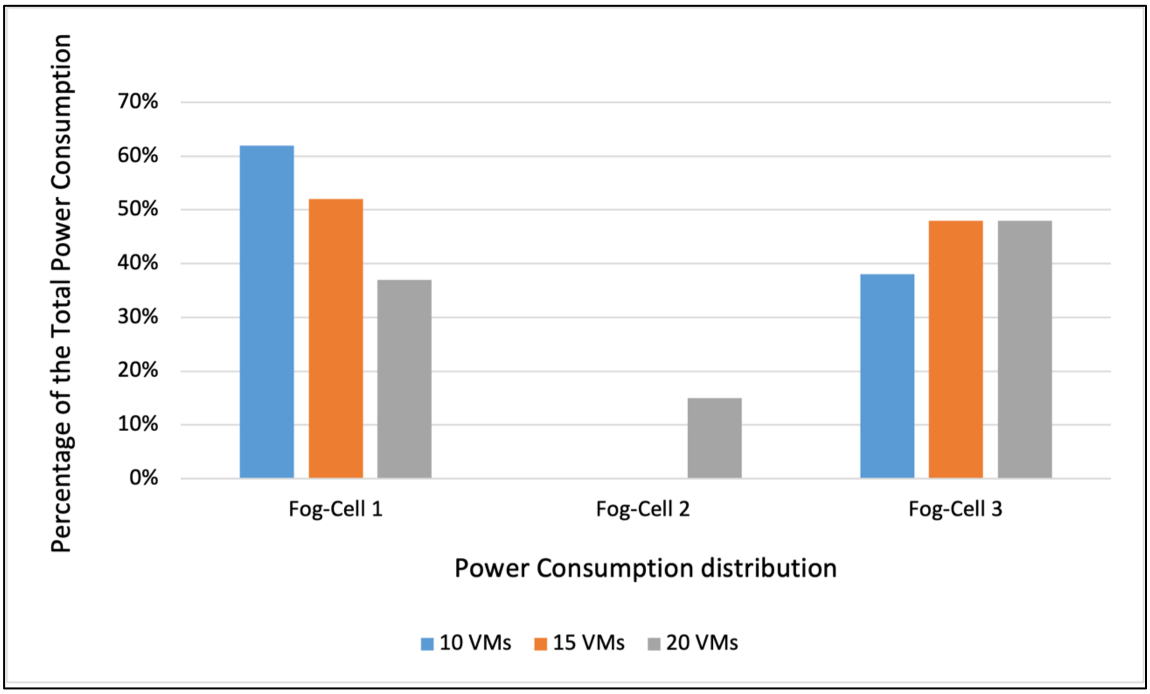

Figure 5.10 Total power consumption distribution

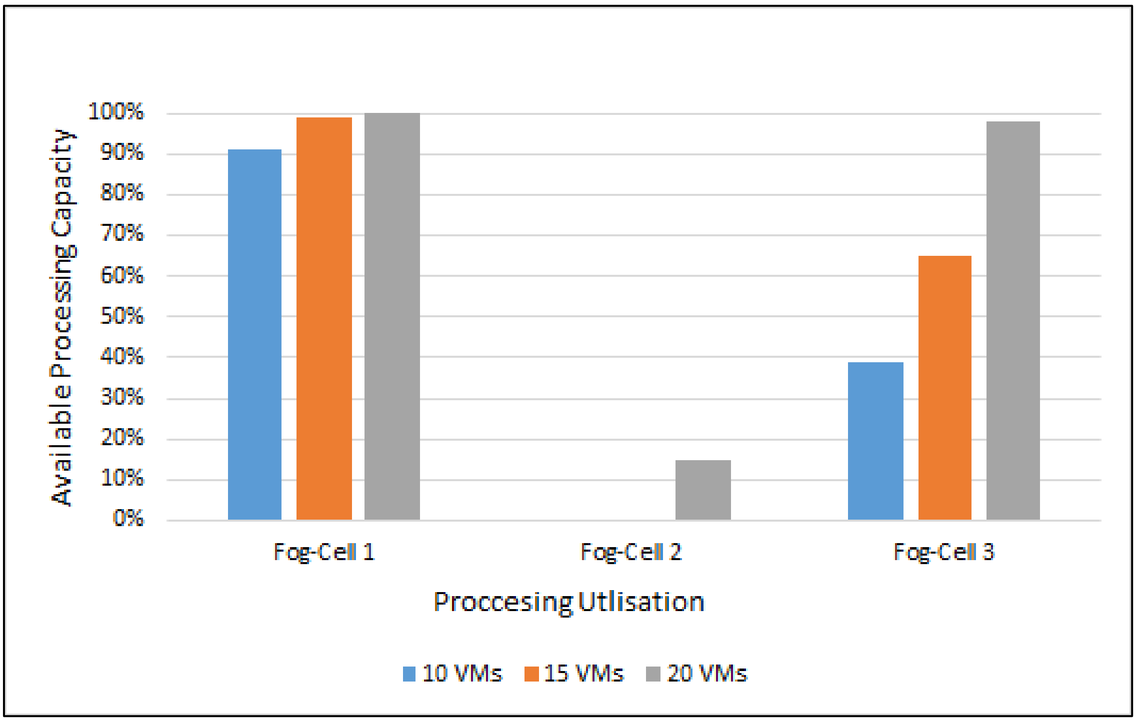

Figure 5.11 The processing utilisation.

5.6 Summary

This chapter evaluated the energy efficiency improvement obtained by the collaborative fog architecture where neighbouring fog cells can collaborate in processing intensive demands.

We compared the collaborative fog approach to the non-collaborative fog approach. The results showed that the collaborative approach improves the energy efficiency by allowing server consolidating across the fog cells facilitated by the passive AWGR based connectivity. Also, this chapter studied the VM placement problem in an architecture of heterogeneous fog cells. The results showed that VMs were better placed in the energy efficient fog servers. The networking power consumption impact is minimal due to the passive nature of PON.

Chapter 6 User Mobility-Aware Collaborative Fog computing Units Architecture

6.1 Introduction

Recent years have witnessed remarkable developments in wireless networking and computing systems related to delay-sensitive applications, which are occasionally associated with non-stationary users. This led researchers to study user-mobility patterns in depth and propose mobility models that can be applied while optimising systems so they can modify allocations of resources across multiple access points in a way that has no impact on the overall performance of networking and computing systems. Considering the user-mobility pattern in fog computing is a key aspect to be considered to overcome challenges such as processing offloading, resources capacity, delay, VM migration, and power consumption [28], [29], [124].

VMs migration, known as VMs mobility, is an optimal management technique for addressing several challenges in both cloud and fog computing, including resources utilisation, load balancing, reduction of the power consumption, and realising mobile applications. VMs migration is considered as a notable feature of virtualisation that allows moving the VMs entirely from one hosted server to another to satisfy the end-users' and the service provider requirements. In the interest of end-users, VMs migration occurs to get closer to the required computational resources which helps in improving the quality of the service and in reducing the latency, which can help attract new users. In the interest of the service provider, VMs migration occurs to reallocate computational resources to reduce power consumption and to meet the end-users' requirements [125], [126]. In addition, the end-users can move across different locations that are served by the same fog units or different fog units, while getting continuous service.

Therefore, user mobility-aware VMs migration plays a crucial role in reducing latency and power consumption [127].

This chapter consider the user-mobility in different time slots among different fog units of the extended proposed collaborative fog computing architecture presented in chapter 5 to achieve an optimal VMs placement for the delay sensitive applications in term of power consumption and propagation delay . We propose a MILP model to minimise the total power consumption and propagation delay in cases where VMs migration are conducted for delay-sensitive application.

6.2 Related Work

Several research projects have investigated end-user mobility in access networks to optimally allocate the resources in term of VMs migration, computation offloading, resource managements, and power consumption [128]–[135]. The author in [128] proposed an algorithm that provided a computation offloading and migration technique to optimally allocate the available resources to minimise the cost of VM migration. The proposed algorithms investigated user-mobility among three fog layers and are characterised by the sojourn time, which is the amount of time spent by the mobile nodes next to the fog computing units (time available to carry out the task) before moving to another computing unit's area. The author in [129] proposed a user mobility framework in fog computing to reduce the latency in IoT application and improve the QoS called Follow Me Fog (FMF). The proposed framework alleviates the impact of user-mobility from one fog computing unit to another while executing the task by avoiding task interruption during the handover. The author in [130] integrated a mobility model and network connectivity with the task offloading decision using genetic algorithms in a smart city for robotics applications to improve the quality of service and minimise power consumption and delay. The proposed genetic algorithm considers three layers of important factors which are task offloading, mobility plan, and access points layer. The authors in [131] proposed a model for resources management in a mobile edge network by predicting user-mobility. The proposed model aims to optimally manage resources by predicating the location of end-users while collecting task to allocate the closest resource for processing. The authors in [132] proposed a handover algorithm and architecture which supports user-mobility in cellular networks. The proposed algorithm effectively managed the resources in mobile edge networking by alleviating the signalling costs resulting from unnecessary handover due to the resource capacities being over utilised at the designated MEC. The author in [133] proposed energy efficient fog computing based on a node-to-node communication architecture and user-mobility algorithms for 5G networks. The proposed model investigated user-mobility from one access point (next-generation evolved nodeB) to another to minimise power consumption. The authors in [134] proposed an energy-aware mobility management framework for MEC, utilising Lyapunov optimisation to minimise the total delay of communication and computation based on various practical deployment scenarios of base stations (BSs). The end-user's choice of candidate BS to offload each task aims to minimise the total delay under the constraint of the end-users' total energy consumption cost of data transmission. The author in [135] proposed a resource allocation algorithm considering user mobility and VMs migration in fog computing based on the Fat Tree data centre architecture to reduce the delay. The proposed algorithm considered different scenarios. First, the VMs are migrated to the cell where the end-users have just moved, which is considered to be the optimal scenario. Second, the VMs migrate to a different cell. The number of fat-tree hops between the end-users and fog nodes plays a significant role in the resource allocation. The more fat-tree hops needed; the more VMs-execution time is needed.

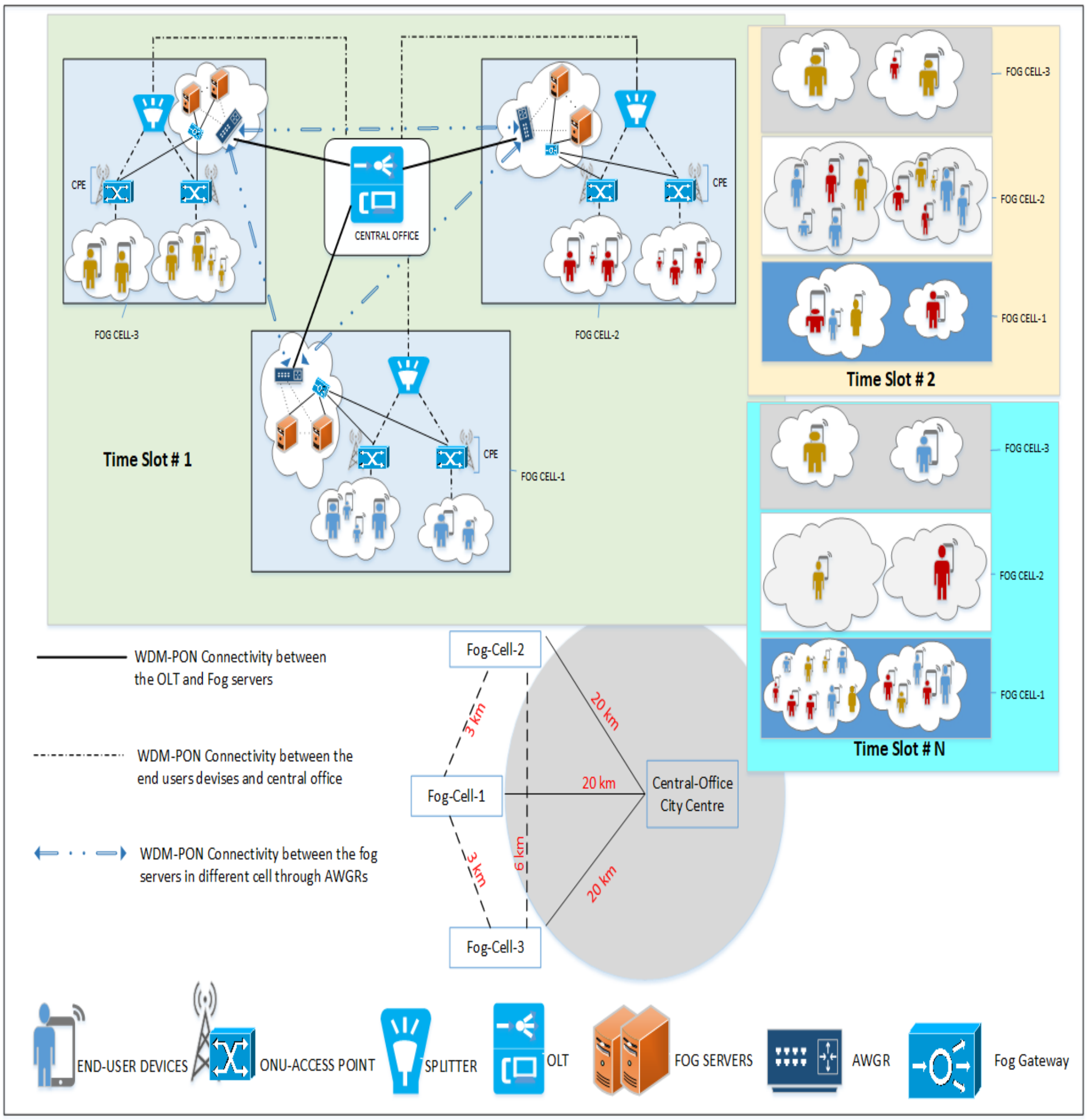

Figure 6.1 User-mobility aware collaborative fog units over PON.

6.3 User-Mobility scenarios

Mobility models are designed to describe the pattern of the mobile users' movements, as well as their current and future positions [74]–[76]. In our optimisation model framework, we consider the Random Waypoint model as a user mobility pattern. The Random Waypoint model, as explained in Chapter 2, is an individual random mobility model, which denotes the unconstrained mobility of the end users [80]. The proposed mobility model uses random movements of end users, however, pause time is included before choosing another random destination to move to. The end user mobile nodes in the Random Waypoint model select a destination randomly. Then they move towards the selected destination. When it arrives at the selected destination, the node pauses for a stated period and then chooses a random destination again and continues with the process [80]. Figure 6.1 illustrates the user's movement between fog units in different time slots. The connectivity between the ONUs within a fog unit the access network and the fog server is assumed to be similar to the work in [136].

6.4 MILP Model

Considering the architecture presented in Chapter 3 and the mobility model in Section 6.3, we developed a MILP model that jointly minimises the total power consumption and the propagation delay by optimising the placement of VM demands, while considering the end-user mobility in different time slots. In the first time slot VM requests from users are optimally placed in servers so the power consumption and propagation delay are minimised. In the second time slot, users move between fog cells and the VMs are migrated to a new server according to the new location of users to ensure minimum power consumption and delay. In the third time slot. Users move again and VMs are migrated to follow them and so on.

The propagation delay between users and servers and between servers (when migrating VMs between servers) is calculated based on the distance between the fog cells, and the distance between the fog cell and the OLT, as shown in Figure 6.1, using:

$$\text{Propagation Delay} = \frac{Đ}{Ç} \qquad (6.1)$$

where Đ represents the distance, and the Ç represents the speed of light. The distances are based on the following assumptions:

The following notations are the sets, parameters and variables used in the optimisation model:

Sets:

F	Set of fog cells.
N	Set of all nodes in the proposed architecture.
N_m	Set of neighboring nodes to node $m, m \in N$.
ONU	Set of access point ONUs in all fog cells, where $ONU \subset N$.
OLT	Set of OLTs, where $OLT \subset N$.
S	Set of servers in all fog cells, where $S \subset N$.
F_S_k	Set of servers within fog cell $k, k \in F$.
F_ONU_k	Set of access point ONUs within fog cell $k, k \in F$.
VM	Set of all VM requests.
VM_ONU_i	Set of VM requests originating from users connected to access point ONU, $i \in ONU$.
I_AWG	Set of input ports in all the AWG Couplers/splitters where $I\_AWG \subset N$.
O_AWG	Set of output ports in all the AWG couplers/splitters, where $O\_AWG \subset N$.

I_AWGR Set of input ports in all the AWGR router in the fog cells, where $I\_AWGR \subset N$.

O_AWGR Set of output ports in all the AWGR router in the fog cells, where $O\_AWGR \subset N$.

T Set of time slots.

Parameters:

WF_{vdt} Weight function for VMs migration with user-mobility, where $v \in VM,\ d \in S$ and $t \in T$.

$Đ_{sd}$ The distance between source $s \in ONU \cup S$ and destination $d \in S$.

$Ç$ Speed of light, $Ç = 299792\ km/s$.

$\mathcal{MU}$ Maximum power consumption of an access point ONU.

$\mathcal{IU}$ Idle power consumption of an access point ONU.

$\mathcal{DU}$ Maximum data rate of an access point ONU.

$\mathcal{EU}$ Energy per bit of an access point ONU, where:

$$\mathcal{EU} = \left(\frac{\mathcal{MU} - \mathcal{IU}}{\mathcal{DU}}\right) \qquad (6.2)$$

$\mathcal{MO}$ Maximum power consumption of an OLT.

$\mathcal{IO}$ Idle power consumption of an OLT.

$\mathcal{DO}$ Maximum data rate of an OLT.

$\mathcal{EO}$ Energy per bit of an OLT port, where:

$$\mathcal{EO} = \left(\frac{\mathcal{MO} - \mathcal{IO}}{\mathcal{DO}}\right) \qquad (6.3)$$

C_{mn} Capacity of the physical link (m, n), where $m, n \in N$.

$\mathcal{M}$ Maximum power consumption of a server.

I Idle power consumption of a server.

C CPU capacity of a server.

R RAM memory capacity of a server.

O The proportional power consumption of a server, where

$$O = \mathcal{M} - I \quad (6.4)$$

ρ Maximum power consumption of an ONU attached to a server.

σ Data rate of an ONU attached to a server.

C_v CPU demand of VM v, $v \in VM$ in MIPS.

R_v RAM memory demand of VM v, $v \in VM$ in GB.

T_v Traffic Demand of each VM $v, v \in VM$ in Gbps.

M A large enough number.

α A unitless weighting parameter for the networking power consumption.

β A unitless weighting parameter for the processing power consumption.

γ A unitless weighting parameter for the propogation delay.

Variables:

L_{sdvt} Traffic demand between source node s and destination node d at time slot t as a result of placing VM v , where $s \in ONU \cup S$, $d \in S$, $v \in VM$, and $t \in T$ (Note that we consider the traffic flow between access point ONUs (users) and servers hosting VMs and traffic flow between servers as a result of VMs migration).

$ßL_{sdvt}$	$ßL_{sdvt}$=1, if there is traffic demand between source node s and destination node d at time slot t as a result of placing VM v , where $s \in ONU \cup S$, $d \in S$, $v \in VM$, and $t \in T$, otherwise $ßL_{sdvt} = 0$.
L_{sdt}^{mnv}	Traffic flow between source node s and destination node d at time slot t as a result of placing VM v traversing physical link link (m, n), where $s \in ONU \cup S$, $d \in S$, $v \in VM$, $t \in T$ and $m, n \in N$.
$ßL_{sdt}^{mnv}$	$ßL_{sdt}^{mnv}$=1, if there is traffic flow between source node s and destination node d at time slot t as a result of placing VM v traversing physical link (m, n), otherwise $ßL_{sdt}^{mnv} = 0$, where $s \in ONU \cup S$, $d \in S$, $v \in VM$, $t \in T$ and $m, n \in N.$
P_{vdt}	Processing demand of VM $v \in VM$ hosted by server $d \in S$ at time slot $t \in T$.
RAM_{vdt}	RAM memory demand of VM $v \in VM$ hosted by server $d \in S$ at time slot $t \in T$.
$Þ_{vdt}$	$Þ_{vdt}$ =1, if processing, and memory demands of VM $v \in VM$ are hosted by server $d \in S$ at time slot $t \in T$ otherwise $Þ_{vdt} = 0$.
$\mathcal{A}_{it}$	Amount of traffic transmitted by access point ONU $i \in ONU$ at time slot $t \in T$.
$\mathcal{B}_{it}$	Amount of traffic gathered by the OLT node i, where $i \in OLT$ and $t \in T$.

$\mathcal{C}_{it}$ Amount of traffic received by the server $i \in S$ at time slot $t \in T$

$\mathcal{D}_{it}$ $\mathcal{D}_{it}$=1, if OLT $i \in OLT$ is activated at time slot $\in T$, otherwise $\mathcal{D}_{it}$=0.

$\mathcal{E}_{it}$ $\mathcal{E}_{it}$ =1, if access point ONU $i \in ONU$ is activated at time slot $t \in T$, otherwise $\mathcal{E}_{it}$=0.

$\mathcal{F}_{it}$ $\mathcal{F}_{it}$=1, if server $i \in S$ is activated at time slot $t \in T$, otherwise $\mathcal{F}_{it} = 0$.

θ_{it} Defined as the AND of two variables $\mathcal{B}_{it}$ and $\mathcal{D}_{it}$, where $i \in OLT$ and $t \in T$.

$\mathbb{N}$ Networking power consumption.

$\mathbb{P}$ Processing power consumption.

$\mathbb{Y}$ Propagation delay.

The total power consumption at each time slot is composed of : networking power consumption($\mathbb{N}$), and processing power consumption ($\mathbb{P}$).

- The networking power consumption at time slot $t \in T$, ($\mathbb{N}$), is composed of:

  a. The power consumption of the access point ONUs at time slot $t \in T$:

$$\left(\sum_{i \in ONU} \mathcal{EU}\, \mathcal{A}_{it} + \sum_{i \in ONU} \mathcal{IU}\, \mathcal{E}_{it} \right) \qquad (6.5)$$

$$\forall \; t \in T$$

  b. The power consumption of OLTs at time slot $t \in T$:

$$\left(\sum_{i \in OLT} \mathcal{EO}\, \mathcal{B}_{it} + \sum_{i \in OLT} \mathcal{IO}\, \frac{\theta_{it}}{\mathcal{DO}} \right) \qquad (6.6)$$

$$\forall \; t \in T$$

- The Processing power consumption at time slot $t \in T$, ($\mathbb{P}$), is composed of:

  a. The power consumption of the servers at time slot $t \in T$,:

$$\left(\sum_{d \in S} I \; \mathcal{F}_{dt} + \frac{O}{C} \sum_{\substack{v \in VM \\ d \in S}} P_{vdt} \right) \quad (6.7)$$

$$\forall \; t \in T$$

$$\text{where}, \; P_{vdt} = C_v \; Þ_{vdt}$$

  b. The power consumption of ONU attached to servers at time slot $t \in T$:

$$\frac{\rho}{\sigma} \sum_{d \in S} \mathcal{F}_{dt} \quad (6.8)$$

$$\forall \; t \in T$$

Note that as explained in Chapter 5, the ONU devices are of two types: 1) the ONUs attached to processing servers which work as transceivers and these have an on/off power consumption profile, 2) the ONUs used at access points and these have a proportional plus an idle power consumption profile [121].

- The propagation delay experienced by traffic flows at time slot $t \in T$, ($\mathbb{Y}$) is given as:

$$\mathbb{Y} = \sum_{v \in VM} ßL_{sdvt} \; * \; \frac{Đ_{sd}}{R\hat{I} \quad Ç} \qquad (6.9)$$

$$\forall s \in N, d \in \mathrm{S} \text{ and } t \in \mathrm{T}$$

where $R\hat{I}$ is added to equation (6.9) as a refractive index to define the ratio of the speed of light in WDM-PON connection (fibre link) to the speed of light in free space. It is given as $\frac{2}{3}$ [137].

The MILP model is defined as follows:

The objective: To minimise the total power consumption, including networking power consumption and processing power consumption and the propagation delay and maximise the VM migration reward function at each time slot considering user mobility [121]:

$$(\alpha \; \mathbb{N} \; + \; \beta \, \mathbb{P} + \gamma \, \mathbb{Y}) \; - \; M \sum_{\substack{v \in VM \\ s \in ONU \cup S \\ d \in S}} ßL_{sdvt} \quad WF_{vdt} \qquad (6.10)$$

$$\forall \;\; t \in T$$

Subject to the following constraints:

$$\sum_{\substack{n \in N_m \\ m \neq n}} L_{sdt}^{mnv} - \sum_{\substack{n \in N_m \\ m \neq n}} L_{sdt}^{nmv} = \begin{cases} L_{sdvt} & m = s \\ -L_{sdvt} & m = d \\ 0 & otherwise \end{cases} \qquad (6.11)$$

$$\forall \;\; s \in ONU \;\cup\; S \,, d \in S, s \neq d$$

$$\forall \; v \; \in VM \,, m \in \mathrm{N}, t \in \mathrm{T}$$

Constraints (6.11) is the traffic flow conservation constraint to ensure that the traffic demand for each VM that enters a node leaves it at same level (except for the source and destination nodes). Constraint (6.11) is for both traffic demands initiating from access point ONUs (users) and from servers.

$$\mathcal{A}_{it} = \sum_{\substack{s \in ONU \cup S \\ d \in S \\ v \in VM \\ n \in N_i}} L_{sdt}^{inv} + \sum_{\substack{s \in ONU \cup S \\ d \in S \\ v \in VM \\ n \in N_i}} L_{sdt}^{niv} \qquad (6.12)$$

$$\forall\ i \in ONU,\ t \in T$$

$$\mathcal{B}_{it} = \sum_{\substack{s \in ONU \cup S \\ d \in S \\ v \in VM \\ n \in N_i}} L_{sdt}^{inv} + \sum_{\substack{s \in ONU \cup S \\ d \in S \\ v \in VM \\ n \in N_i}} L_{sdt}^{niv} \qquad (6.13)$$

$$\forall\ i \in OLT,\ t \in \mathrm{T}$$

$$\mathcal{C}_{it} = \sum_{\substack{s \in ONU \cup S \\ d \in S \\ v \in VM \\ n \in N_i}} L_{sdt}^{inv} + \sum_{\substack{s \in ONU \cup S \\ d \in S \\ v \in VM \\ n \in N_i}} L_{sdt}^{niv} \qquad (6.14)$$

$$\forall\ i \in S,\ t \in \mathrm{T}$$

The relations in (6.12), (6.13), and (6.14) are given to calculate the amount of traffic that is transmitted/received by the access point ONUs, OLT, and fog servers.

$$\theta_{it} \leq M\,\mathcal{D}_{it} \qquad (6.15)$$

$$\forall\ i \in OLT,\ t \in T$$

$$\theta_{it} \leq M\,\mathcal{B}_{it} \qquad (6.16)$$

$$\forall\ i \in OLT,\ t \in T$$

$$\theta_{it} \geq \mathcal{D}_{it} - (1 - \mathcal{B}_{it})M \qquad (6.17)$$

$$\forall\ i \in OLT,\ t \in T$$

$$\theta_{it} \geq 0 \qquad (6.18)$$

$$\forall\, i \in OLT \;\;,\;\; t \in T$$

Constraints (6.15), (6.16), (6.17) and (6.18) are used to linearise the multiplication of two variables $\mathcal{D}_{it}$ and $\mathcal{B}_{it}$ (i.e., to linearise $\theta_{it} = \mathcal{D}_{it}\, \mathcal{B}_{it}$), where $i \in OLT$, and $t \in T$.

$$\sum_{\substack{s \in ONU \,\cup\, S \\ d \in S \\ s \neq d}} L_{sdvt} = T_v \qquad (6.19)$$

$$\forall\, v \in VM \,, t \in T$$

Constraint (6.19) ensures that the traffic demand for each VM source node s $\in \gamma$ is met at a given destination node.

$$M\, L_{sdvt} \geq\; ßL_{sdvt}$$

$$\forall\, s \in ONU \;\cup\; S\; \forall\, d \in S \;, s \neq d \qquad (6.20)$$

$$\forall\, v \in VM \,, t \in T$$

$$L_{sdvt} \leq\; M\;\; ßL_{sdvt}$$

$$\forall\, s \in ONU \;\cup\; S\; \forall\, d \in S, s \neq d \qquad (6.21)$$

$$\forall\, v \in VM \,, t \in T$$

Constraint (6.20) and (6.21) are given to relate the binary traffic demand variable $ßL_{sdvt}$ to the non-binary variable L_{sdvt} .

$$\sum_{d\in S} L_{sdvt} = T_v \qquad (6.22)$$

$\forall\ s \in VM\_ONU, v \in VM, t = 1$

$$\sum_{s\in ONU \cup S} L_{sdvt'} = \sum_{s\in S} L_{dsvt} \qquad (6.23)$$

$\forall\ d \in S, v \in VM, t' = t-1, t > 1$

Constraints (6.22) and (6.23) are given to ensure that the traffic demand for each $v \in VMs$ at time slot $t' = t-1, t > 1$ is equivalent to the traffic demand served in the following time slot $t \in T, t > 1$.

$$\sum_{d\in S} P_{vdt} = C_v \qquad (6.24)$$

$\forall\ v \in VM , t \in T$

Constraint (6.24) ensures that the processing demand for each $v \in VMs$ at each time slot $t \in T$ is met at servers.

$$M\ P_{vdt} \geq Þ_{vdt} \qquad (6.25)$$

$\forall\ d \in S, v \in VM , t \in T$

$$P_{vdt} \leq M\ Þ_{vdt} \qquad (6.26)$$

$\forall\ d \in S, v \in VM , t \in T$

Constraints (6.25) and (6.26) are given to relate the binary processing demand variable $Þ_{vdt}$ to the non-binary variable P_{vdt}.

$$\sum_{d \in S} RAM_{vdt} = R_v \tag{6.27}$$

$$\forall\, v \in VM, t \in T$$

Constraint (6.27) ensures that the processing demand for each $v \in VM$ at each time slot $t \in T$ is met by servers.

$$M\, RAM_{vdt} \geq Þ_{vdt} \tag{6.28}$$

$$\forall\, d \in S, v \in VM, t \in T$$

$$RAM_{vdt} \leq M\, Þ_{vdt} \tag{6.29}$$

$$\forall\, d \in S, v \in VM, t \in T$$

Constraints (6.28) and (6.29) are given to relate the binary variable for the memory demand $Þ_{vdt}$ to the non-binary variable RAM_{vdt} .

$$M \sum_{s \in ONU \cup S} L_{sdvt} \geq Þ_{vdt} \tag{6.30}$$

$$\forall\, d \in S, v \in VM, t \in T$$

$$\sum_{s \in ONU \cup S} L_{sdvt} \leq M Þ_{vdt} \tag{6.31}$$

$$\forall\, d \in S, v \in VM, t \in T$$

Equation (6.30) and (6.31) are given to relate the binary variable that indicates that the processing and memory demands of a VM are met by a server, $Þ_{vdt}$, at time slot $t \in T$ to the traffic demand between the source of the VM and the sever, i.e. these equations ensure that the processing, memory and traffic of a VM are served by a the same sever. each $v \in VM$

$$\sum_{v \in VM} C_v \, P_{vdt} \leq C \qquad (6.32)$$
$$\forall \; d \in S \;, t \in T$$

Equation (6.32) ensures that the processing demands of VMs hosted by a server at each time slot do not exceed the processing capacity of the server.

$$\sum_{v \in VM} R_v \, RAM_{vdt} \leq R \qquad (6.33)$$
$$\forall \; d \in S \;, t \in T$$

Equation (6.33) ensures that the memory demand of VMs hosted by a server at each time slot does not exceed the memory capacity of the server.

$$\mathcal{A}_{it} \leq \mathcal{DU} \qquad (6.34)$$
$$\forall \; i \in ONU \;, \qquad t \in T$$

Equation (6.34) ensures that the total traffic load on an access point ONU does not exceed the data rate of the ONU.

$$\mathcal{C}_{it} \leq \sigma \qquad (6.35)$$
$$\forall \; i \in S, t \in T$$

Equation (6.35) ensures that the total traffic load on a server does not exceed the data rate of the ONU attached to the server.

$$\sum_{v \in VM} \sum_{d \in S} L_{sdt}^{mnv} \leq C_{mn} \qquad (6.36)$$
$$\forall \; s \in ONU \; \cup \; S \;, n \in N, m \in N_m, t \in T$$

Equation (6.36) ensures that the total traffic demand traversing physical link (m, n) does not exceed the capacity of the link.

$$\sum_{d \in S} Þ_{vdt} \leq 1 \quad (6.37)$$

$$v \in VM, t \in T$$

Equation (6.37) ensures that the number of servers that host each VM request is limited to one.

$$\mathcal{A}_{it} \geq \mathcal{E}_{it} \quad (6.38)$$

$$\forall \; i \in ONU, \; t \in \mathrm{T}$$

$$\mathcal{A}_{it} \leq M \, \mathcal{E}_{it} \quad (6.39)$$

$$\forall \; i \in ONU, \; t \in T$$

Constraints (6.38) and (6.39) relate the binary variable for the access point ONU $\mathcal{E}_{it}$ to the non-binary variable $\mathcal{A}_{it}$.

$$\mathcal{B}_{it} \geq \mathcal{D}_{it} \quad (6.40)$$

$$\forall \; i \in OLT, \quad t \in \mathrm{T}$$

$$\mathcal{B}_{it} \leq M \, \mathcal{D}_{it} \quad (6.41)$$

$$\forall \; i \in OLT, \; t \in \mathrm{T}$$

Equations (6.40) and (6.41) ensure that, the binary variable for the OLT $\mathcal{D}_{it}$ to the non-binary variable $\mathcal{B}_{it}$.

$$\sum_{v \in VM} P_{vit} \geq \mathcal{F}_{it} \tag{6.42}$$

$$\forall \; i \in S, \quad t \in T$$

$$\sum_{v \in VM} P_{vit} \leq M \, \mathcal{F}_{it} \tag{6.43}$$

$$\forall \; i \in S, t \in T$$

Equations (6.42) and (6.43) relate the binary variable for the server $\mathcal{F}_{it}$ to the sum of the processing demand of VMs hosted by the server.

$$\sum_{v \in VM} L_{sdt}^{mnv} \leq 0$$

$$\forall s \in ONU \cup S, \forall d \in S, s \neq d$$

$$\forall m \in O\_AWG, \forall n \in I\_AWG \tag{6.44}$$

$$\forall t \in T$$

Equation (6.44) demonstrates the flow direction inside the AWG couplers / splitters, i.e., the flow direction is only from the input ports to the output ports.

$$\sum_{v \in VM} L_{sdt}^{mnv} \leq 0$$

$$\forall s \in ONU \cup S, \forall d \in S, s \neq d$$

$$\forall m \in O\_AWGR, \forall n \in I\_AWGR \tag{6.45}$$

$$\forall t \in T$$

Equation (6.45) ensures the correct flow direction inside the AWGR routers, i.e., the flow direction is only from the input ports to the output ports. It is important to note that the connectivity between the fog cells based on the wavelength assignment discussed in Chapter 3 is considered in this model.

6.5 MILP MODEL RESULT

To evaluate the impact of user-mobility on the total power consumption of the collaborative fog computing architecture, we consider placing and migrating 10 VM requests between the fog units at three time slots. The CPU capacity, memory capacity and traffic data rate of the VMs are randomly distributed between the values given in Table 6.1.

The distance between the ONUs in access points and the OLT is based on the typical PON architecture. As shown in Figure 6.1, the OLT is located in the central office and the access points ONUs are located at the end-users' location. Therefore, we have assumed 20 km as the distance between them. The distance between fog servers located in the fog cells and the OLT is 20 km based on the typical PON architecture. The distances between the collaborative fog units connected over the AWGR-PON are as follow:

- The distance between Fog-Cell-1 and Fog-Cell-2 is 3 km.
- The distance between Fog-Cell-1 and Fog-Cell-3 is 3 km.
- The distance between Fog-Cell-2 and Fog-Cell-3 is 6 km.

Table 6.1 The input data for the user mobility model.

Server's maximum power consumption [109].	457 W
Server's idle power consumption (66% of Maximum power) [109].	301 W
Processing capacity of the server [109].	280k MIPS
Processing capacity of the VMs.	10k MIPS - 280k MIPS
Memory capacity (RAM) of the server [109].	16 GB

Memory capacity (RAM) of the VMs.	100 MB - 500 MB
OLT Maximum power consumption [102].	1940 W
OLT idle power consumption (90% of Maximum power).	1746 W
OLT data rate [102].	8600 Gbps
ONU Maximum power consumption [104].	2.5 W
ONU idle power consumption (60% of Maximum power) [104].	1.5 W
ONU data rate [104].	10 Gbps
VMs Traffic Demands.	1 Gbps – 5 Gbps
Capacity of Optical physical link.	6 wavelengths per fibre at 10 Gbps per wavelength

Figure 6.2 show how the processing load of the fog cells changes over three time slots. As shown in Figure 6.2, the processing load of fog cell 1 for had decreased by 45% in time slot 2 compared to time slot 1 while it has increased by 81% in the time slot 3 compared to the time slot 2. For fog cell 2, the processing load has increased by 60% in time slot 2 compared to time slot 1 while it has decreased by 81% in time slot 3 compared to time slot 2 . For fog cell 3, there are no VM assignment in time slots 2 and 3 as no end-users were nearby this cell and hence, no VMs were migrated to fog cell 3 in these time slots.

Figure 6.3 shows the VMs placement in the fog cells at the three time slots. We have classified the VMs into three groups coloured red, blue, and green based on the fog cell they were assigned to in the first time slot. As shown in Figure 6.3, the red and green groups have been migrated over the three time slots, while the blue group have only migrated in the last time slot. Also, despite the similarity in VMs number, Figure 6.2 shows that the red group of VMs have utilised more processing capacity of the fog servers compared to the blue group as the VMs' processing demand of the red group is higher than the blue group.

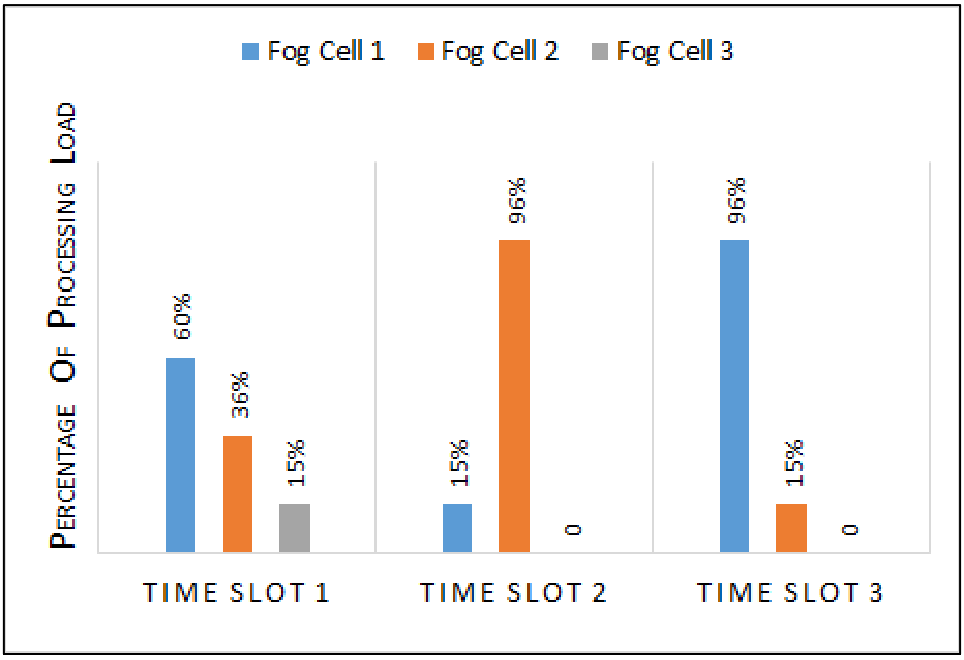

Figure 6.2 Processing load among collaborative fog units in different time slots.

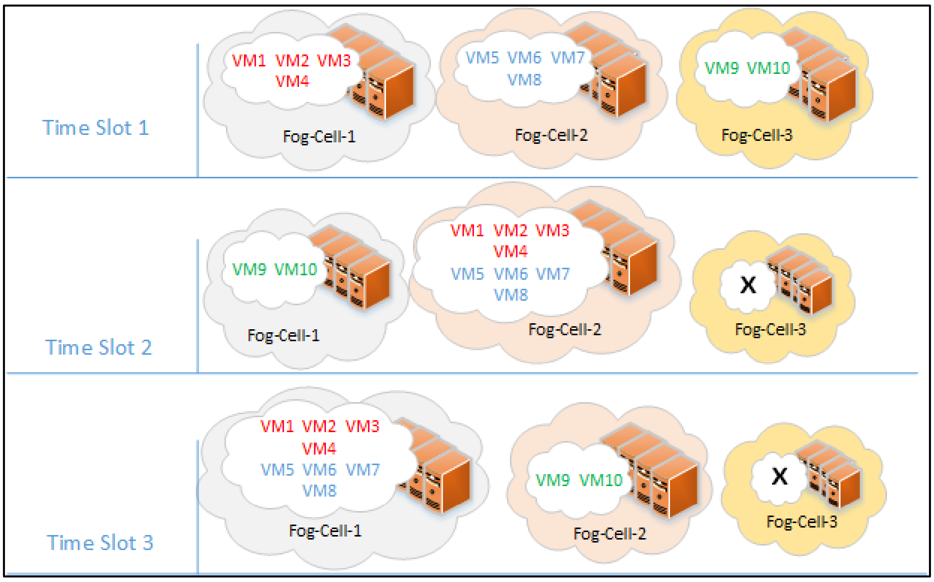

Figure 6.3 Placement of VMs in collaborative fog units in different time slots.

6.5.1 Scenario 1: Joint minimisation model of Total Power Consumption and Propagation Delay (Ô)

We evaluate the efficiency of the proposed joint minimisation objectives, as shown in equation 6.10 of the placement and migration of VMs for different paths in the proposed collaborative fog units over PON architecture, either over AWGRs or over the OLT. To minimise the total power consumption ($\mathbb{N} + \mathbb{P}$) and the propagation delay ($\mathbb{Y}$) jointly, we have set up the values of $\alpha,\ \beta,\ and\ \gamma$ to 1 in equation 6.10.

Figure 6.4, and Figure 6.5 show the total power consumption, including the processing power consumption and the networking power consumption. We found that the processing power consumption is the same value on both paths, as shown in Figure 6.4 and Figure 6.5, due to it utilising the same number of activated servers as shown in Figure 6.6. Notice the difference in networking power consumption in both paths especially in time slot 2 and time slot 3. Note that, time slot 1 represents the VMs original placement where the OLT must be used (the OLT is used for users to communicate with fog). The VMs migration occurred in time slot 2 and time slot 3 along with user mobility and either the OLT or the AWGRs are used to migrate the VMs. Therefore, the impact of VMs migration on the power consumption and delay can be clearly noticed in time slot 2 and time slot 3. The networking power consumption for VMs migration over the collaborative fog units over AWGRs is minimised by 100%, compared to the VMs migration over the collaborative fog units over OLT, as shown in Figure 6.4 and Figure 6.5. This has result in a reduction in the total networking power consumption over three time slots by 55%, as shown in Figure 6.7.

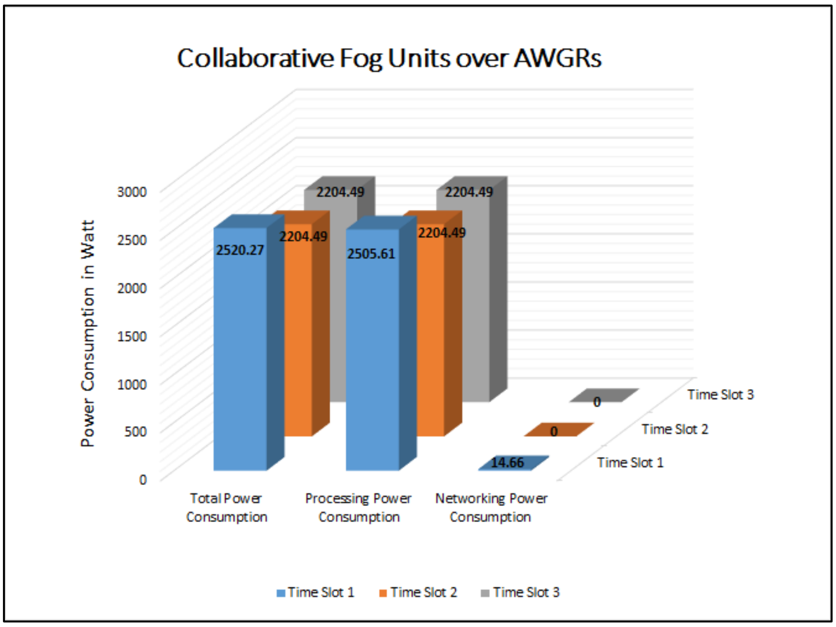

Figure 6.4 Power Consumption of VMs placement and migration among collaborative fog units over AWGRs.

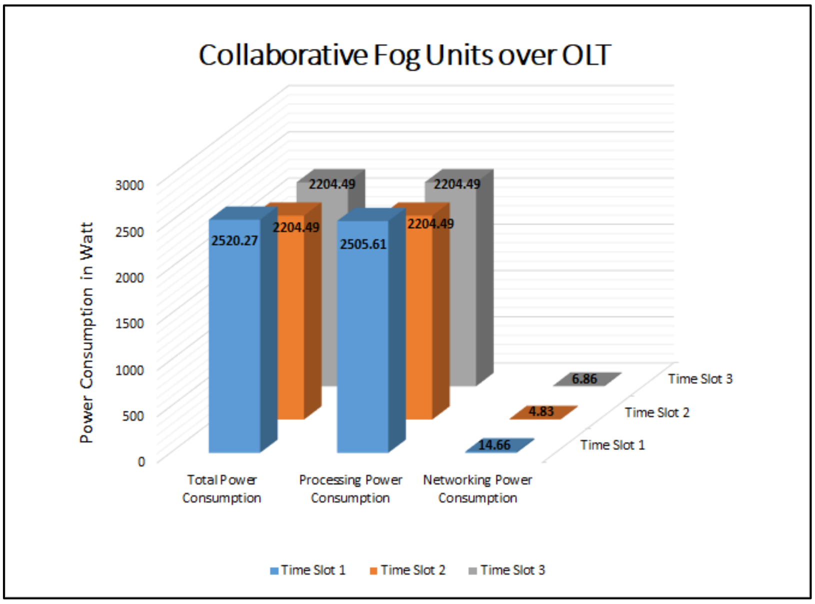

Figure 6.5 Power Consumption of VMs placement and migration among collaborative fog units over OLT.

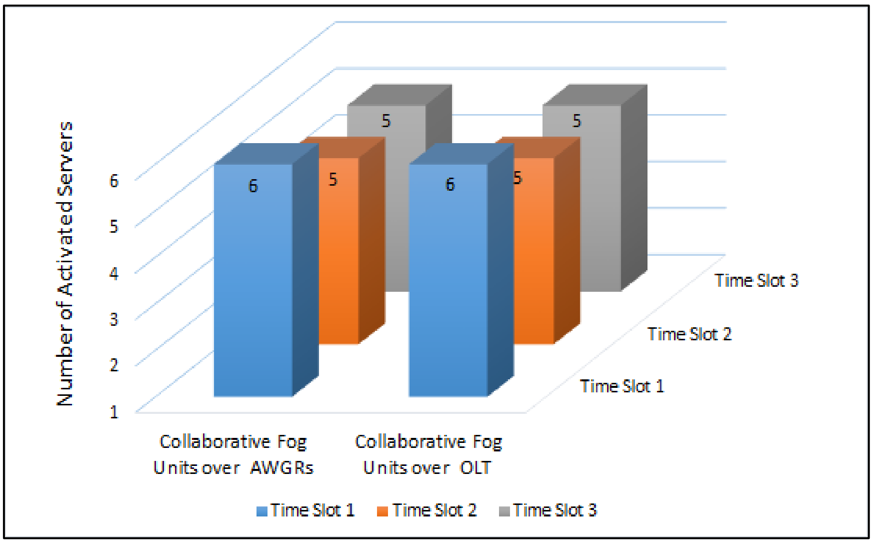

Figure 6.6 Number of Activated Servers of joint minimisation model.

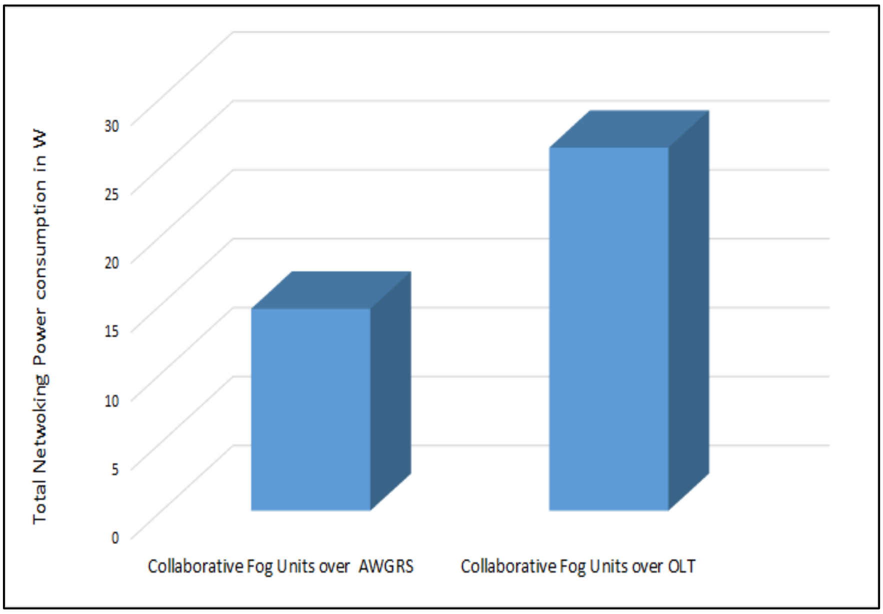

Figure 6.7 Total Networking Power consumption of joint minimisation model.

Figure 6.8 and Figure 6.9. give the propagation delay in milliseconds (ms) of the placement and migration of VMs for both paths, either over AWGRs or over the OLT. In time slot 1, as shown in Figure 6.8 and Figure 6.9, the propagation delay is the same, 0.2 ms, which is the propagation time from the end-users' access point ONU to the OLT and from the OLT to the closer fog servers from which the end user sent the VMs requests. In time slot 2 and time slot 3, the propagation delay is minimised when the VMs have migrated over AWGRs by 92% compared to the case where the VMs have been migrated over the OLT. As we can see in time slot 2 in Figure 6.8 and Figure 6.9 that the propagation delay for the blue group is 0, because the end users stayed within the same fog cell. Figure 6.10 summarises the average of the propagation delay of VMs migration over both routes, AWGRs or OLT. There is a remarkable reduction in propagation delay when the VMs migrated over AWGRs.

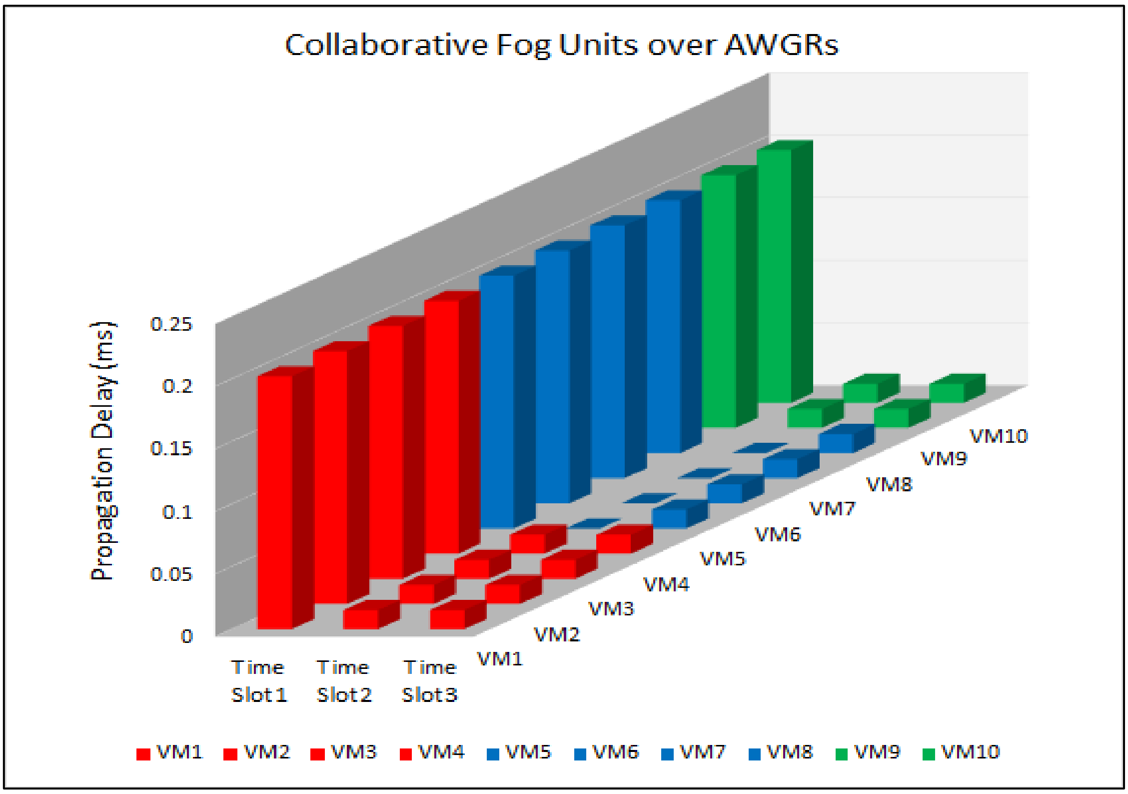

Figure 6.8 Propagation delay of VMs migration among collaborative fog units over AWGRs in the joint minimisation model.

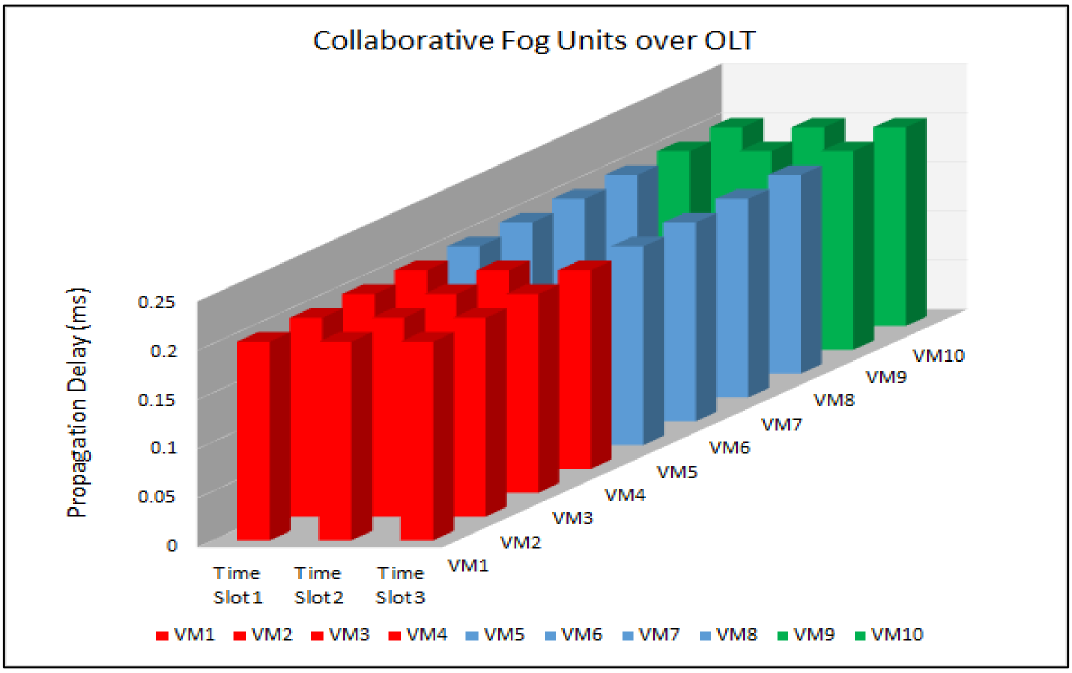

Figure 6.9 Propagation delay of VMs migration among collaborative fog units over OLT in the joint minimisation model.

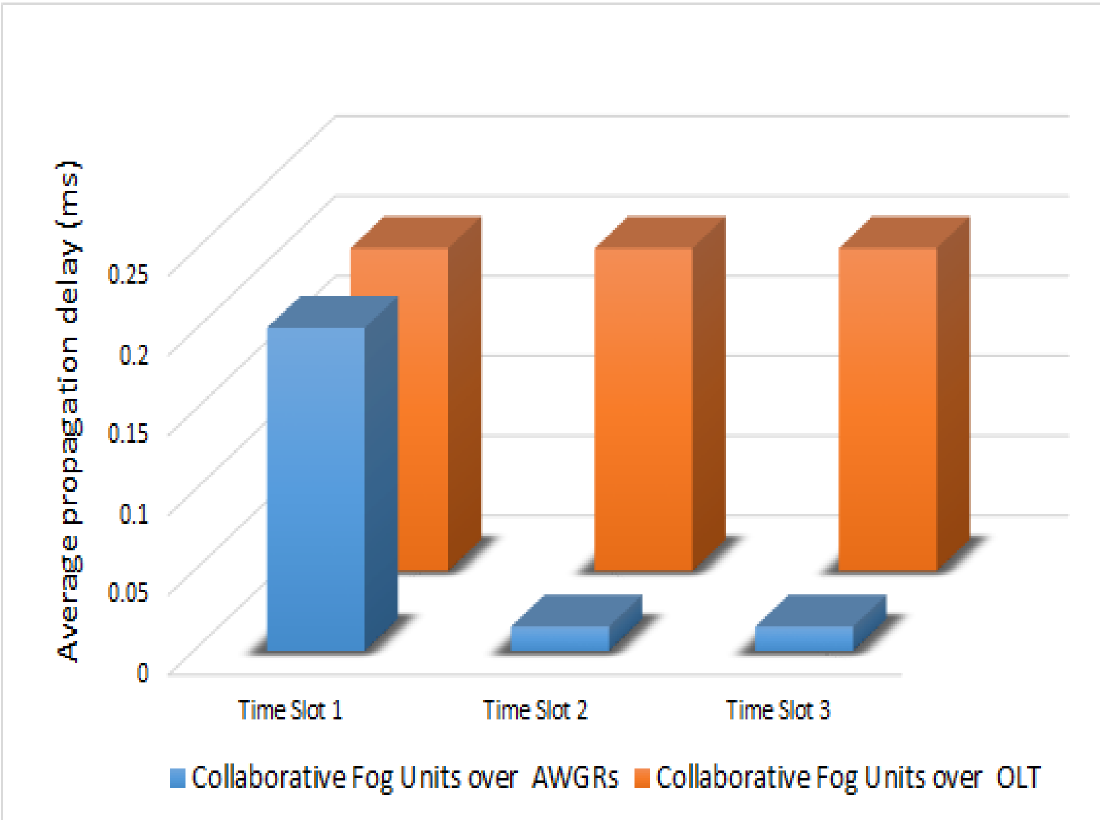

Figure 6.10 Average propagation delay.

6.5.2 Scenario 2: Variation of the objectives

In this scenario, we study the collaborative fog architecture with user mobility under the following variations of the objectives:

- Minimising the processing power consumption only **(Ä)**, by setting the values of $\alpha\ to\ 1;\ and\ \ \beta\ and\ \ \gamma$ to 0 in Equation (6.10).
- Minimising the networking power consumption only **(þ)**, by setting the values of $\beta\ to\ 1;\ and\ \ \alpha\ and\ \ \gamma$ to 0 in Equation (6.10).
- Minimising the propagation delay only **(ÿ)**, by setting the values of $\gamma\ to\ 1;\ and\ \ \alpha\ and\ \ \beta$ to 0 in Equation (6.10).

All the above objectives have considered that the VMs migration can occur over OLT or AWGRs for the previous set of 10 VMs (i.e., the red, blue, and green groups).

6.5.2.1 Minimising the processing power consumption only (Ä)

In this section, we study the results of the proposed model with the objective of only minimising the processing power consumption and compare it to the results of the joint minimisation model of total power consumption and delay (Ô)

Figure 6.11 shows the total power consumption, including the processing power consumption and the networking power consumption, while Figure 6.12 shows the propagation delay in (ms). The total power consumption results obtained from only minimising the processing power consumption objective, as shown in Figure 6.11, matches the optimal total power consumption obtained from the joint minimisation model as shown in Figure 6.4 as both models have migrated the VMs over the AWGRs. Both models with different objectives use the same number of activated servers, as shown in Figure 6.13 which are 6 activated servers in time slot 1 and 5 activated servers in time slot 2 and time slot 3. However, the propagation delay obtained from minimising only the processing power consumption was higher compared to the joint minimisation model results, as shown in Figure 6.12, especially in time slot 1 compared to the optimal results as shown in Figure 6.8. That is because some VMs (e.g., VM1, VM2, and VM3) have crossed among multiple fog cells through AWGRs before reaching the final fog server destination.

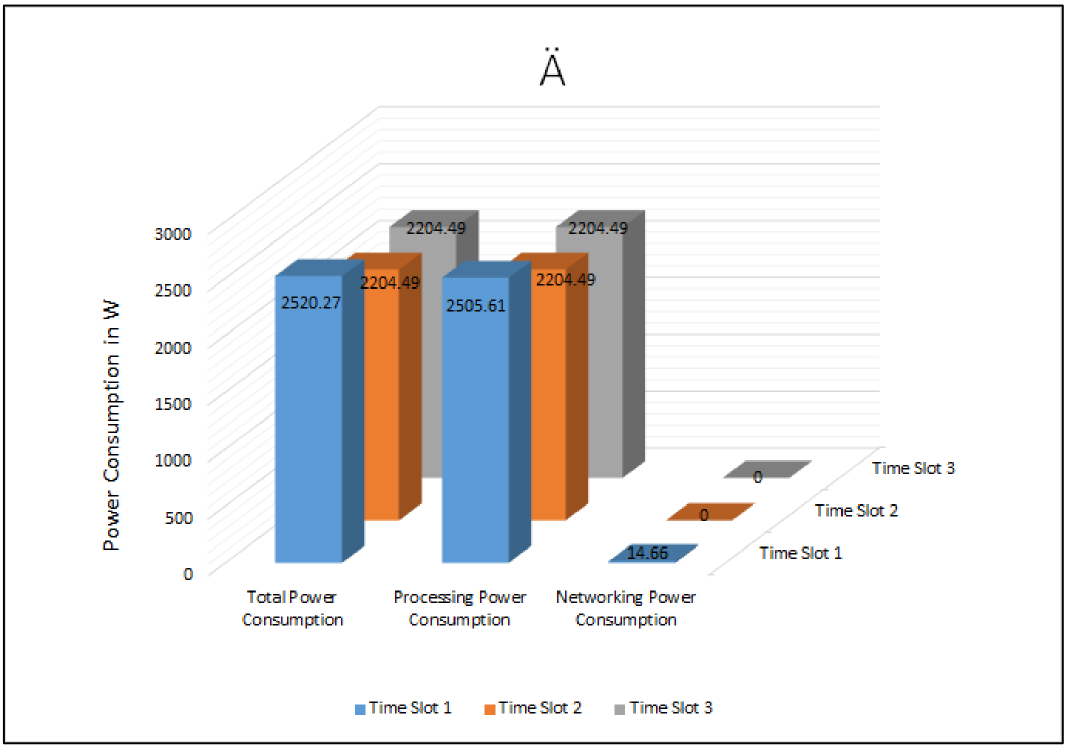

Figure 6.11 Power consumption when minimising only the processing power consumption.

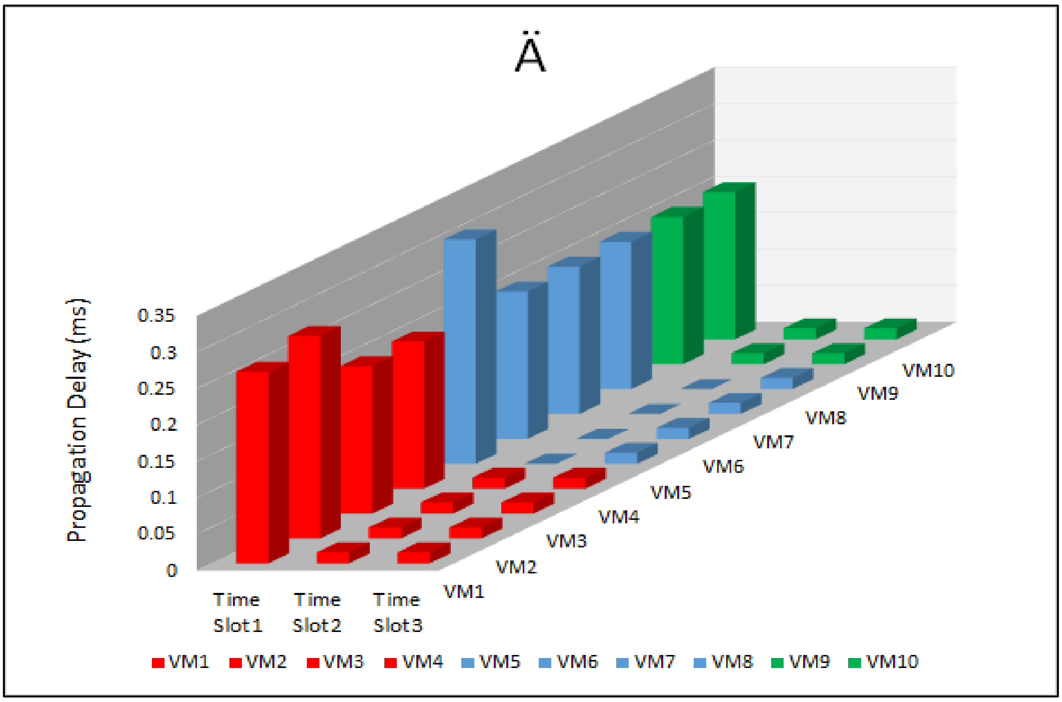

Figure 6.12 Propagation delay when minimising only the processing power consumption.

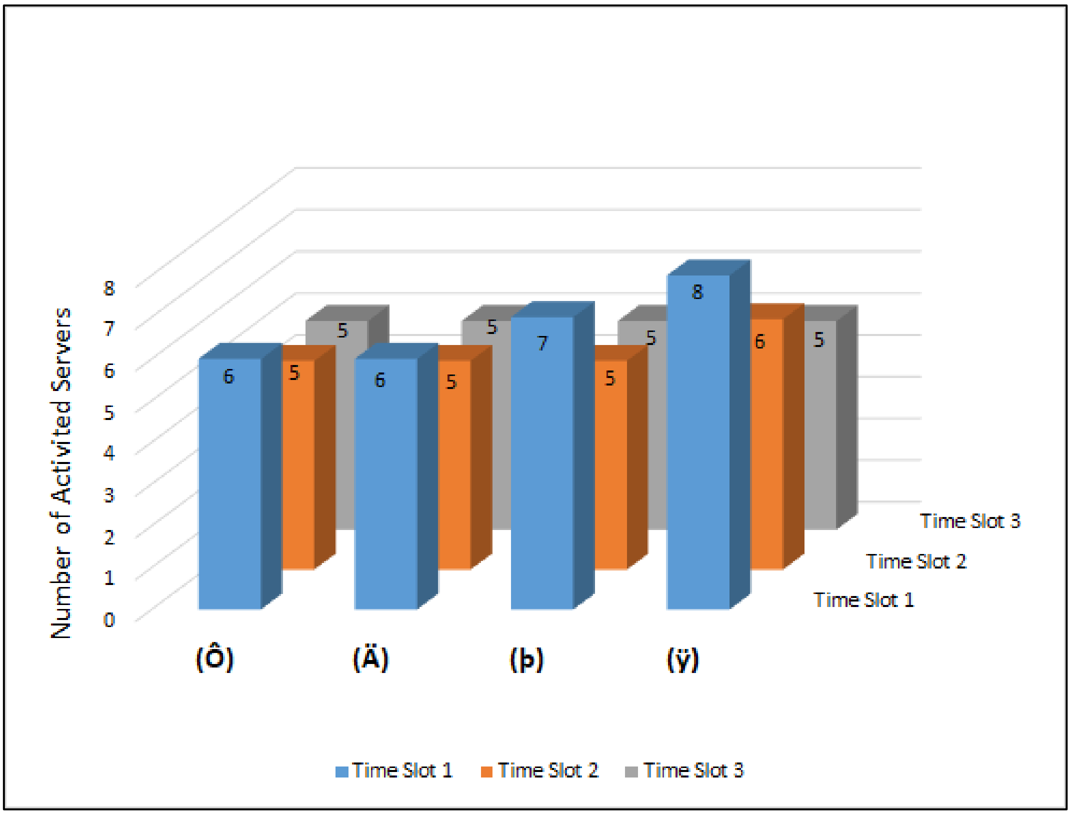

Figure 6.13 Number of activated severs when considering the different objectives.

6.5.2.2 Minimising the networking power consumption only (Þ)

In this section, we study the results of the proposed model with the objective of minimising the networking power consumption only and compare them to the joint minimisation objective (Ô) of total power consumption and delay model results and to the minimisation objective (Ä) of the processing power consumption only model results.

Figure 6.14 shows an increase in the total power consumption by 10%, compared to the joint minimisation model and the minimising only the processing power consumption model. Most of this increase occurs in time slot 1. The reason behind the increased processing power consumption is that the number of activated servers has increased in time slot 1, as shown in Figure 6.13, as the processing power consumption is not considered. Figure 6.15 shows more propagation delay compared to all other scenarios.

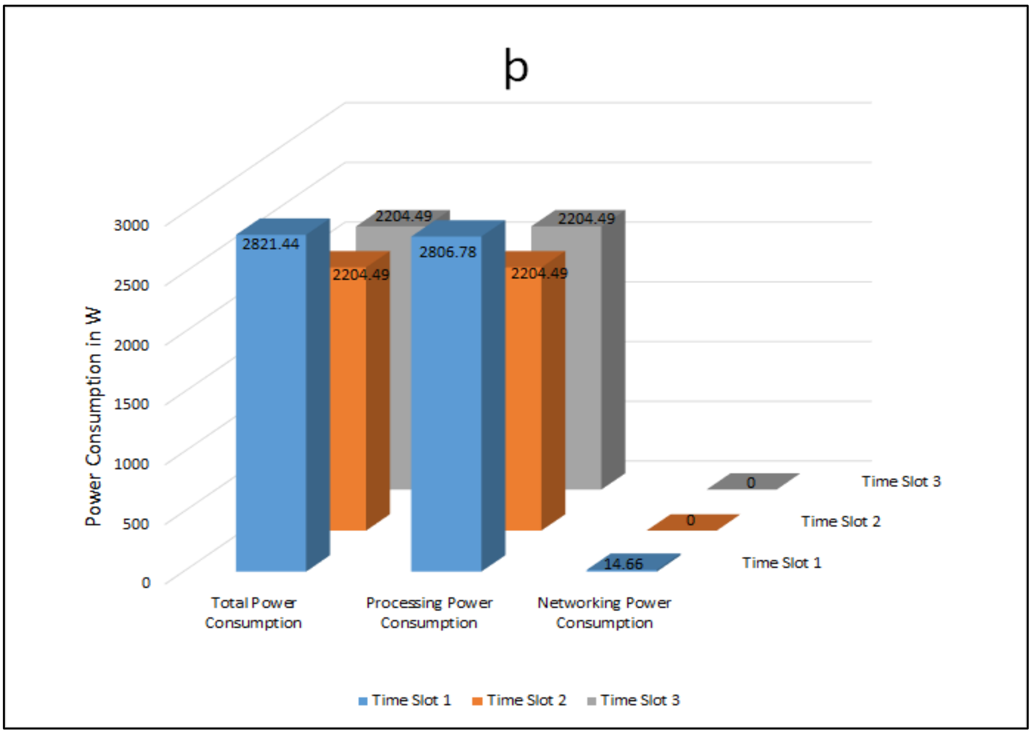

Figure 6.14 Power consumption when minimising the networking power consumption only.

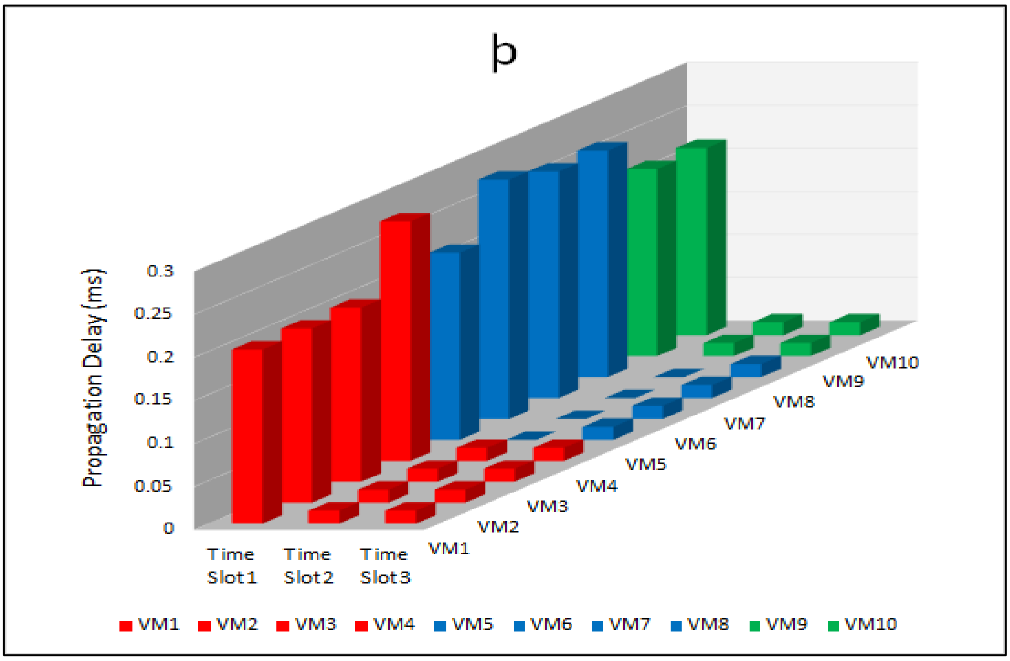

Figure 6.15 Propagation delay when minimising the networking power consumption only.

6.5.2.3 Minimising the propagation delay only (ÿ)

In this section, we study the results of the proposed model with the objective (ÿ) of only minimising the propagation delay and compare it to all previous minimisation models (Ô, Ä, and þ).

Figure 6.16 shows the total power consumption, which is higher than all the results in all previous minimisation models due to the high number of activated servers, as shown in Figure 6.13. The propagation delay, as shown in Figure 6.17, matches the propagation delay in the previous minimisation objective, as shown in Figure 6.8, Figure 6.12, and Figure 6.15.

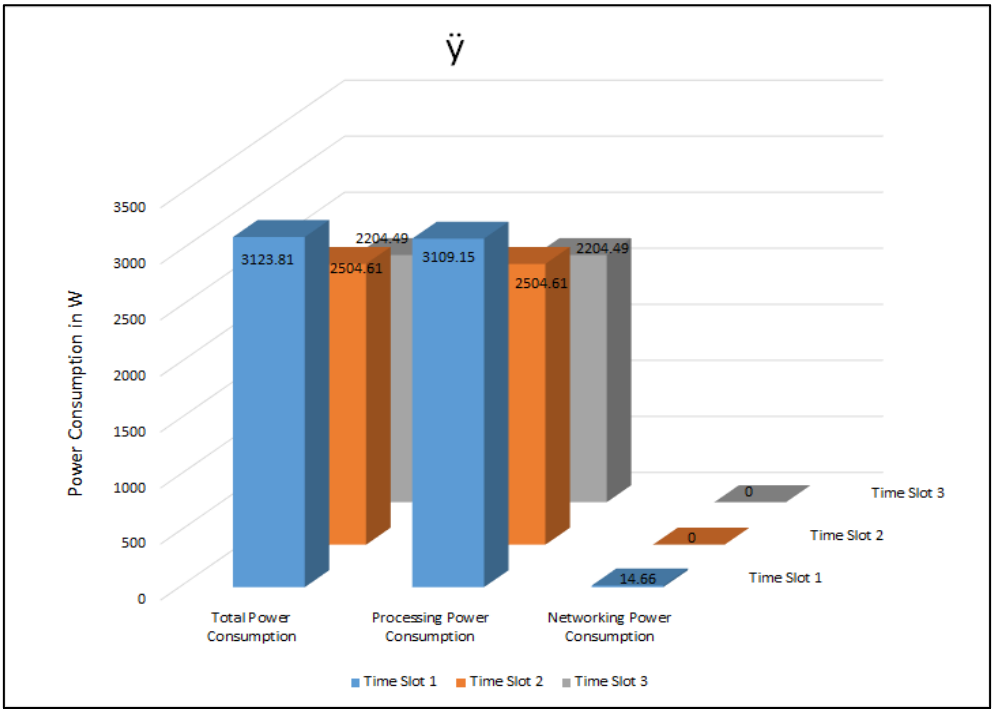

Figure 6.16 Power consumption when minimising only the propagation delay.

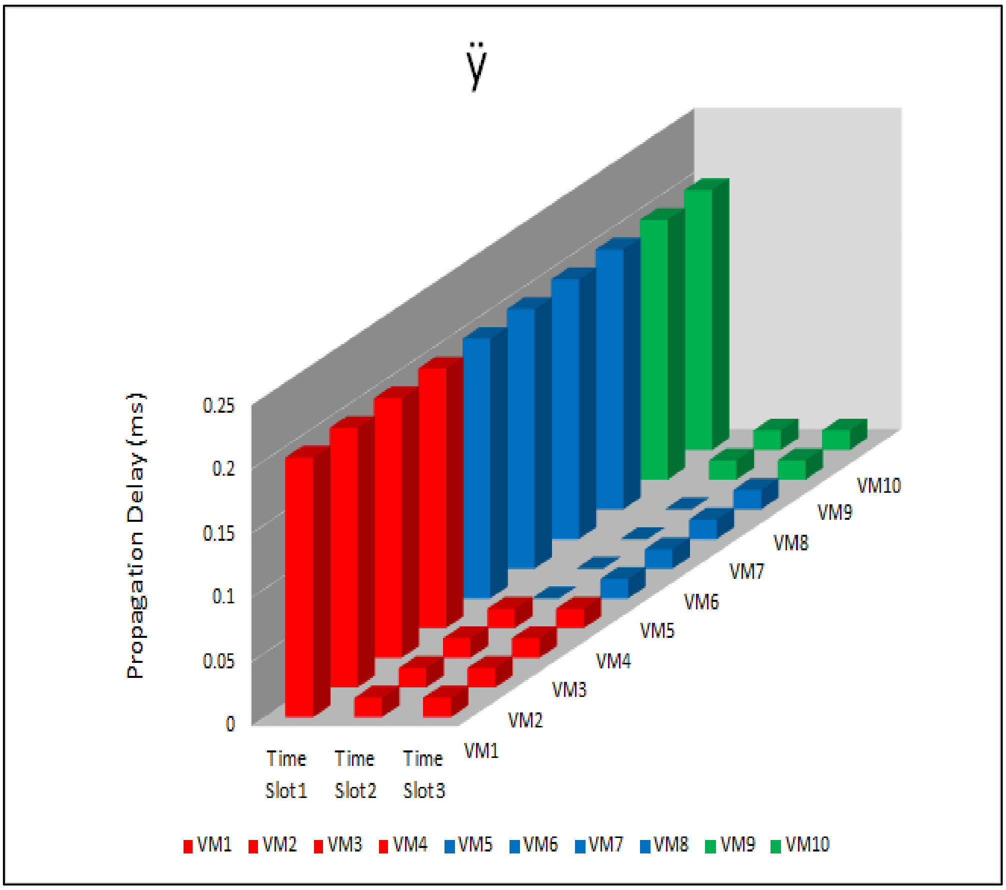

Figure 6.17 Propagation delay when minimising only the propagation delay.

6.6 Summary

In this chapter, we studied user-mobility among fog units in the collaborative fog computing architecture. We developed a MILP that optimise the migration of VMs according to the end user's mobility to be close to the end users to satisfy the requirements of delay-sensitive applications. The objective function of the model is to jointly minimise power consumption and propagation delay. The results indicated that VMs migration over AWGRs minimises power consumption and propagation delay by 55% and 92% respectively, compared to VMs migration over OLT. We investigated three more scenarios for the objective function which are: minimising the processing power consumption only, minimising the networking power consumption only, and minimising the propagation delay only. Over the different scenarios, the optimal result for the power consumption and delay occurred when the VMs have migrated over AWGR with the joint objective of minimising the total power consumption and minimising the propagation delay.

Chapter 7 Conclusions and Future Work

This chapter provides the conclusions of the work discussed in this thesis and highlights some potential future research directions.

7.1 Conclusions

This thesis has tackled some of the challenges in terms of power consumption, processing resources capacity, and delay that were raised due to the continuous growth in demand for delay-sensitive applications in access network which has shifted the cloud paradigm from a centralised computing architecture towards distributed heterogeneous computing platforms, the fog paradigm. Collaborative fog computing units over PON architecture have been proposed in this thesis to address these challenges through the following contributions:

- We proposed a collaborative fog computing architecture based on SDN-enabled PONs to achieve full connectivity among distributed fog computing units. The PON architecture, which utilises AWGs and AWGRs, has some remarkable advantages over other technologies used in connecting distributed or centralised computing units, especially in terms of the power consumption, due to the passive components used in this technology.
- We developed a MILP model to achieve all-to-all connectivity in the proposed collaborative architecture.
- The energy consumption of the proposed PON-based fog computing connectivity was compared to a spine and leaf architecture connecting the collaborative fog units. Power consumption saving by up to 81% was reported.

- Also, we developed a MILP model to optimise the VM placement in the proposed collaborative fog computing units with the objective of minimising the total power consumption while considering inter-VM traffic. Moreover, a heuristic was developed to realise energy efficient VMs resource allocation in real time. The results show power savings up to 44% by energy efficient placement of VMs compared to a baseline VMs placement neglecting the power consumption and inter-VMs traffic.
- We also studied a collaborative fog computing architecture where multiple distributed fog cells collaborate in serving end-users demand. We optimised the placement of VM demands originating from the end-users by formulating a MILP model to minimise the total power consumption. The results showed that the collaborative approach improves the energy efficiency by enabling server consolidation across the fog cells facilitated by the passive AWGR based connectivity. Also, this chapter studied the impact of the heterogeneity of the fog units in the proposed architecture. The results showed that VMs were better placed in the energy efficient fog servers. The networking power consumption impact is minimal due to the passive nature of PON.

- The user-mobility across the proposed collaborative fog units over PON in different time slots was discussed. We developed a MILP model to minimise the total power consumption and propagation delay while considering VMs migrations so that the VMs are placed closer to the end-users requesting them. We evaluated the model by comparing the VMs migration being routed through collaborative fog units over AWGRs or through a collaborative fog unit over the OLT. The results indicated that VMs migration over AWGRs minimises power consumption and propagation delay by 55% and 92% respectively, compared to VMs migration over OLT.

- Also, we investigated the proposed collaborative architecture considering the user with consideration of a number of objectives which are minimising the processing power consumption only, minimising the networking power consumption only, and minimising the propagation delay only. All these objectives have considered an architecture where the VMs can be migrated over OLT or AWGRs. Over the different scenarios, the optimal result for the power consumption and delay occurred when the VMs have migrated over AWGR with the joint objective of minimising the total power consumption and minimising the propagation delay.

7.2 Future Work

In the following, we list some of the future research directions related to the work presented in this thesis:

7.2.1 Architecture and Model Optimisation

The MILP models in this work connected three PON cells, each of which consists of two PON groups, and each PON group is assumed to contain up to16 servers. As future work, we plan to extend our models to more than two PON group in each cell. By increasing the number of PON groups in each cell, oversubscription increases. The oversubscription issue can be reduced by developing an optimal solution that can handle the increase in PON groups within a fog cell.

The VM placement and migration models in this thesis are based on the assumption that the connection through AWGs and AWGRs between all PON cells are based on fixed optimal routing. Future work can develop heuristics to achieve a flexible topology optimised based on variations in traffic and processing demands to choose the optimal number of connections needed to achieve connectivity between different PON cells.

7.2.2 Resilience in the Proposed Architecture

The proposed architecture in this thesis is a composed of distributed PON cells which are construct a fog computing system. Resilience has not been considered in our work. In future work, a new architecture and MILP models and heuristics can be developed to introduce a resilient collaborative fog architecture capable of handling server failure or link failure.

7.2.3 Experimental demonstration

The work in this thesis is based on mathematical models and simulations. In future experimental demonstrations can be developed to validate and verify the results obtained from the MILP models and the heuristic models.

7.2.4 Extending the model's objective

The joint optimisation objectives of users' mobility can be extended to include queuing delay and transmission delay to extend the evaluation of delay. Considering the total service time of such delay-sensitive application demands will help in the optimal resource allocation.

References

[1] S. H. Mohamed, T. E. H. El-Gorashi, and J. M. H. Elmirghani, ‘Energy Efficiency of Server-Centric PON Data Center Architecture for Fog Computing’, in *2018 20th International Conference on Transparent Optical Networks (ICTON)*, 2018, pp. 1–4, doi: 10.1109/ICTON.2018.8473877.

[2] A. C. Baktir, A. Ozgovde, and C. Ersoy, ‘How Can Edge Computing Benefit From Software-Defined Networking: A Survey, Use Cases, and Future Directions’, *IEEE Commun. Surv. Tutorials*, vol. 19, no. 4, pp. 2359–2391, 2017, doi: 10.1109/COMST.2017.2717482.

[3] M. Satyanarayanan, ‘The emergence of edge computing’, *Computer (Long. Beach. Calif).*, vol. 50, no. 1, pp. 30–39, Jan. 2017, doi: 10.1109/MC.2017.9.

[4] K. Dolui and S. K. Datta, ‘Comparison of edge computing implementations: Fog computing, cloudlet and mobile edge computing’, in *GIoTS 2017 - Global Internet of Things Summit, Proceedings*, 2017, doi: 10.1109/GIOTS.2017.8016213.

[5] S. Yi, Z. Hao, Z. Qin, and Q. Li, ‘Fog Computing: Platform and Applications’, in *2015 Third IEEE Workshop on Hot Topics in Web Systems and Technologies (HotWeb)*, 2015, pp. 73–78, doi: 10.1109/HotWeb.2015.22.

[6] F. Bonomi, R. Milito, J. Zhu, and S. Addepalli, ‘Fog computing and its role in the internet of things’, *Proc. first Ed. MCC Work. Mob. cloud Comput. - MCC ’12*, p. 13, 2012, doi: 10.1145/2342509.2342513.

[7] Cisco, ‘Fog Computing and the Internet of Things: Extend the Cloud to Where the Things Are’, *WHITE PAPER*, 2015. [Online]. Available: https://www.cisco.com/c/dam/en_us/solutions/trends/iot/docs/computing-overview.pdf. [Accessed: 15-Dec-2019].

[8] V. B. C. Souza, W. Ramirez, X. Masip-Bruin, E. Marin-Tordera, G. Ren, and G. Tashakor, ‘Handling service allocation in combined Fog-cloud scenarios’, in *2016 IEEE International Conference on Communications, ICC 2016*, 2016, doi: 10.1109/ICC.2016.7511465.

[9] P. O. Ostberg *et al.*, ‘Reliable capacity provisioning for distributed cloud/edge/fog computing applications’, in *EuCNC 2017 - European Conference on Networks and Communications*, 2017, doi: 10.1109/EuCNC.2017.7980667.

[10] M. T. Thai, Y. D. Lin, Y. C. Lai, and H. T. Chien, ‘Workload and Capacity Optimization for Cloud-Edge Computing Systems with Vertical and Horizontal Offloading’, *IEEE Trans. Netw. Serv. Manag.*, vol. 17, no. 1, pp. 227–238, Mar. 2020, doi: 10.1109/TNSM.2019.2937342.

[11] E. Bonetto, L. Chiaraviglio, D. Cuda, G. A. G. Castillo, and F. Neri, ‘Optical technologies can improve the energy efficiency of networks’, in *2009 35th European Conference on Optical Communication*, 2009, pp. 1–

4.

[12] E. Bonetto, D. Cuda, G. A. G. Castillo, and F. Neri, ‘The role of Arrayed Waveguide Gratings in energy-efficient optical switching architectures’, in *2010 Conference on Optical Fiber Communication (OFC/NFOEC), collocated National Fiber Optic Engineers Conference*, 2010, pp. 1–3, doi: 10.1364/OFC.2010.OWY4.

[13] R. S. Tucker, ‘The Role of Optics and Electronics in High-Capacity Routers’, *J. Light. Technol.*, vol. 24, no. 12, pp. 4655–4673, 2006, doi: 10.1109/JLT.2006.885774.

[14] R. S. Tucker, ‘Green Optical Communications—Part I: Energy Limitations in Transport’, *IEEE J. Sel. Top. Quantum Electron.*, vol. 17, no. 2, pp. 245–260, 2011, doi: 10.1109/JSTQE.2010.2051216.

[15] Y. Zhang, P. Chowdhury, M. Tornatore, and B. Mukherjee, ‘Energy Efficiency in Telecom Optical Networks’, *IEEE Commun. Surv. Tutorials*, vol. 12, no. 4, pp. 441–458, 2010, doi: 10.1109/SURV.2011.062410.00034.

[16] J. Baliga, R. Ayre, W. V. Sorin, K. Hinton, and R. S. Tucker, ‘Energy consumption in access networks’, *OFC/NFOEC 2008 - 2008 Conf. Opt. Fiber Commun. Fiber Opt. Eng. Conf.*, 2008, doi: 10.1109/OFC.2008.4528538.

[17] T. Crosby, ‘How Fiber-to-the-home Broadband Works’, *HowStuffWorks.com*. [Online]. Available: https://computer.howstuffworks.com/fiber-to-the-home.htm.

[18] G. Kramer and G. Pesavento, ‘Ethernet passive optical network (EPON): building a next-generation optical access network’, *IEEE Commun. Mag.*, vol. 40, no. 2, pp. 66–73, 2002, doi: 10.1109/35.983910.

[19] C. Gray, R. Ayre, K. Hinton, and R. S. Tucker, ‘Power consumption of IoT access network technologies’, in *2015 IEEE International Conference on Communication Workshop (ICCW)*, 2015, pp. 2818–2823, doi: 10.1109/ICCW.2015.7247606.

[20] J. Baliga, R. Ayre, K. Hinton, and R. S. Tucker, ‘Energy consumption in wired and wireless access networks’, *IEEE Commun. Mag.*, vol. 49, no. 6, pp. 70–77, 2011, doi: 10.1109/MCOM.2011.5783987.

[21] Y. Jin, Y. Wen, and Q. Chen, ‘Energy efficiency and server virtualization in data centers: An empirical investigation’, in *Proceedings - IEEE INFOCOM*, 2012, pp. 133–138, doi: 10.1109/INFCOMW.2012.6193474.

[22] A. Varasteh and M. Goudarzi, ‘Server Consolidation Techniques in Virtualized Data Centers: A Survey’, *IEEE Syst. J.*, vol. 11, no. 2, pp. 772–783, Jun. 2017, doi: 10.1109/JSYST.2015.2458273.

[23] S. Das, F. Slyne, A. Kaszubowska, and M. Ruffini, ‘Virtualized EAST-WEST PON architecture supporting low-latency communication for mobile functional split based on multiaccess edge computing’, *J. Opt. Commun. Netw.*, vol. 12, no. 10, pp. D109–D119, Oct. 2020, doi: 10.1364/JOCN.391929.

[24] S. N. Mthunzi, E. Benkhelifa, M. A. Alsmirat, and Y. Jararweh, ‘Analysis of VM communication for VM-based cloud security systems’, in *2018 Fifth*

International Conference on Software Defined Systems (SDS), 2018, pp. 182–188, doi: 10.1109/SDS.2018.8370441.

[25] H. A. Alharbi, T. E. H. Elgorashi, A. Q. Lawey, and J. M. H. Elmirghani, ‘The Impact of Inter-Virtual Machine Traffic on Energy Efficient Virtual Machines Placement’, in *2019 IEEE Sustainability through ICT Summit, StICT 2019*, 2019, doi: 10.1109/STICT.2019.8789381.

[26] X. Meng, V. Pappas, and L. Zhang, ‘Improving the scalability of data center networks with traffic-aware virtual machine placement’, *Proc. - IEEE INFOCOM*, 2010, doi: 10.1109/INFCOM.2010.5461930.

[27] S. Ayoubi, S. Sebbah, K. Shaban, and C. Assi, ‘Traffic engineering in cloud data centers: A column generation approach’, in *2014 IEEE Network Operations and Management Symposium (NOMS)*, 2014, pp. 1–5, doi: 10.1109/NOMS.2014.6838351.

[28] A. Jain, E. Lopez-Aguilera, and I. Demirkol, ‘Are Mobility Management Solutions Ready for 5G?’, *Comput. Commun.*, vol. 161, pp. 50–75, Feb. 2019, doi: 10.1016/j.comcom.2020.07.016.

[29] M. Waqas, Y. Niu, M. Ahmed, Y. Li, D. Jin, and Z. Han, ‘Mobility-Aware Fog Computing in Dynamic Environments: Understandings and Implementation’, *IEEE Access*, vol. 7, pp. 38867–38879, 2019, doi: 10.1109/ACCESS.2018.2883662.

[30] A. Hammadi, T. E. H. El-Gorashi, and J. M. H. Elmirghani, ‘High performance AWGR PONs in data centre networks’, in *2015 17th International Conference on Transparent Optical Networks (ICTON)*, 2015, pp. 1–5, doi: 10.1109/ICTON.2015.7193567.

[31] C. Lange, D. Kosiankowski, C. Gerlach, F.-J. Westphal, and A. Gladisch, ‘Energy consumption of telecommunication networks’, *2009 35th Eur. Conf. Opt. Commun.*, 2009.

[32] R. A. Patterson and E. Rolland, ‘Hybrid Fiber Coaxial Network Design’, *https://doi.org/10.1287/opre.50.3.538.7737*, vol. 50, no. 3, pp. 538–551, Jun. 2002, doi: 10.1287/OPRE.50.3.538.7737.

[33] Cisco, ‘Broadband Network Gateway Overview’. [Online]. Available: https://www.cisco.com/c/en/us/td/docs/routers/asr9000/software/asr9k_r4-3/bng/configuration/guide/b_bng_cg43xasr9k/b_bng_cg43asr9k_chapter_01.pdf.

[34] R. Santitoro, ‘Metro Ethernet Services – A Technical Overview .’, *Metro Ethernet forum*, pp. 1–19, 2003.

[35] R. Ballart and Y. C. Ching, ‘SONET: Now It’s the Standard Optical Network’, *IEEE Commun. Mag.*, vol. 27, no. 3, pp. 8–15, 1989, doi: 10.1109/35.20262.

[36] ‘What is WDM? Wavelength Division Multiplexing - Smartoptics’. [Online]. Available: https://www.smartoptics.com/this-is-wdm/. [Accessed: 30-Jan-2022].

[37] L. Bernstein and C. M. Yuhas, ‘Managing the last mile [access network]’, *IEEE Commun. Mag.*, vol. 35, no. 10, pp. 72–76, 1997, doi: 10.1109/35.623989.

[38] H. S. Abbas and M. Gregory, ‘The next generation of passive optical networks: A review’, *J. Netw. Comput. Appl.*, 2016.

[39] P. Ossieur *et al.*, ‘An overview of passive optical networks’, in *Signals, Circuits and Systems, 2003. SCS 2003. International Symposium on*, 2003, vol. 1, pp. 113–116 vol.1, doi: 10.1109/SCS.2003.1226961.

[40] M. M. Rad, K. Fouli, H. A. Fathallah, L. A. Rusch, and M. Maier, ‘Passive optical network monitoring: challenges and requirements’, *IEEE Commun. Mag.*, vol. 49, no. 2, pp. s45-S52, 2011, doi: 10.1109/MCOM.2011.5706313.

[41] A. Hammadi, M. Musa, T. E. H. El-Gorashi, and J. H. Elmirghani, ‘Resource provisioning for cloud PON AWGR-based data center architecture’, in *2016 21st European Conference on Networks and Optical Communications (NOC)*, 2016, pp. 178–182, doi: 10.1109/NOC.2016.7507009.

[42] D. Hood and L. Lu, ‘Current and future ITU-T PON systems and standards’, in *17th Opto-Electronics and Communications Conference*, 2012, p. 125, doi: 10.1109/OECC.2012.6276402.

[43] G. S. Rajiv Ramaswami, Kumar Sivarajan, *OPTICAL NETWORK A Practical Perspective*, 3rd ed. Morgan Kaufmann, 2009.

[44] F. Effenberger *et al.*, ‘An introduction to PON technologies [Topics in Optical Communications]’, *IEEE Commun. Mag.*, vol. 45, no. 3, pp. S17–S25, 2007, doi: 10.1109/MCOM.2007.344582.

[45] D. J. Shin *et al.*, ‘Hybrid WDM/TDM-PON with wavelength-selection-free transmitters’, *J. Light. Technol.*, vol. 23, no. 1, pp. 187–195, 2005, doi: 10.1109/JLT.2004.840031.

[46] N. Cvijetic, ‘OFDM for Next-Generation Optical Access Networks’, *J. Light. Technol.*, vol. 30, no. 4, pp. 384–398, 2012, doi: 10.1109/JLT.2011.2166375.

[47] S. S. W. Lee, K. Y. Li, and M. S. Wu, ‘Design and Implementation of a GPON-Based Virtual OpenFlow-Enabled SDN Switch’, *J. Light. Technol.*, vol. 34, no. 10, pp. 2552–2561, 2016, doi: 10.1109/JLT.2016.2540244.

[48] H. Khalili, S. Sallent, J. R. R. Piney, and D. Rincón, ‘A proposal for an SDN-based SIEPON architecture’, *Opt. Commun.*, vol. 403, no. July, pp. 9–21, 2017, doi: 10.1016/j.optcom.2017.07.009.

[49] A. S. Thyagaturu, A. Mercian, M. P. McGarry, M. Reisslein, and W. Kellerer, *Software Defined Optical Networks (SDONs): A Comprehensive Survey*, vol. 18, no. 4. 2016.

[50] R. Gu, Y. Ji, P. Wei, and S. Zhang, ‘Software defined flexible and efficient passive optical networks for intra-datacenter communications’, *Opt. Switch. Netw.*, vol. 14, no. PART 3, pp. 289–302, 2014, doi: 10.1016/j.osn.2014.05.015.

[51] M. Nakamura, H. Ueda, S. Makino, T. Yokotani, and K. Oshima, ‘Proposal of networking by PON technologies for full and ethernet services in FTTx’, *J. Light. Technol.*, vol. 22, no. 11, pp. 2631–2640, 2004, doi: 10.1109/JLT.2004.836765.

[52] C. Kachris and I. Tomkos, 'Power consumption evaluation of hybrid WDM PON networks for data centers', in *2011 16th European Conference on Networks and Optical Communications*, 2011, pp. 118–121.

[53] J. M. H. Elmirghani, E.-G. T.E., and A. Hammadi, 'PASSIVE OPTICAL - BASED DATA CENTER NETWORKS', WO2016083812, 2016.

[54] A. Hammadi, T. E. H. El-Gorashi, M. O. I. Musa, and J. M. H. Elmirghani, 'Server-centric PON data center architecture', in *2016 18th International Conference on Transparent Optical Networks (ICTON)*, 2016, pp. 1–4, doi: 10.1109/ICTON.2016.7550695.

[55] A. Hammadi, T. E. H. El-Gorashi, and J. M. H. Elmirghani, 'Energy-efficient software-defined AWGR-based PON data center network', in *2016 18th International Conference on Transparent Optical Networks (ICTON)*, 2016, pp. 1–5, doi: 10.1109/ICTON.2016.7550697.

[56] P. Mell and T. Grance, 'The NIST Definition of Cloud Computing', *Natl. Inst. Stand. Technol.*, 2011, doi: 10.6028/NIST.SP.800-145.

[57] D. Puthal, B. P. S. Sahoo, S. Mishra, and S. Swain, 'Cloud Computing Features, Issues, and Challenges: A Big Picture', in *2015 International Conference on Computational Intelligence and Networks*, 2015, pp. 116–123, doi: 10.1109/CINE.2015.31.

[58] D. Rani and R. K. Ranjan, 'A Comparative Study of SaaS , PaaS and IaaS in Cloud Computing', *Int. J. Adv. Res. Comput. Sci. Softw. Eng.*, vol. 4, no. 6, pp. 458–461, 2014.

[59] A. Hammadi and L. Mhamdi, 'A survey on architectures and energy efficiency in Data Center Networks', *Comput. Commun.*, vol. 40, pp. 1–21, 2014, doi: 10.1016/j.comcom.2013.11.005.

[60] J. Wang, D. Wang, M. Qiu, Y. Chen, and B. Guo, 'A locality-aware shuffle optimization on fat-tree data centers', *Futur. Gener. Comput. Syst.*, vol. 89, pp. 31–43, 2018, doi: https://doi.org/10.1016/j.future.2018.06.016.

[61] R.Niranjan *et al.*, 'Portland:a scalable fault-tolerant layer 2 data center network fabric', *SIGCOMM Comput. Commun*, pp. 66–105, 2011, doi: 10.5949/upo9781846312953.004.

[62] 'Cisco Data Center Spine-and-Leaf Architecture: Design Overview White Paper - Cisco'. [Online]. Available: https://www.cisco.com/c/en/us/products/collateral/switches/nexus-7000-series-switches/white-paper-c11-737022.html. [Accessed: 26-Jul-2021].

[63] C.Guo, H.Wu, K.Tan, L.Shi, Y.Zhang, and S.Lu, 'DCell: A Scalable and Fault-Tolerant Network Structure for Data Centers', *Sigcomm*, pp. 75–86, 2008, doi: 10.1145/1402958.1402968.

[64] H. R. H. Andersson, A. d. Blanche, and T. Lundqvist, 'Flipping the Data Center Network: Increasing East-West Capacity Using Existing Hardware', in *2017 IEEE 42nd Conference on Local Computer Networks (LCN)*, 2017, pp. 211–214, doi: 10.1109/LCN.2017.92.

[65] C. Guo *et al.*, 'BCube: A High Performance, Server-centric Network Architecture for Modular Data Centers', *ACM SIGCOMM Comput. Commun. Rev.*, vol. 39, no. 4, p. 63, 2009, doi: 10.1145/1594977.1592577.

[66] C. Mouradian, D. Naboulsi, S. Yangui, R. H. Glitho, M. J. Morrow, and P. A. Polakos, ‘A Comprehensive Survey on Fog Computing: State-of-the-Art and Research Challenges’, *IEEE Commun. Surv. Tutorials*, vol. 20, no. 1, pp. 416–464, 2018, doi: 10.1109/COMST.2017.2771153.

[67] OpenFog Consortium Working Group, C. B. (Cisco), and R. S. (Intel), ‘OpenFog Reference Architecture for Fog Computing’, 2017.

[68] P. Hu, S. Dhelim, H. Ning, and T. Qiu, ‘Survey on fog computing: architecture, key technologies, applications and open issues’, *J. Netw. Comput. Appl.*, vol. 98, no. April, pp. 27–42, 2017, doi: 10.1016/j.jnca.2017.09.002.

[69] M. Chiang and T. Zhang, ‘Fog and IoT: An Overview of Research Opportunities’, *IEEE Internet Things J.*, vol. 3, no. 6, pp. 854–864, 2016, doi: 10.1109/JIOT.2016.2584538.

[70] S. Sarkar and S. Misra, ‘Theoretical modelling of fog computing: a green computing paradigm to support IoT applications’, *IET Networks*, vol. 5, no. 2, pp. 23–29, 2016, doi: 10.1049/iet-net.2015.0034.

[71] F. Jalali, K. Hinton, R. Ayre, T. Alpcan, and R. S. Tucker, ‘Fog Computing May Help to Save Energy in Cloud Computing’, *IEEE J. Sel. Areas Commun.*, vol. 34, no. 5, pp. 1728–1739, 2016, doi: 10.1109/JSAC.2016.2545559.

[72] A. Khan, A. Zugenmaier, D. Jurca, and W. Kellerer, ‘Network virtualization: A hypervisor for the internet?’, *IEEE Commun. Mag.*, vol. 50, no. 1, pp. 136–143, Jan. 2012, doi: 10.1109/MCOM.2012.6122544.

[73] R. A. T. Alani, T. E. H. El-Gorashi, and J. M. H. Elmirghani, ‘Virtual machines embedding for cloud PON AWGR and server based data centres’, in *International Conference on Transparent Optical Networks*, 2019, vol. 2019-July, doi: 10.1109/ICTON.2019.8840217.

[74] E. Halepovic and C. Williamson, ‘Characterizing and modeling user mobility in a cellular data network’, in *PE-WASUN’05 - Proceedings of the Second ACM International Workshop on Performance Evaluation of Wireless Ad Hoc, Sensor, and Ubiquitous Networks*, 2005, pp. 71–78, doi: 10.1145/1089803.1089969.

[75] M. Musolesi and C. Mascolo, ‘Designing mobility models based on social network theory’, *ACM SIGMOBILE Mob. Comput. Commun. Rev.*, vol. 11, no. 3, pp. 59–70, Jul. 2007, doi: 10.1145/1317425.1317433.

[76] T. Camp, J. Boleng, and V. Davies, ‘A survey of mobility models for ad hoc network research’, *Wirel. Commun. Mob. Comput.*, vol. 2, no. 5, pp. 483–502, Aug. 2002, doi: 10.1002/wcm.72.

[77] X. Ge, J. Ye, Y. Yang, and Q. Li, ‘User Mobility Evaluation for 5G Small Cell Networks Based on Individual Mobility Model’, *IEEE J. Sel. Areas Commun.*, vol. 34, no. 3, pp. 528–541, Mar. 2016, doi: 10.1109/JSAC.2016.2525439.

[78] J. Harri, F. Filali, and C. Bonnet, ‘Mobility models for vehicular ad hoc networks: A survey and taxonomy’, *IEEE Commun. Surv. Tutorials*, vol. 11, no. 4, pp. 19–41, 2009, doi: 10.1109/SURV.2009.090403.

[79] X. Hong, M. Gerla, G. Pei, and C. C. Chiang, ‘A group mobility model for

ad hoc wireless networks', in *Proceedings of the 2nd ACM International Workshop on Modeling, Analysis and Simulation of Wireless and Mobile Systems, MSWiM 1999*, 1999, pp. 53–60, doi: 10.1145/313237.313248.

[80] S. Batabyal and P. Bhaumik, 'Mobility models, traces and impact of mobility on opportunistic routing algorithms: A survey', *IEEE Commun. Surv. Tutorials*, vol. 17, no. 3, pp. 1679–1707, Jul. 2015, doi: 10.1109/COMST.2015.2419819.

[81] C. Bettstetter, 'Mobility modeling in wireless networks', *ACM SIGMOBILE Mob. Comput. Commun. Rev.*, vol. 5, no. 3, pp. 55–66, Jul. 2001, doi: 10.1145/584051.584056.

[82] M. M. Zonoozi and P. Dassanayake, 'User mobility modeling and characterization of mobility patterns', *IEEE J. Sel. Areas Commun.*, vol. 15, no. 7, pp. 1239–1252, Sep. 1997, doi: 10.1109/49.622908.

[83] M. M. S. Kowsar and M. R. Karim, 'A survey of mobility management in wireless mesh networks', in *Proceeding of the 15th International Conference on Computer and Information Technology, ICCIT 2012*, 2012, pp. 316–320, doi: 10.1109/ICCITechn.2012.6509775.

[84] Q. Dong and W. Dargie, 'A survey on mobility and mobility-aware MAC protocols in wireless sensor networks', *IEEE Commun. Surv. Tutorials*, vol. 15, no. 1, pp. 88–100, 2013, doi: 10.1109/SURV.2012.013012.00051.

[85] J. Wu and P. Fan, 'A Survey on High Mobility Wireless Communications: Challenges, Opportunities and Solutions', *IEEE Access*, vol. 4, pp. 450–476, 2016, doi: 10.1109/ACCESS.2016.2518085.

[86] E. W. Woolard, A. Einstein, R. Furth, and A. D. Cowper, 'Investigations on the Theory of the Brownian Movement.', *Am. Math. Mon.*, vol. 35, no. 6, p. 318, Jun. 1928, doi: 10.2307/2298685.

[87] R. C. Sofia, 'A survey on mobility models for wireless networks', *Academia.edu*. [Online]. Available: https://www.academia.edu/17676659/A_survey_on_mobility_models_for_wireless_networks. [Accessed: 28-Jul-2020].

[88] I. F. Akyildiz, Y. B. Lin, W. R. Lai, and R. J. Chen, 'New random walk model for PCS networks', *IEEE J. Sel. Areas Commun.*, vol. 18, no. 7, pp. 1254–1260, Jul. 2000, doi: 10.1109/49.857925.

[89] J. Broch and D. A. Maltz, 'A Performance Comparison of Multi-Hop Wireless Ad Hoc Network Routing Protocols'. [Online]. Available: https://www.cs.cornell.edu/people/egs/615/broch98performance.pdf. [Accessed: 28-Jul-2020].

[90] C. Bettstetter, 'Mobility modeling in wireless networks', *ACM SIGMOBILE Mob. Comput. Commun. Rev.*, vol. 5, no. 3, pp. 55–66, Jul. 2001, doi: 10.1145/584051.584056.

[91] D. M. Blough, G. Resta, and P. Santi, 'A statistical analysis of the long-run node spatial distribution in mobile ad hoc networks', in *Proceedings of the 5th ACM international workshop on Modeling analysis and simulation of wireless and mobile systems - MSWiM '02*, 2002, p. 30, doi: 10.1145/570758.570765.

[92] E. M. Royer, P. M. Melliar-Smith, and L. E. Moser, 'An analysis of the

optimum node density for ad hoc mobile networks', in *IEEE International Conference on Communications*, 2001, vol. 3, pp. 857–861, doi: 10.1109/icc.2001.937360.

[93] A. M. Alqahtani, S. H. Mohamed, T. E. H. El-Gorashi, and J. M. H. Elmirghani, 'PON-Based Connectivity for Fog Computing', in *2020 22nd International Conference on Transparent Optical Networks (ICTON)*, 2020, pp. 1–6, doi: 10.1109/ICTON51198.2020.9203425.

[94] Y. Cai, S. Luo, and L. Zhou, 'Software defined passive optical intra-rack networks in data centers', in *2016 IEEE Globecom Workshops, GC Wkshps 2016 - Proceedings*, 2016, doi: 10.1109/GLOCOMW.2016.7849048.

[95] S. H. S. Newaz, W. Susanty Binti Haji Suhaili, G. M. Lee, M. R. Uddin, A. F. Y. Mohammed, and J. K. Choi, 'Towards realizing the importance of placing fog computing facilities at the central office of a PON', in *International Conference on Advanced Communication Technology, ICACT*, 2017, pp. 152–157, doi: 10.23919/ICACT.2017.7890075.

[96] Cisco, 'Cisco Nexus 9332C and 9364C Fixed Spine Switches Data Sheet - Cisco'. [Online]. Available: https://www.cisco.com/c/en/us/products/collateral/switches/nexus-9000-series-switches/datasheet-c78-739886.html. [Accessed: 04-Feb-2020].

[97] R. Alani, A. Hammadi, T. E. H. El-Gorashi, and J. M. H. Elmirghani, 'PON data centre design with AWGR and server based routing', in *2017 19th International Conference on Transparent Optical Networks (ICTON)*, 2017, pp. 1–4, doi: 10.1109/ICTON.2017.8024885.

[98] A. Hammadi, T. E. H. El-Gorashi, and J. M. H. Elmirghani, 'Energy-efficient software-defined AWGR-based PON data center network', in *International Conference on Transparent Optical Networks*, 2016, vol. 2016-Augus, doi: 10.1109/ICTON.2016.7550697.

[99] A. Yousefpour *et al.*, 'All One Needs to Know about Fog Computing and Related Edge Computing Paradigms: A Complete Survey', *Elsevier J. Syst. Archit.*, 2018, doi: 10.1016/j.sysarc.2019.02.009.

[100] K. O. Hill and G. Meltz, 'Fiber Bragg grating technology fundamentals and overview', *J. Light. Technol.*, vol. 15, no. 8, pp. 1263–1276, Aug. 1997, doi: 10.1109/50.618320.

[101] Y. Luo, F. Effenberger, and M. Sui, 'Cloud computing provisioning over passive optical networks', *2012 1st IEEE Int. Conf. Commun. China, ICCC 2012*, pp. 255–259, 2012, doi: 10.1109/ICCChina.2012.6356888.

[102] Cisco, 'Cisco ME 4600 Series Optical Network Terminal Data Sheet', 2013. [Online]. Available: https://www.cisco.com/c/en/us/products/collateral/switches/me-4600-series-multiservice-optical-access-platform/datasheet-c78-730445.html. [Accessed: 02-Mar-2020].

[103] X. Dong, T. El-Gorashi, and J. M. H. Elmirghani, 'Green IP over WDM networks with data centers', *J. Light. Technol.*, vol. 29, no. 12, pp. 1861–1880, 2011, doi: 10.1109/JLT.2011.2148093.

[104] K. Grobe, M. Roppelt, A. Autenrieth, J. P. Elbers, and M. Eiselt, 'Cost and

energy consumption analysis of advanced WDM-PONs', *IEEE Commun. Mag.*, vol. 49, no. 2, pp. 25–32, 2011, doi: 10.1109/MCOM.2011.5706310.

[105] Cisco, 'Cisco Nexus 9200 Platform Switches Data Sheet - Cisco'. [Online]. Available: https://www.cisco.com/c/en/us/products/collateral/switches/nexus-9000-series-switches/datasheet-c78-735989.html. [Accessed: 04-Feb-2020].

[106] L. Gyarmati and T. A. Trinh, 'How can architecture help to reduce energy consumption in data center networking?', *1st Int. Conf. Energy-Efficient Comput. Networking, Passau, Ger.*, p. 183, 2010, doi: 10.1145/1791314.1791343.

[107] M. B. Nagpure, P. Dahiwale, and P. Marbate, 'An efficient dynamic resource allocation strategy for VM environment in cloud', in *2015 International Conference on Pervasive Computing (ICPC)*, 2015, pp. 1–5, doi: 10.1109/PERVASIVE.2015.7087186.

[108] A. M. Alqahtani, B. Yosuf, S. H. Mohamed, T. E. H. El-Gorashi, and J. M. H. Elmirghani, 'Energy Minimized Federated Fog Computing over Passive Optical Networks', May 2021.

[109] Dell, 'SPECpower_ssj2008'. [Online]. Available: https://www.spec.org/power_ssj2008/results/res2017q3/power_ssj2008-20170829-00780.html. [Accessed: 30-Jan-2020].

[110] N. (Cisco) Sorensen, 'Industry Benchmarks Performance', 2011.

[111] S. P. E. Corporation, 'SPECpower_ssj2008', 2017. [Online]. Available: https://www.spec.org/power_ssj2008/results/res2017q3/power_ssj2008-20170829-00780.html. [Accessed: 12-Mar-2021].

[112] A. K. Paul, S. K. Addya, B. Sahoo, and A. K. Turuk, 'Application of greedy algorithms to Virtual Machine Distribution across Data Centers', in *11th IEEE India Conference: Emerging Trends and Innovation in Technology, INDICON 2014*, 2015, doi: 10.1109/INDICON.2014.7030633.

[113] S. S. Seiden, 'On the online bin packing problem', *J. ACM*, vol. 49, no. 5, pp. 640–671, Sep. 2002, doi: 10.1145/585265.585269.

[114] J. Xu and J. A. B. Fortes, 'Multi-objective virtual machine placement in virtualized data center environments', in *Proceedings - 2010 IEEE/ACM International Conference on Green Computing and Communications, GreenCom 2010, 2010 IEEE/ACM International Conference on Cyber, Physical and Social Computing, CPSCom 2010*, 2010, pp. 179–188, doi: 10.1109/GreenCom-CPSCom.2010.137.

[115] S. Kumaraswamy and M. K. Nair, 'Bin packing algorithms for virtual machine placement in cloud computing: A review', *Int. J. Electr. Comput. Eng.*, vol. 9, no. 1, pp. 512–524, Feb. 2019, doi: 10.11591/ijece.v9i1.pp512-524.

[116] C. Wei, Z. H. Hu, and Y. G. Wang, 'Exact algorithms for energy-efficient virtual machine placement in data centers', *Futur. Gener. Comput. Syst.*, vol. 106, pp. 77–91, May 2020, doi: 10.1016/j.future.2019.12.043.

[117] X. Zhang, J. Lu, and X. Qin, 'BFEPM: Best fit energy prediction modeling based on CPU utilization', *Proc. - 2013 IEEE 8th Int. Conf. Networking, Archit. Storage, NAS 2013*, pp. 41–49, 2013, doi: 10.1109/NAS.2013.12.

[118] M. Goudarzi, H. Wu, M. Palaniswami, and R. Buyya, ‘An Application Placement Technique for Concurrent IoT Applications in Edge and Fog Computing Environments’, *IEEE Trans. Mob. Comput.*, vol. 20, no. 4, pp. 1298–1311, 2021, doi: 10.1109/TMC.2020.2967041.

[119] D. G. Roy, D. De, A. Mukherjee, and R. Buyya, ‘Application-aware cloudlet selection for computation offloading in multi-cloudlet environment’, *J. Supercomput.*, vol. 73, no. 4, pp. 1672–1690, Apr. 2017, doi: 10.1007/S11227-016-1872-Y/TABLES/6.

[120] M. H. Chen, B. Liang, and M. Dong, ‘Joint offloading and resource allocation for computation and communication in mobile cloud with computing access point’, *Proc. - IEEE INFOCOM*, Oct. 2017, doi: 10.1109/INFOCOM.2017.8057150.

[121] C. Gray, R. Ayre, K. Hinton, and R. S. Tucker, ‘Power consumption of IoT access network technologies’, in *2015 IEEE International Conference on Communication Workshop, ICCW 2015*, 2015, pp. 2818–2823, doi: 10.1109/ICCW.2015.7247606.

[122] ‘SPECpower_ssj2008’. [Online]. Available: https://www.spec.org/power_ssj2008/results/res2012q1/power_ssj2008-20120306-00434.html. [Accessed: 19-Mar-2022].

[123] ‘SPECpower_ssj2008’. [Online]. Available: https://www.spec.org/power_ssj2008/results/res2012q3/power_ssj2008-20120724-00513.html. [Accessed: 19-Mar-2022].

[124] D. H. S. Lima, A. L. L. Aquino, and M. Curado, ‘A review of mobility prediction models applied in cloud/fog environments’, in *Lecture Notes in Computer Science (including subseries Lecture Notes in Artificial Intelligence and Lecture Notes in Bioinformatics)*, 2019, vol. 11339 LNCS, pp. 263–274, doi: 10.1007/978-3-030-10549-5_21.

[125] R. Boutaba, Q. Zhang, and M. F. Zhani, ‘Virtual Machine Migration in Cloud Computing Environments: Benefits, Challenges, and Approaches’, *https://services.igi-global.com/resolvedoi/resolve.aspx?doi=10.4018/978-1-4666-4522-6.ch017*, pp. 383–408, Jan. 1AD, doi: 10.4018/978-1-4666-4522-6.CH017.

[126] V. Mann, A. Vishnoi, K. Kannan, and S. Kalyanaraman, ‘CrossRoads: Seamless VM mobility across data centers through software defined networking’, *Proc. 2012 IEEE Netw. Oper. Manag. Symp. NOMS 2012*, pp. 88–96, 2012, doi: 10.1109/NOMS.2012.6211886.

[127] F. Zhang, G. Liu, X. Fu, and R. Yahyapour, ‘A Survey on Virtual Machine Migration: Challenges, Techniques, and Open Issues’, *IEEE Commun. Surv. Tutorials*, vol. 20, no. 2, pp. 1206–1243, Apr. 2018, doi: 10.1109/COMST.2018.2794881.

[128] D. Wang, Z. Liu, X. Wang, and Y. Lan, ‘Mobility-Aware Task Offloading and Migration Schemes in Fog Computing Networks’, *IEEE Access*, vol. 7, pp. 43356–43368, 2019, doi: 10.1109/ACCESS.2019.2908263.

[129] W. Bao *et al.*, ‘Follow Me Fog: Toward Seamless Handover Timing Schemes in a Fog Computing Environment’, *IEEE Commun. Mag.*, vol. 55, no. 11, pp. 72–78, 2017, doi: 10.1109/MCOM.2017.1700363.

[130] A. Rahman, J. Jin, A. Cricenti, A. Rahman, and M. Panda, ‘Motion and connectivity aware offloading in cloud robotics via genetic algorithm’, in *2017 IEEE Global Communications Conference, GLOBECOM 2017 - Proceedings*, 2017, vol. 2018-January, pp. 1–6, doi: 10.1109/GLOCOM.2017.8255040.

[131] T. Ojima and T. Fujii, ‘Resource management for mobile edge computing using user mobility prediction’, in *International Conference on Information Networking*, 2018, vol. 2018-January, pp. 718–720, doi: 10.1109/ICOIN.2018.8343212.

[132] W. Nasrin and J. Xie, ‘SharedMEC: Sharing clouds to support user mobility in mobile edge computing’, in *IEEE International Conference on Communications*, 2018, vol. 2018-May, doi: 10.1109/ICC.2018.8422241.

[133] S. K. Biswash, ‘Node-to-Node Communication and Mobility Management Scheme for 5G Fog Networks’, in *International Symposium on Advanced Networks and Telecommunication Systems, ANTS*, 2019, vol. 2019-December, doi: 10.1109/ANTS47819.2019.9118111.

[134] Y. Sun, S. Zhou, and J. Xu, ‘EMM: Energy-aware mobility management for mobile edge computing in ultra dense networks’, *IEEE J. Sel. Areas Commun.*, vol. 35, no. 11, pp. 2637–2646, Nov. 2017, doi: 10.1109/JSAC.2017.2760160.

[135] P. J. Roig, S. Alcaraz, K. Gilly, and C. Juiz, ‘Study on Mobility and Migration in a Fog Computing Environment’, *2018 22nd Int. Conf. Electron. Electron. 2018*, Aug. 2018, doi: 10.1109/ELECTRONICS.2018.8443636.

[136] K. Deep Singh, ‘Role of Optical Network in Cloud/Fog Computing’, *Telecommun. Syst. - Princ. Appl. Wireless-Optical Technol.*, Oct. 2019, doi: 10.5772/INTECHOPEN.84404.

[137] A. A. Alahmadi, T. E. H. El-Gorashi, and J. M. H. Elmirghani, ‘Energy efficient and delay aware vehicular edge cloud’, *Int. Conf. Transparent Opt. Networks*, vol. 2020-July, Jul. 2020, doi: 10.1109/ICTON51198.2020.9203156.